The Science Case for a Southern Wide field of view detector

G. Di Sciascio
INFN - Roma Tor Vergata
disciascio@roma2.infn.it

RICAP 2018 - 7th Roma International Conference on Astroparticle Physics
Rome, September 04-07, 2018

The currently standard model

- CRs below 10^{17} eV are predominantly Galactic.
- ***Standard paradigm***: *Galactic CRs accelerated in SuperNova Remnants*
  ➜ *But smoking gun still missing !!!*
- Galactic CRs via *diffusive* shock acceleration ?
  $n_{CR} \propto E^{-\gamma}$ (at source), $\gamma \approx 2.1$
- Energy-dependent *diffusion* through Galaxy
  $n_{CR} \propto E^{-\gamma-\delta}$ (observed), $\delta \approx 0.6$

all-particle energy spectrum

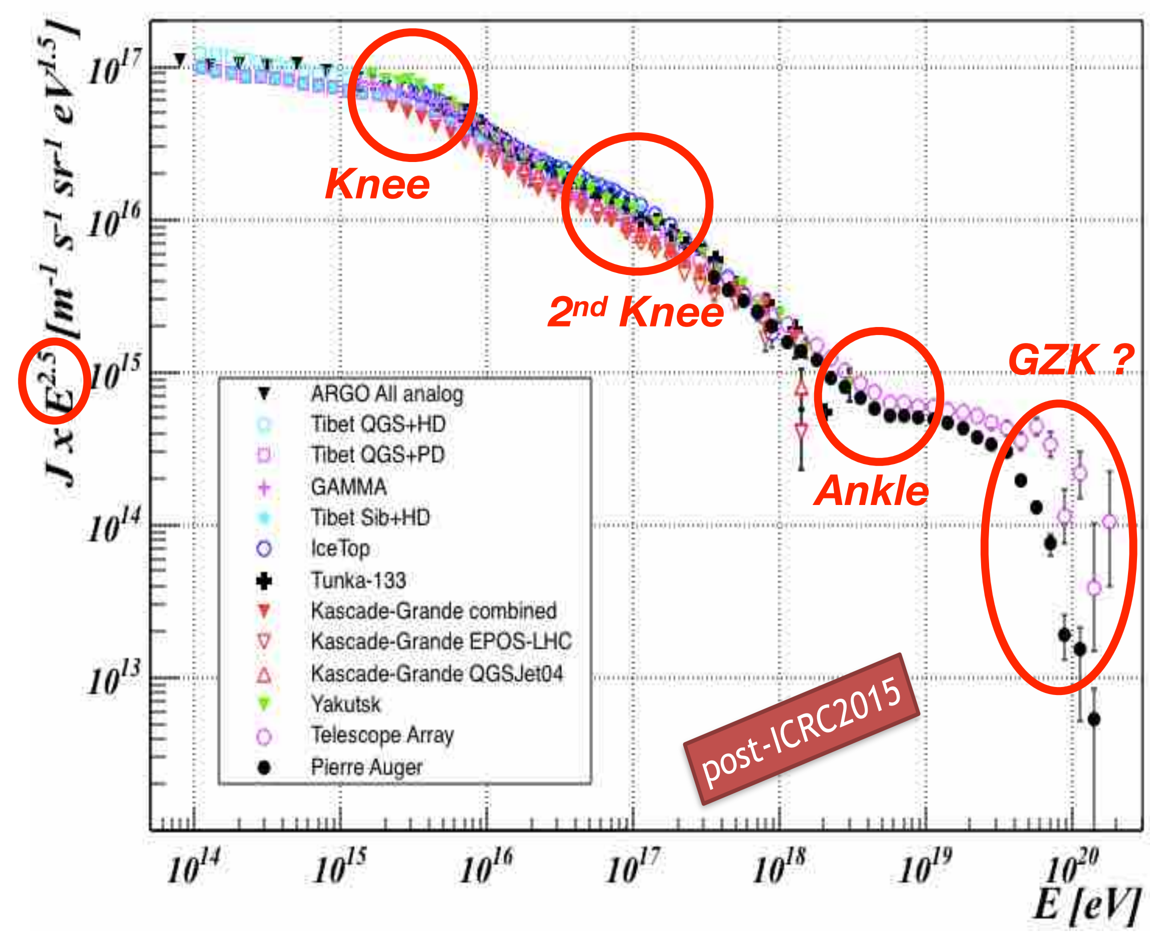

- Galactic CRs are scrambled by galactic magnetic field over very long time
  ➜ arrival direction *mostly isotropic*
- Transition to extragalactic CRs occurs somewhere between 10^{17} and 10^{19} eV

The key questions

✦ ***Origin of Cosmic Rays***: what are ***the sites*** that can accelerate particles up to > 10^{20} eV ? How many classes of sources at work ? Which cosmic accelerators dominate the CR flux in which energy range ?

- which *acceleration* mechanism? ➜ injection spectrum
- total energy in CRs
- *maximum energy of accelerated particles: the ‘proton knee’*

  The description of how particles escape from a SNR shock has not been completely understood yet, the reason being the uncertainties related to *how particles reach the maximum energies.*

✦ ***Cosmic Ray propagation***: How do CRs propagate ?

- injected ➜ observed spectrum
- Diffusion coefficients
- Why are CR confined in the Galaxy ? ➜ magnetic field in the Galaxy
- spatial distribution of sources
- spatial distribution of CRs ➜ anisotropy

✦ What is the ***elemental composition*** of the radiation as a function of the energy ?

Knee as end of Galactic population ?

Understanding the origin of the "knee" is the key for a comprehensive theory of the origin of CRs up to the highest observed energies.

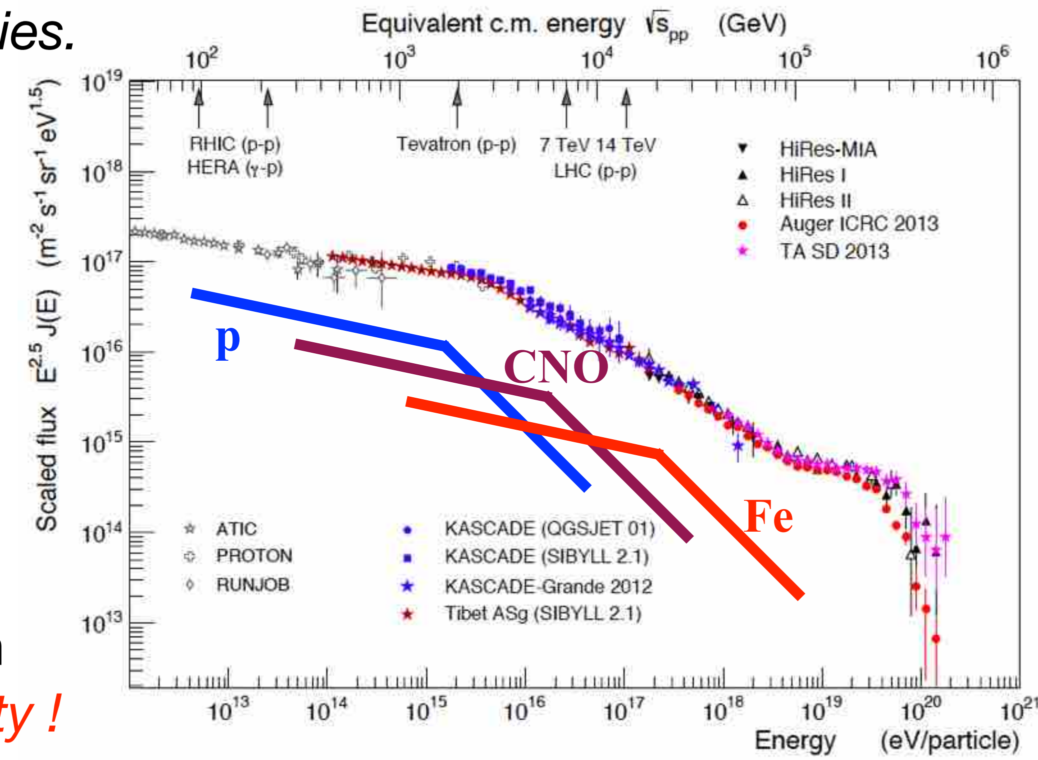

In fact, the knee is connected with the issue of the end of the Galactic CR spectrum and the transition from Galactic to extra-galactic CRs.

★ *Rigidity* models can be *rigidity-acceleration* models or *rigidity-confinement* models

- *Accelerator feature*: maximum energy of acceleration
  ➜ implies that all accelerators are similar: *source property !*

- *Structure generated by propagation:* ➜ we should observe a *knee that is potentially dependent on location*, because the propagation properties depend on position in the Galaxy
  ➜ the (main) Galactic CR accelerators must be capable to accelerate to much higher energy
  ➜ the Galaxy contains *"super-PeVatrons" !* ➜ *Gamma-Ray Astronomy above 100 TeV*

If the mass of the knee is *light* according to the standard model
➜ Galactic CR spectrum is expected to end around 10^{17} eV

If the composition at the knee is *heavier* due to CNO / MgSi
➜ we have a problem !

Knee as end of Galactic population ?

Understanding the origin of the "knee" is the key for a comprehensive theory of the origin of CRs up to the highest observed energies.

In fact, the knee is connected with the issue of the end of the Galactic CR spectrum and the transition from Galactic to extra-galactic CRs.

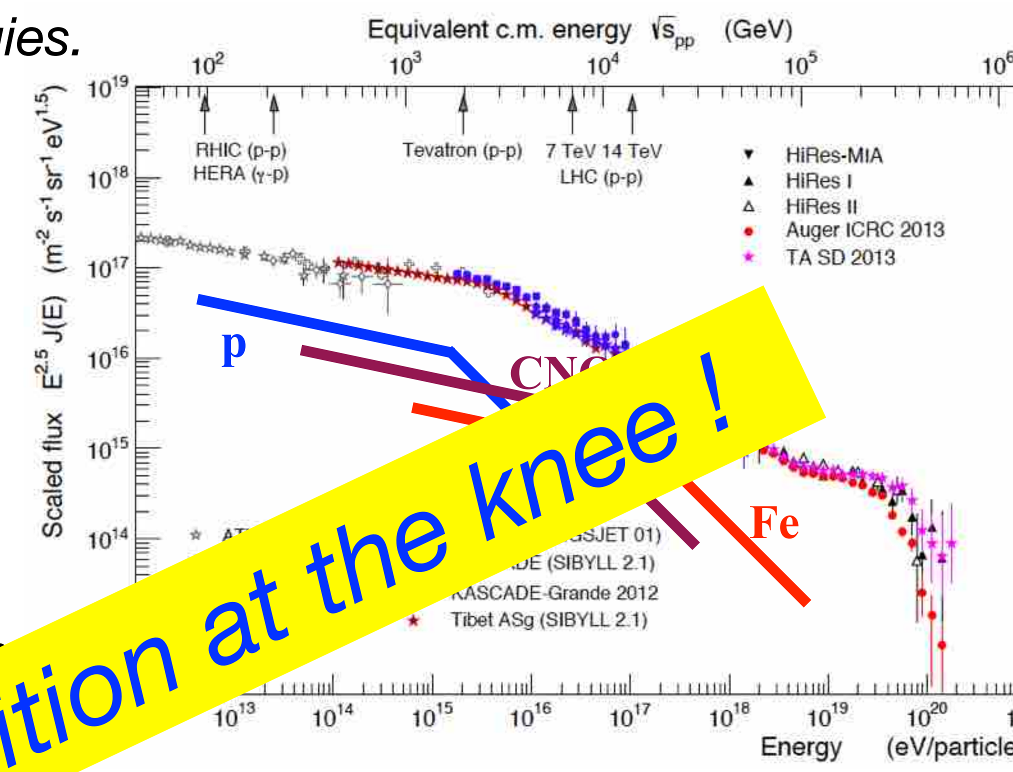

★ *Rigidity* models can be *rigidity-acceleration* models or *rigidity-confinement* models

- *Accelerator feature*: maximum energy of acceleratio
  ➜ implies that all accelerators are similar: *source*
- *Structure generated by propagati* ...uld observe a *knee that is potentially dependent on location*, because t ...n properties depend on position in the Galaxy
  ➜ the (main) Galactic CR ac ... ust be capable to accelerate to much higher energy
  ➜ the Galaxy contains ... trons" ! ➜ *Gamma-Ray Astronomy above 100 TeV*

Strong Message: composition at the knee !

...s of the knee is *light* according to the standard model
...alactic CR spectrum is expected to end around 10^{17} eV

If the composition at the knee is *heavier* due to CNO / MgSi
➜ we have a problem !

Ground-based gamma-ray detectors

Detecting Extensive Air Showers

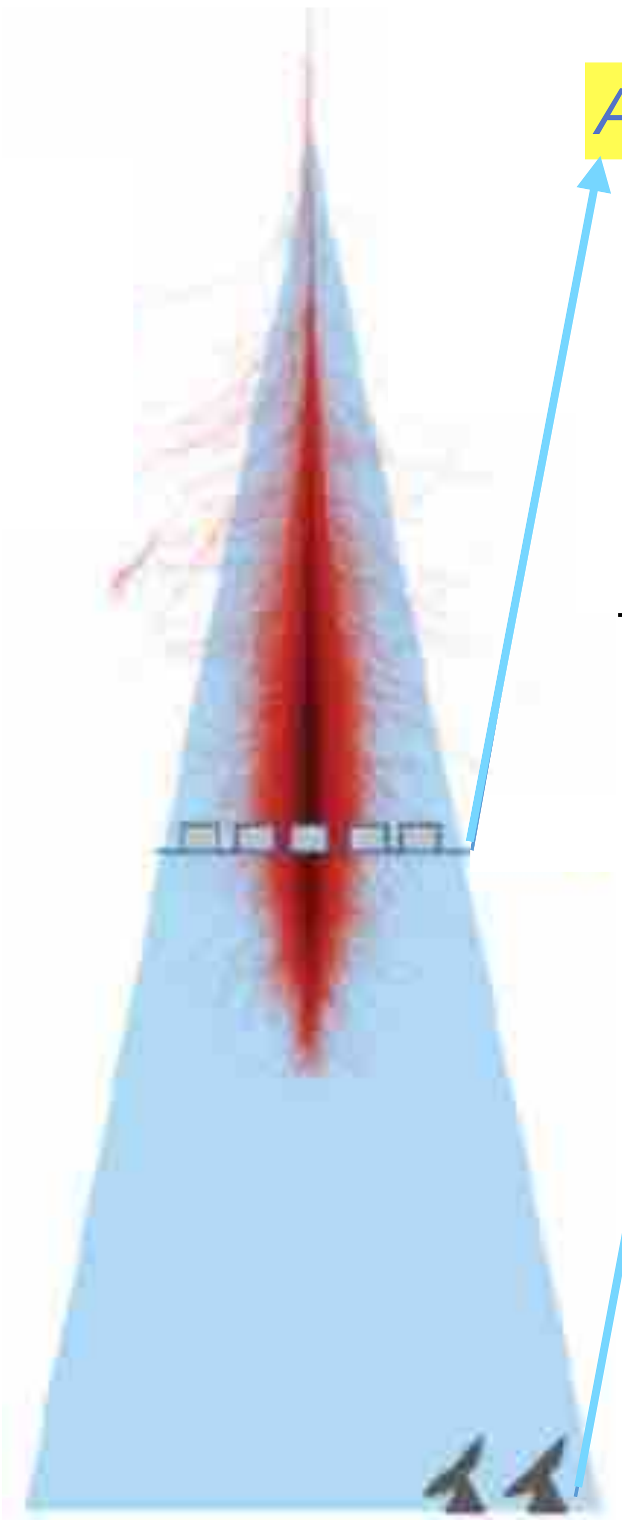

Air Shower Arrays (≈100 GeV → 1 PeV)

- High duty-cycle (≈100%)
- Large field of view (≈2 sr)
- Large energy range (≈PeV)
- Higher energy threshold (ARGO ≈300 GeV),
- Very strong zenith angle dependent ($\approx \cos\theta^{-(6-7)}$)
- Good bkg rejection (>80%)
- Good angular resolution (0.2-0.8 deg)
- Modest energy resolution (≈50%)
- Good Sensitivity (5-10% Crab flux)
- Effective area shrinks with large zenith angle

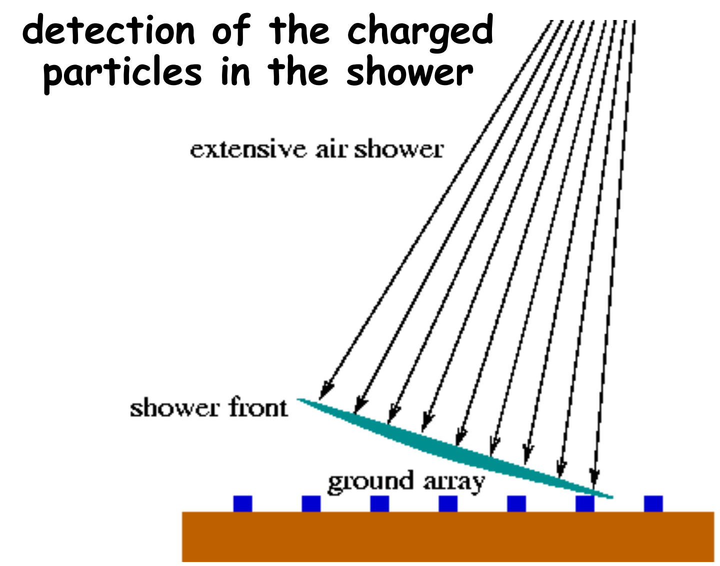

Cherenkov Telescopes (≈10 GeV → 100 TeV)

- Very low energy threshold (≈10 GeV)
- Excellent bkg rejection (>99%)
- Excellent angular resolution (≈0.05 deg)
- Very good energy resolution (≈15%)
- High Sensitivity (< % Crab flux)
- Effective area increase with zenith angle
- Small zenith angle dependent ($\approx \cos\theta^{-2.7}$)
- Low duty-cycle (≈10-15%)
- Small field of view (≈4-5 deg)
- Reduced maximum energy (≈100 TeV)

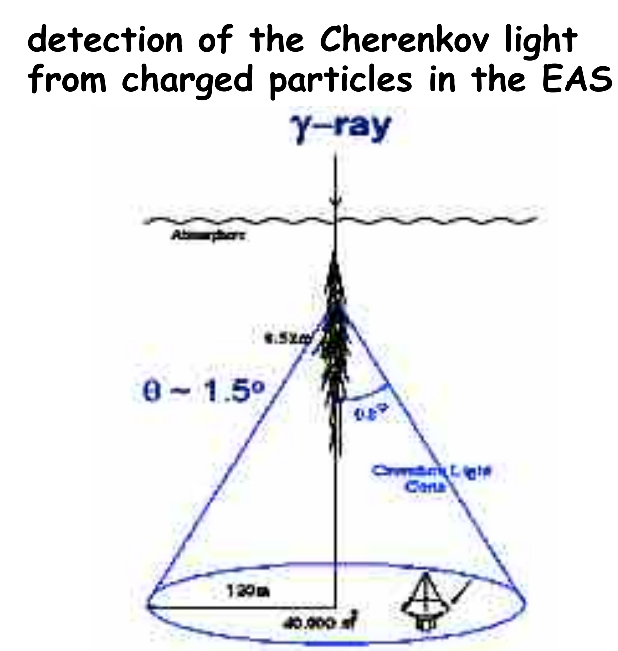

Wide field of view detectors

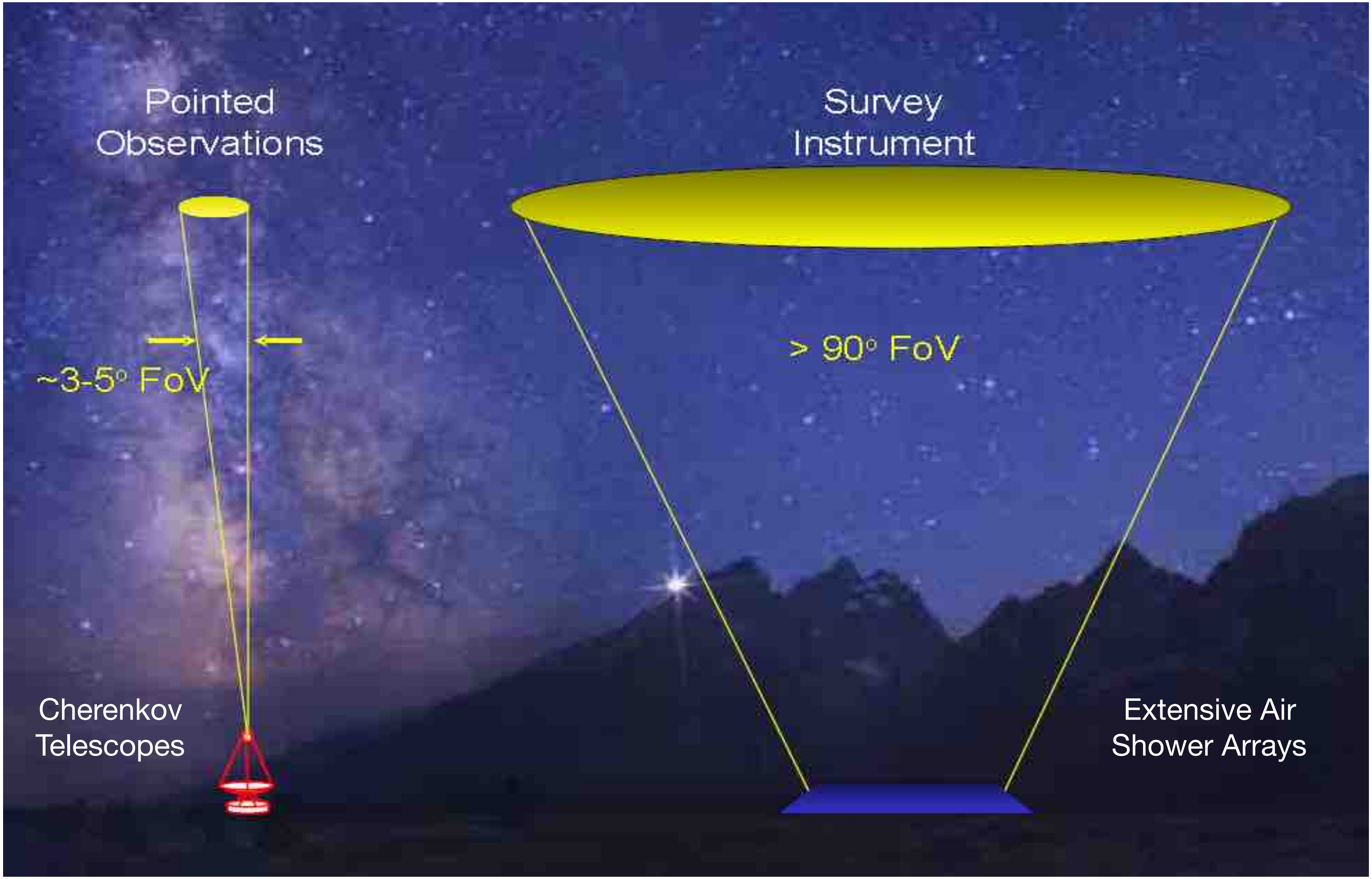

Wide field of view detectors

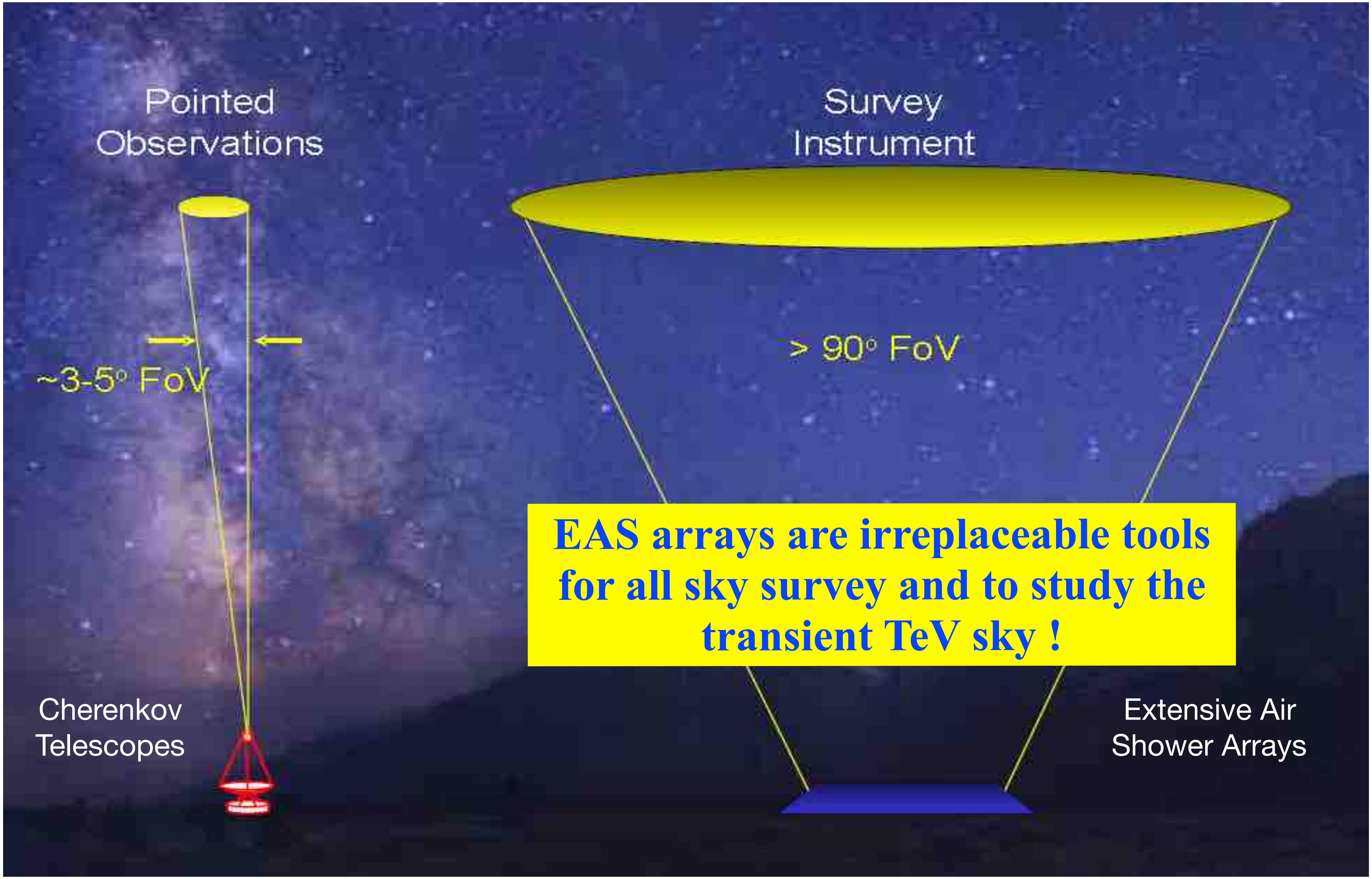

Why are Wide FoV instruments so cool ?

✦ ***Origin of Cosmic Rays***: what are ***the sites*** that can accelerate particles up to > 10^{20} eV ? How many classes of sources at work ? Which cosmic accelerators dominate the CR flux in which energy range ?

- which *acceleration* mechanism? ➜ injection spectrum
- total energy in CRs
- *maximum energy of accelerated particles: the 'proton knee'*

The description of how particles escape from a SNR shock has not been completely understood yet, the reason being the uncertainties related to *how particles reach the maximum energies.*

✦ ***Cosmic Ray propagation***: How do CRs propagate ?

- injected ➜ observed spectrum
- Diffusion coefficients
- Why are CR confined in the Galaxy ? ➜ magnetic field in the Galaxy
- spatial distribution of sources
- spatial distribution of CRs ➜ anisotropy

✦ What is the ***elemental composition*** of the radiation ?

Why are Wide FoV instruments so cool ?

✦ ***Origin of Cosmic Rays***: what are ***the sites*** that can accelerate particles up to > 10^{20} eV ? How many classes of sources at work ? Which cosmic accelerators dominate the CR flux in which energy range ?

- which *acceleration* mechanism? ➜ injection spectrum
- total energy in CRs
- *maximum energy of accelerated particles: the 'proton knee'*

The description of how particles escape from a SNR shock has not been completely understood yet, the reason being the uncertainties related to *how particles reach the maximum energies.*

✦ ***Cosmic Ray propagation***: How do CRs propagate ?

- injected ➜ observed spectrum
- Diffusion coefficients
- Why are CR confined in the Galaxy ? ➜ magnetic field in the Galaxy
- spatial distribution of sources
- spatial distribution of CRs ➜ anisotropy

✦ What is the ***elemental composition*** of the radiation ?

Why are Wide FoV instruments so cool ?

✦ ***Origin of Cosmic Rays***: what are ***the sites*** that can accelerate particles up to > 10^{20} eV ? How many classes of sources at work ? Which cosmic accelerators dominate the CR flux in which energy range ?

- which *acceleration* mechanism? ➜ injection spectrum
- total energy in CRs
- *maximum energy of accelerated particles: the '<u>proton knee</u>'*

The description of how particles escape from a SNR sho … completely understood yet, the reason being the uncertainties related to *h… …ach the maximum energies*.

✦ ***Cosmic Ray propagation***: How … …pagate ?

- injected ➜ observed s…
- Diffusion coeff…
- Why a… …ed in the Galaxy ? ➜ magnetic field in the Galaxy
- …ribution of sources
- …patial distribution of CRs ➜ anisotropy

✦ What is the ***elemental composition*** of the radiation ?

Wide FoV detectors = Multi-Messenger Instruments (by definition)

Why a new Wide FoV detector in the CTA era ?

- Galactic/Extragalactic *unbiased survey*: detection of *unexpected sources*
- "Finder" telescope for CTA: provides *targets for in-depth observations*
- *Extended objects* (PWN, diffuse gamma-ray emission)
- High exposure for *flaring activity* (AGN, GRBs, solar flares): *transient factory*
- *Fundamental physics* (high mass dark matter > 10 TeV)
- "Classical" *Cosmic Ray Physics* (energy spectrum, elemental composition, anisotropy, hadronic interactions)
- *Multi-Messenger Instrument* (by definition)

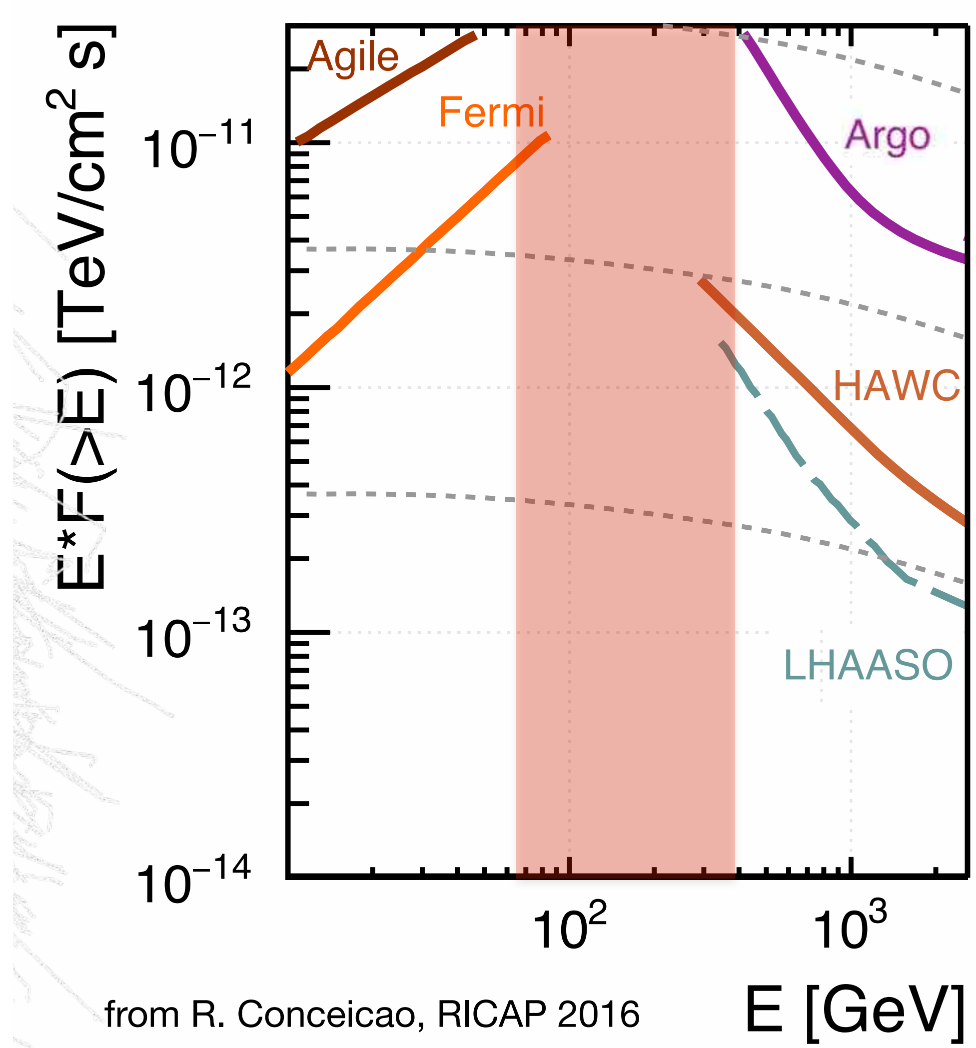

from R. Conceicao, RICAP 2016

No Wide FoV experiment to:

- Explore the 100 GeV energy region
- *Survey the Inner Galaxy and the Galactic Center*

The fascinating TeV γ-sky

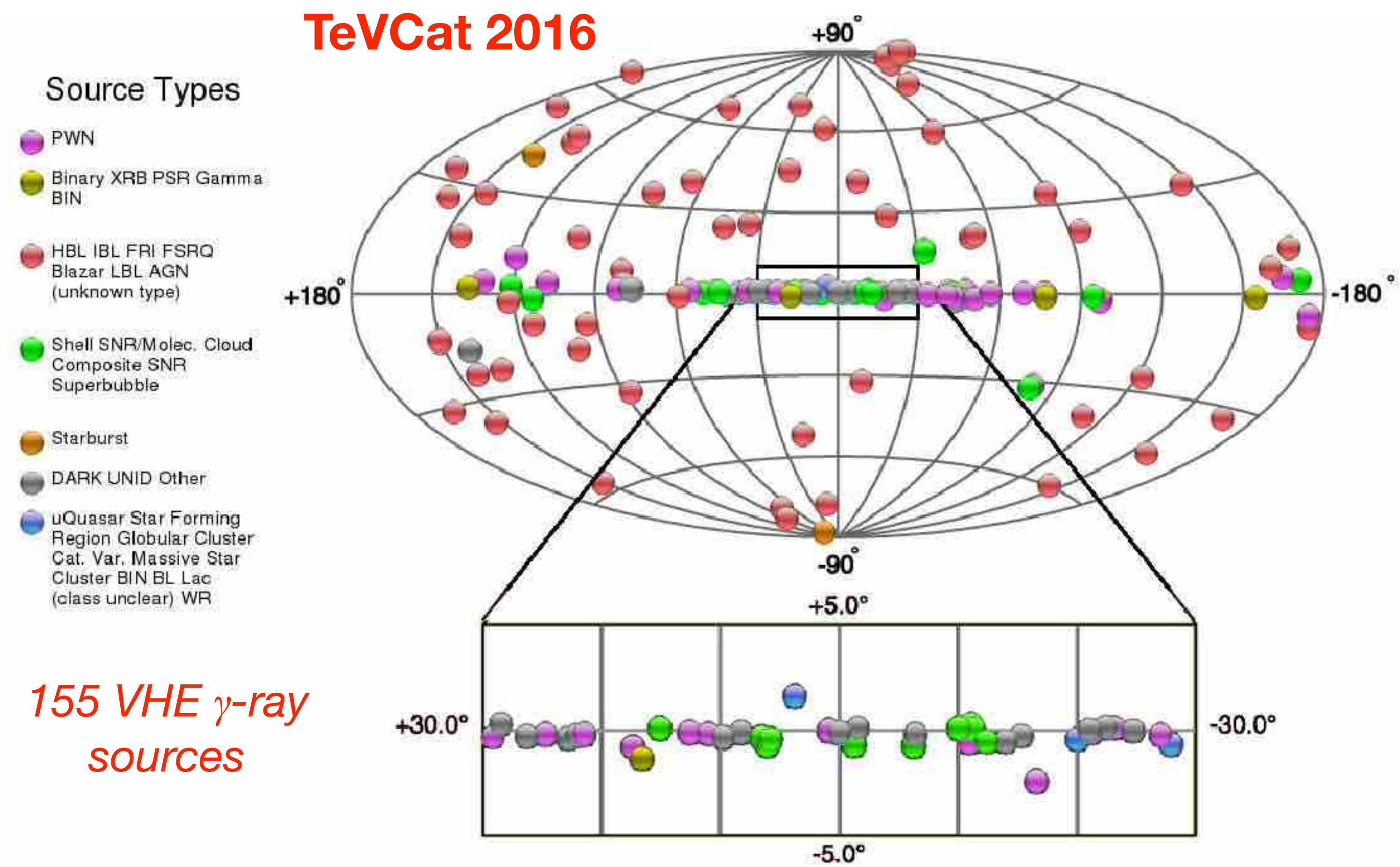

155 VHE γ-ray sources

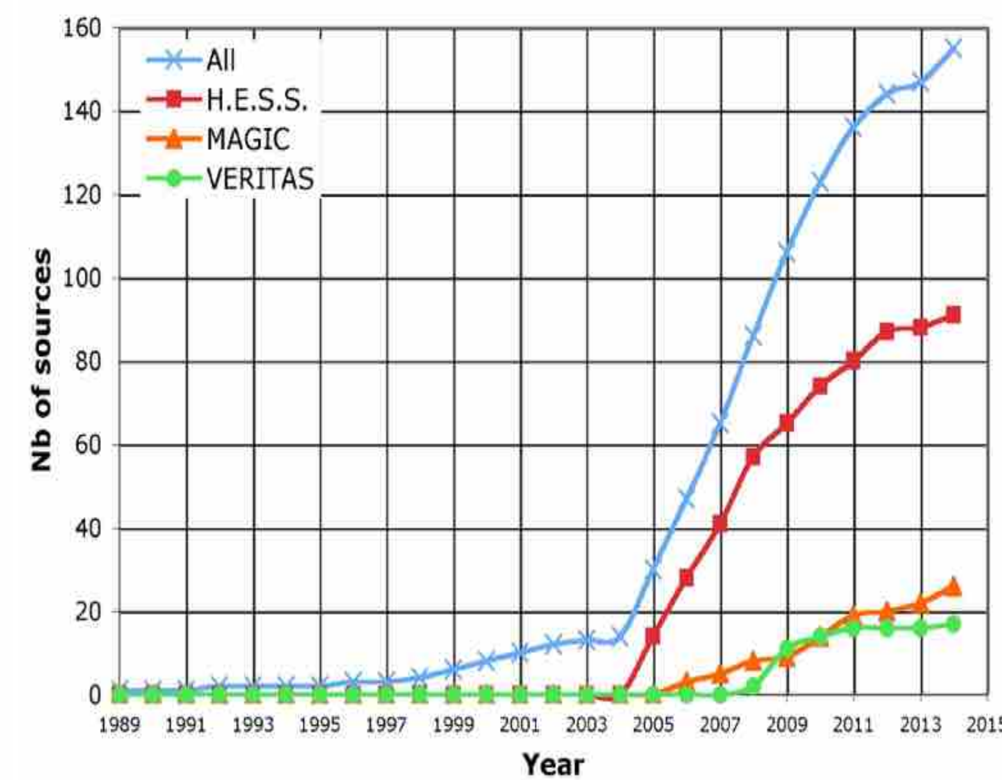

How complete is the Survey ?

If there is a (bright) PeVatron out there, would we have detected it already ?

- *Wide Field of View:* all-sky survey provides un *unbiased map of the sky*
- *Survey of the Southern sky*
- *High Energy Survey (100 TeV range)*

HESS Galactic Plane Survey

arXiv:1804.02432

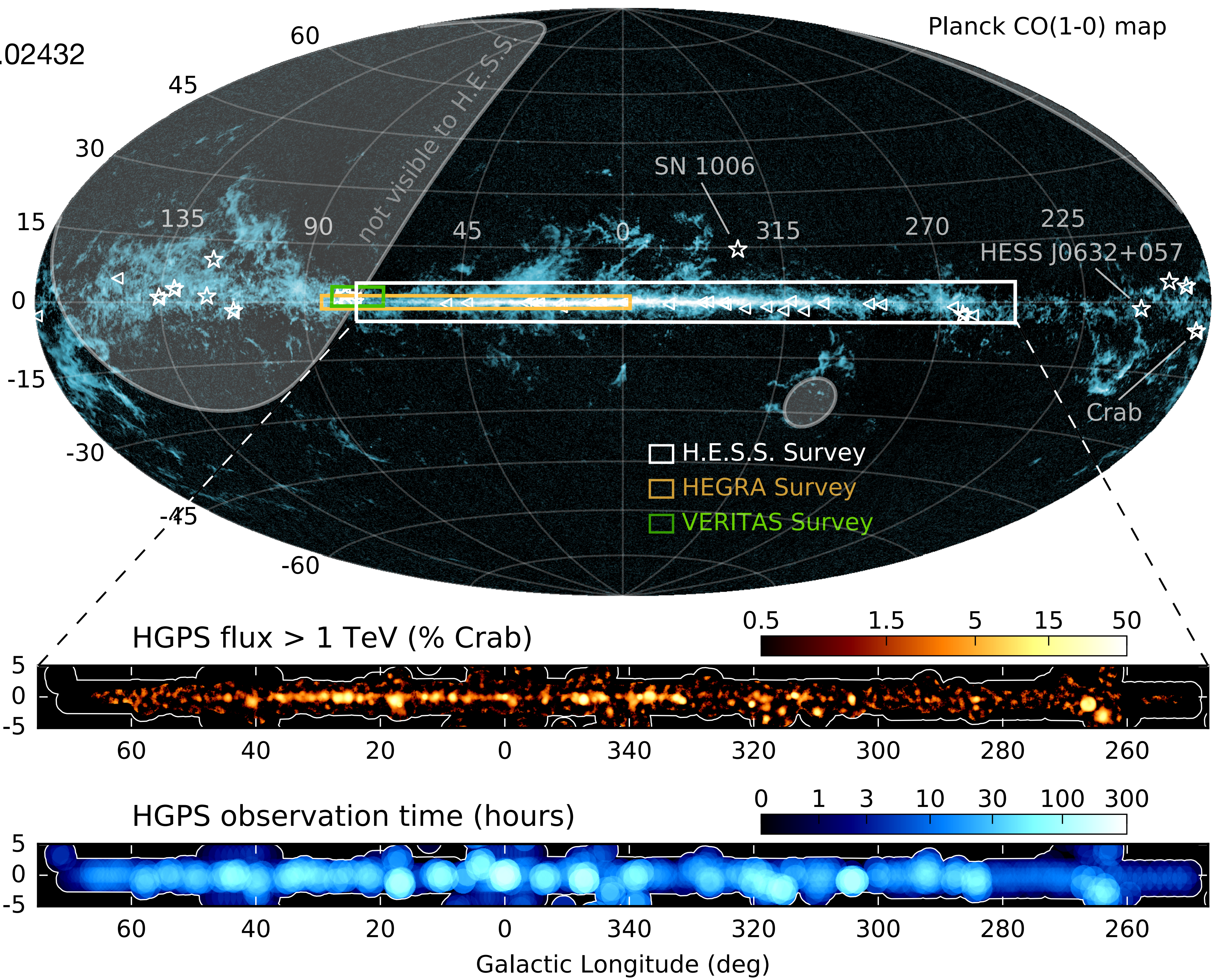

HESS Galactic Plane Survey

2700 hours observation from 2004 to 2013 at longitudes from l=250° to 65° and latitudes $|b|\leq 3°$, angular resolution ≈0.08° (≈5 arcmin), *sensitivity ≤1.5% Crab*, energy range *0.2 TeV ➔ 100 TeV*.

Table 3. Table of 31 firmly-identified objects among the HGPS sources. The object classes are γ-ray binary, shell-type supernova remnant (SNR), pulsar wind nebula (PWN), and composite SNR (in cases where it is not possible to distinguish between the shell and interior nebula). The evidence used to identify the VHE γ-ray emission include position, morphology, variability, and energy-dependent morphology (ED Morph.).

Source name	Identified object	Class	Evidence	Reference
HESS J1018−589 A	1FGL J1018.6−5856	Binary	Variability	H.E.S.S. Collaboration et al. (2015e)
HESS J1302−638	PSR B1259−63	Binary	Variability	Aharonian et al. (2005c)
HESS J1826−148	LS 5039	Binary	Variability	Aharonian et al. (2006e)
HESS J0852−463	Vela Junior	SNR	Morphology	Aharonian et al. (2005e)
HESS J1442−624	RCW 86	SNR	Morphology	H.E.S.S. Collaboration et al. (2016e)
HESS J1534−571	G323.7−1.0	SNR	Morphology	H.E.S.S. Collaboration et al. (2017a)
HESS J1713−397	RX J1713.7−3946	SNR	Morphology	Aharonian et al. (2004b)
HESS J1718−374	G349.7+0.2	SNR	Position	H.E.S.S. Collaboration et al. (2015b)
HESS J1731−347	G353.6−0.7	SNR	Morphology	H.E.S.S. Collaboration et al. (2011a)
HESS J1801−233	W 28	SNR	Position	Aharonian et al. (2008d)
HESS J1911+090	W 49B	SNR	Position	H.E.S.S. Collaboration et al. (2016b)
HESS J0835−455	Vela X	PWN	Morphology	Aharonian et al. (2006c)
HESS J1303−631	G304.10−0.24	PWN	ED Morph.	H.E.S.S. Collaboration et al. (2012)
HESS J1356−645	G309.92−2.51	PWN	Position	H.E.S.S. Collaboration et al. (2011b)
HESS J1418−609	G313.32+0.13	PWN	Position	Aharonian et al. (2006f)
HESS J1420−607	G313.54+0.23	PWN	Position	Aharonian et al. (2006f)
HESS J1514−591	MSH 15−52	PWN	Morphology	Aharonian et al. (2005d)
HESS J1554−550	G327.15−1.04	PWN	Morphology	Section 5.6.5
HESS J1747−281	G0.87+0.08	PWN	Morphology	Aharonian et al. (2005a)
HESS J1818−154	G15.4+0.1	PWN	Morphology	H.E.S.S. Collaboration et al. (2014a)
HESS J1825−137	G18.00−0.69	PWN	ED Morph.	Aharonian et al. (2006g)
HESS J1837−069	G25.24−0.19	PWN	Morphology	Marandon et al. (2008)
HESS J1849−000	G32.64+0.53	PWN	Position	Section 5.6.15
HESS J1119−614	G292.2−0.5	Composite	Position	Section 5.6.1
HESS J1640−465	G338.3−0.0	Composite	Position	Abramowski et al. (2014b), Gotthelf et al. (2014)
HESS J1714−385	CTB 37A	Composite	Position	Aharonian et al. (2008c)
HESS J1813−178	G12.8−0.0	Composite	Position	Funk et al. (2007), Gotthelf & Halpern (2009)
HESS J1833−105	G21.5−0.9	Composite	Position	Section 5.6.10
HESS J1834−087	W 41	Composite	Morphology	H.E.S.S. Collaboration et al. (2015a)
HESS J1846−029	G29.7−0.3	Composite	Position	Section 5.6.13
HESS J1930+188	G54.1+0.3	Composite	Position	Acciari et al. (2010), Sect. 5.4

arXiv:1804.02432

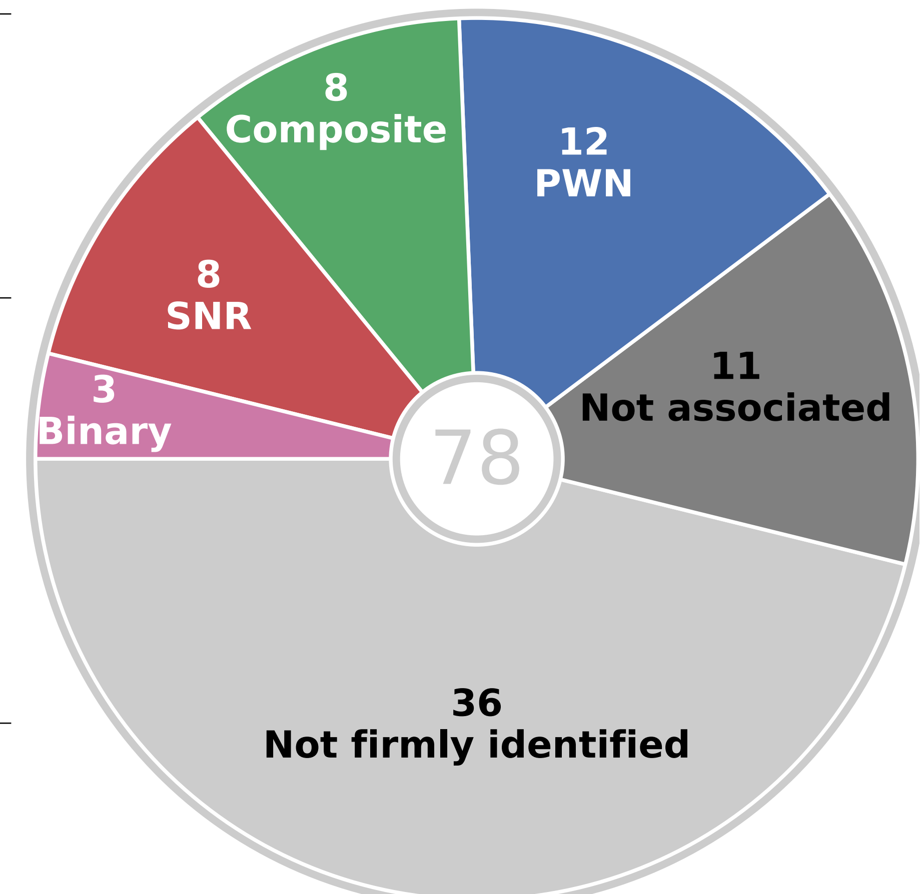

Important finding by HESS in the GC

A proton PeVatron: a machine accelerating particles *up to 10^{15} eV* and beyond presently operates *in R<10 pc* region of the Galactic Center with acceleration rate of protons above energy 10 TeV *at level $10^{37\text{-}38}$ erg/s*

This conclusion is based on *spectroscopic and morphological studies* of *diffuse VHE gamma-ray component* in so-called ~200 pc radius Central Molecular Zone (CMZ) of the GC

✓ for the first time, a gamma-ray spectrum is registered that continues without a cutoff or a break up to 20-30 TeV (most likely, 50 TeV)

✓ for the first time, the density profile of parent protons is derived based on analysis of spatial distributions of VHE gamma-rays and the gas in GC

VHE γ-ray spectra of the diffuse emission and the central source (HESS J1745-290)

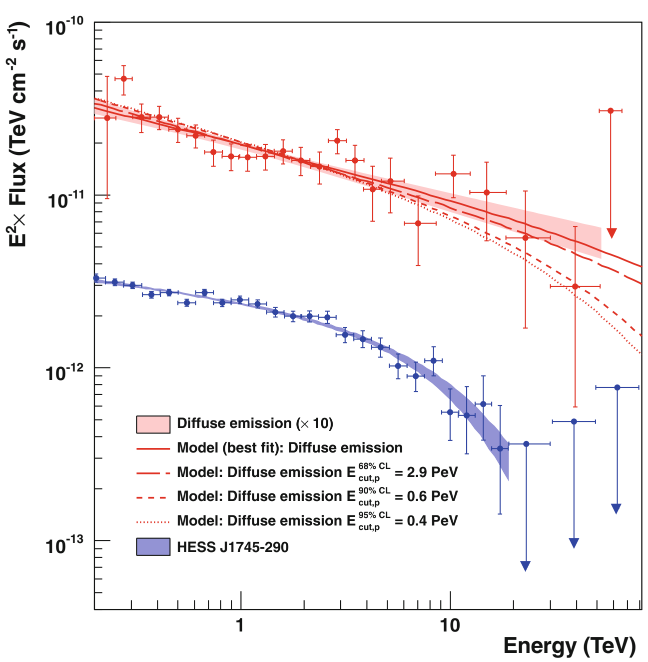

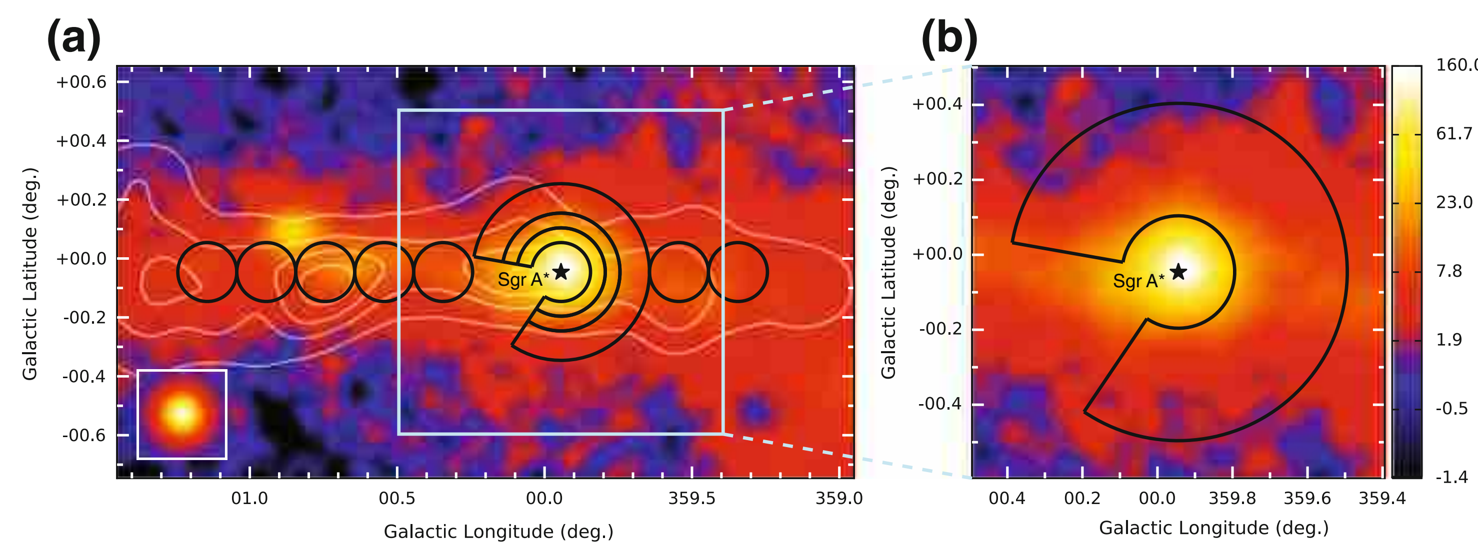

Fig. 17 VHE γ-ray image of the Galactic Centre region (from Ref. [55]). *Left panel* The *black lines* outline the regions used to extract the energy density of CRs. White contours indicate the density distribution of molecular gas. *Right panel* Zoomed view of the inner ~70 pc and the contour of the region used to extract the spectrum of the diffuse emission

Diffuse γ-rays from the Galactic Plane

Diffuse γ-rays are produced by relativistic electrons by bremsstrahlung or inverse Compton scattering on bkg radiation fields, or by protons and nuclei via the decay of π^o produced in *hadronic interactions* with interstellar gas.

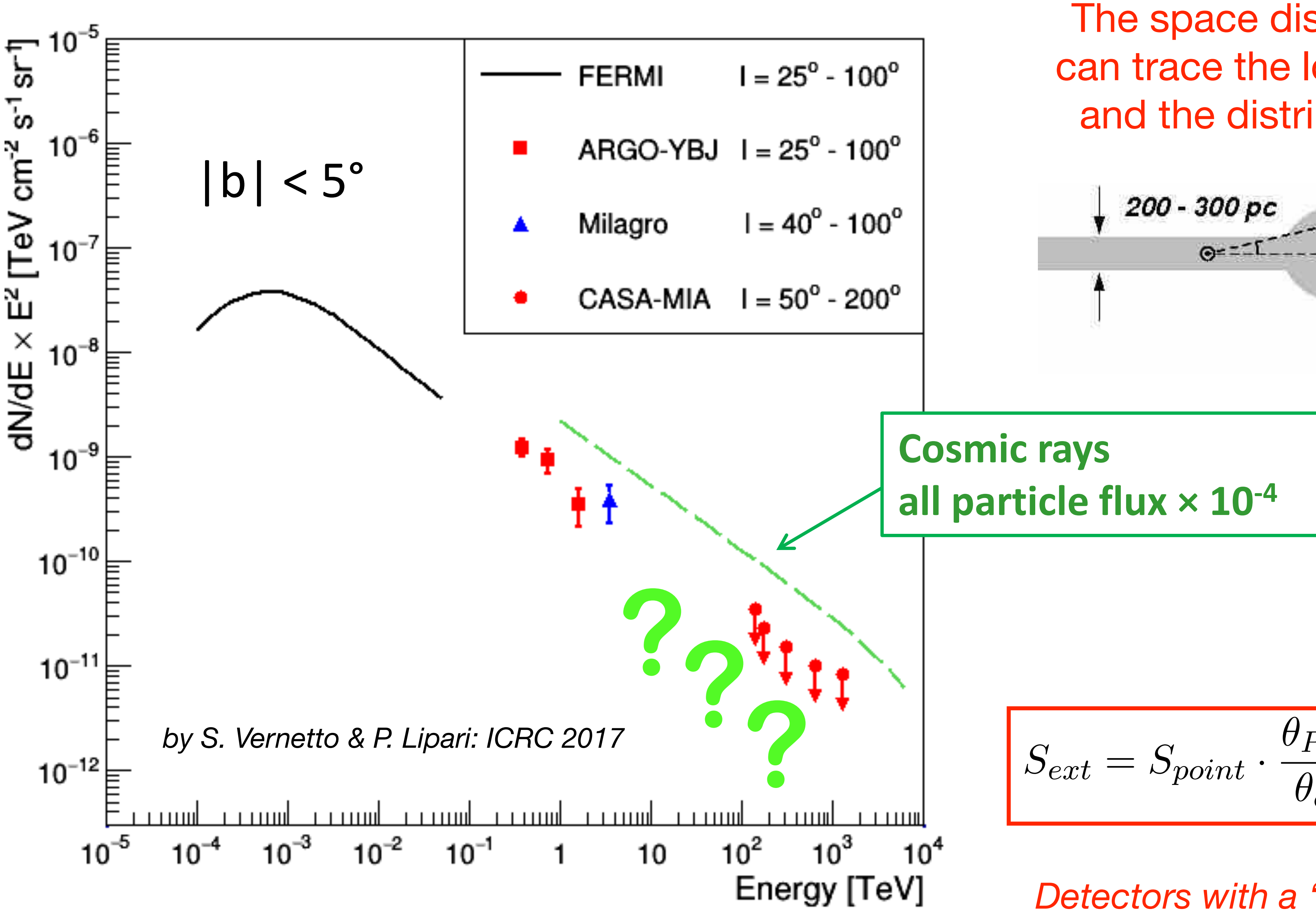

The space distribution of this emission can trace the location of the CR sources and the distribution of interstellar gas.

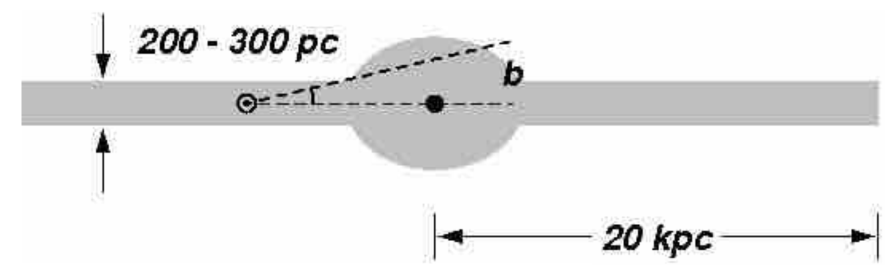

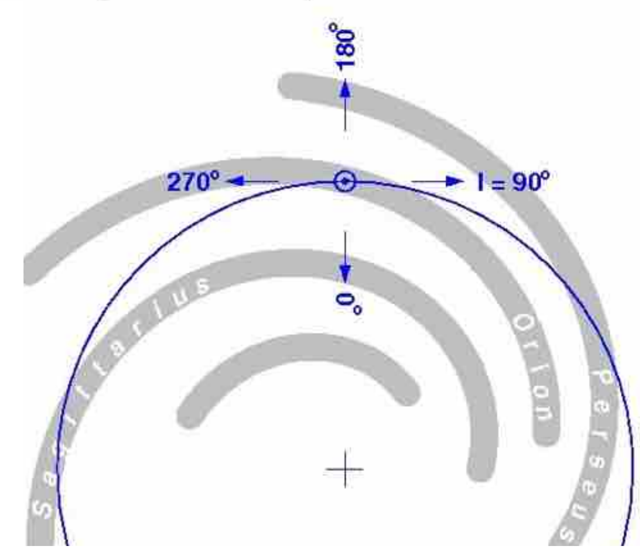

$$S_{ext} = S_{point} \cdot \frac{\theta_{PSF}}{\theta_{ext}}$$

Detectors with a 'poor' angular resolution are favoured in the extended source studies.

Expected Galactic diffuse γ-ray flux

Is the knee a source property, in which case we should see a corresponding spectral feature in the gamma-ray spectra of CR sources, or the result of propagation, so we should observe *a knee that is potentially dependent on location*, because the propagation properties depend on position in the Galaxy ?

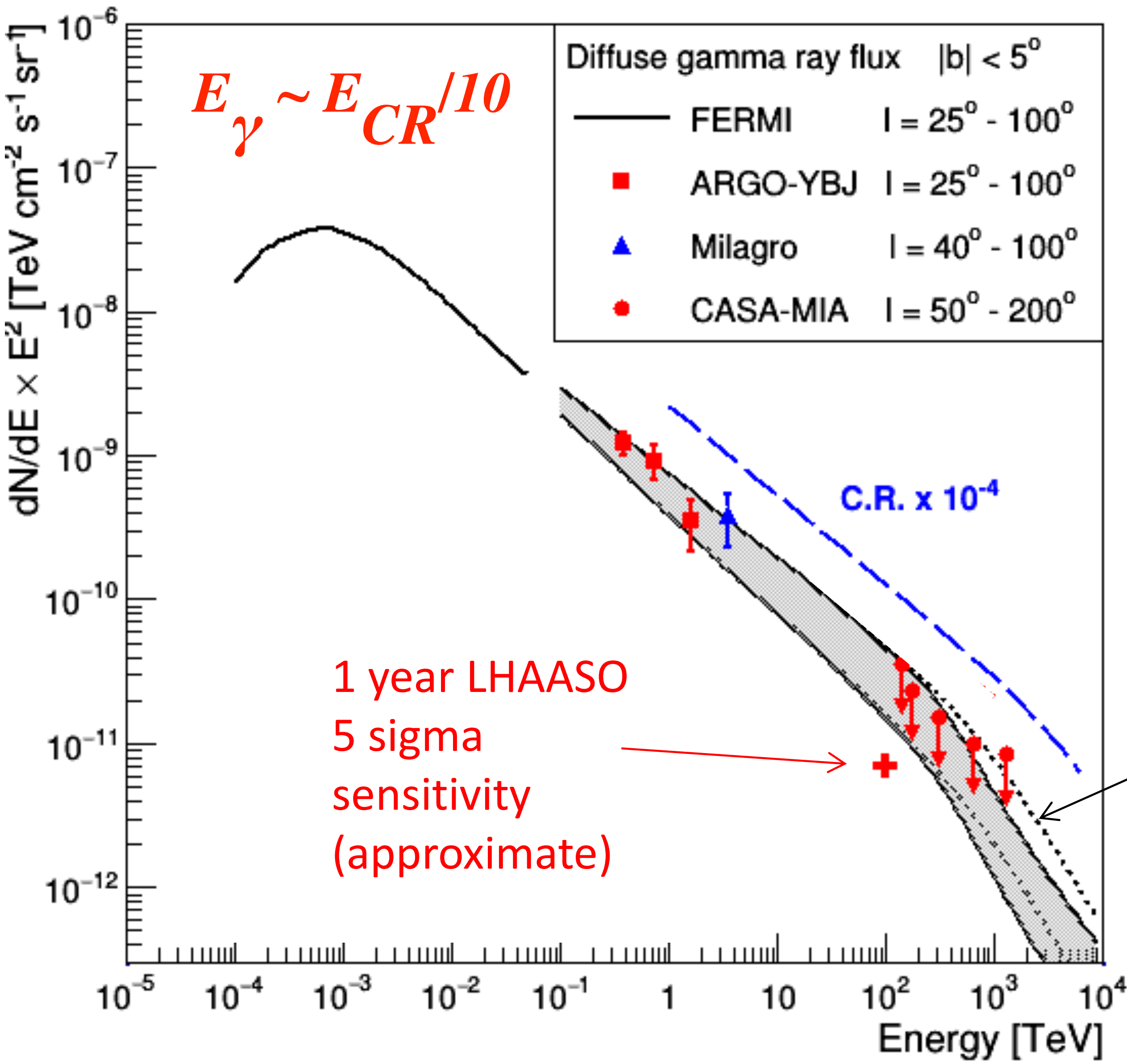

Observing a location dependence of the knee energy (or of the spectral index !) would provide important clues on the nature of the knee.

Grey band: expected γ-ray flux in the region |lat|<5°, long=25°-100°

Unabsorbed flux

Extrapolation of the Fermi spectrum $E^{-2.65\pm0.05}$ with a steepening due to CR knee

by S. Vernetto & P. Lipari: ICRC 2017

Diffuse Gamma Emission

Diffuse gamma-ray emission from the Galactic plane for |b| < 5°

l Intervals	Significance	Spectral index	Energy(GeV)	Flux[a]
$25° < l < 100°$	6.9 s.d.	-2.80 ± 0.26	390	8.06 ± 1.49
			750	1.64 ± 0.43
			1640	0.13 ± 0.05
			1000[b]	0.60 ± 0.13
$40° < l < 100°$	6.1 s.d.	-2.90 ± 0.31	350	10.94 ± 2.23
			680	2.00 ± 0.60
			1470	0.14 ± 0.08
			1000[b]	0.52 ± 0.15
$65° < l < 85°$	4.1 s.d.	-2.65 ± 0.44	440	5.38 ± 1.70
			780	1.13 ± 0.60
			1730	0.15 ± 0.07
			1000[b]	0.62 ± 0.18
$25° < l < 65°$ & $85° < l < 100°$	5.6 s.d.	-2.89 ± 0.33	380	9.57 ± 2.18
			730	1.96 ± 0.59
			1600	0.12 ± 0.07
			1000[b]	0.60 ± 0.17
$130° < l < 200°$	-0.5 s.d.	–	–	< 5.7[c]

[a]In units of 10^{-9} TeV^{-1} cm^{-2} s^{-1} sr^{-1}.

ApJ 806 (2015) 20

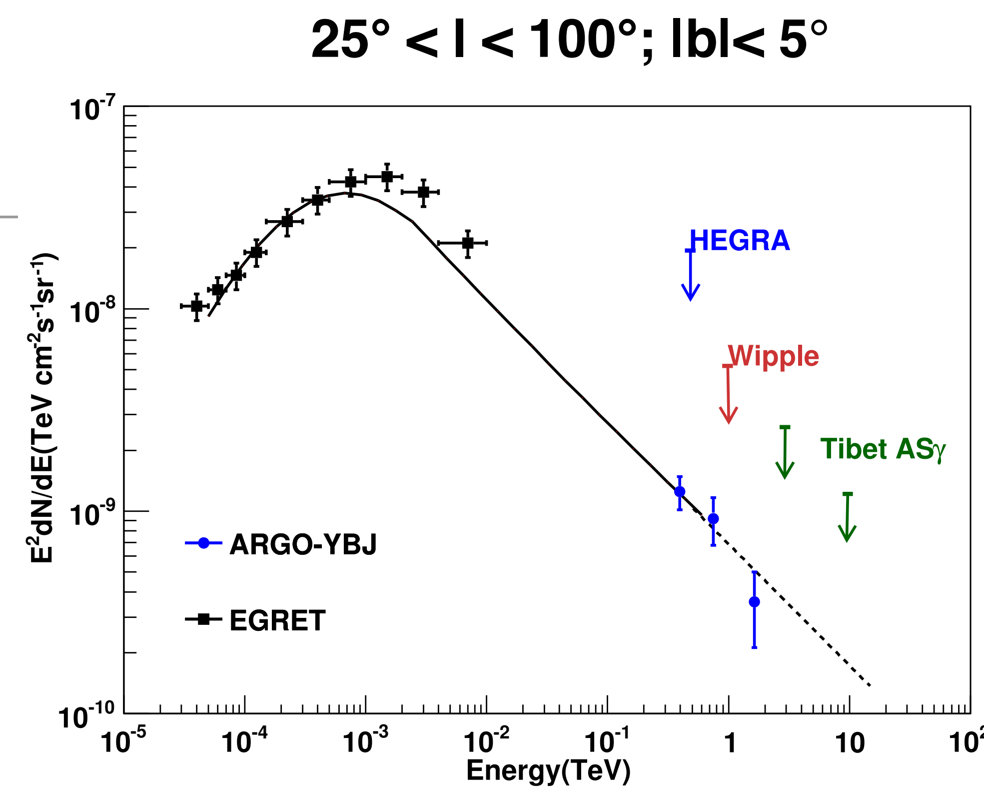

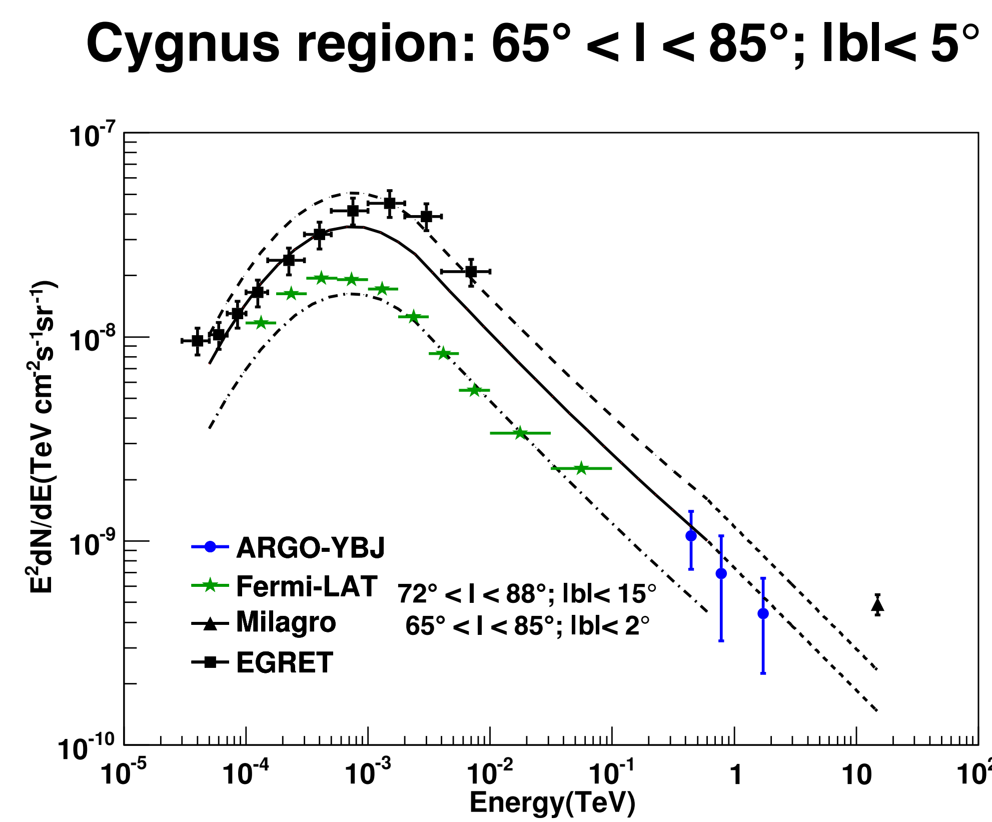

Interestingly, *the energy spectrum of the light component (p+He) up to 700 TeV measured by ARGO-YBJ follows the same spectral shape as that found in the Cygnus region.*

A precise comparison of the spectrum of young CRs, as those supposed in the Cygnus region, with the spectrum of old CRs resident in other places of the Galactic plane, could help to determine the *distribution of the sources of CRs*.

The flaring γ-ray sky: Mrk421

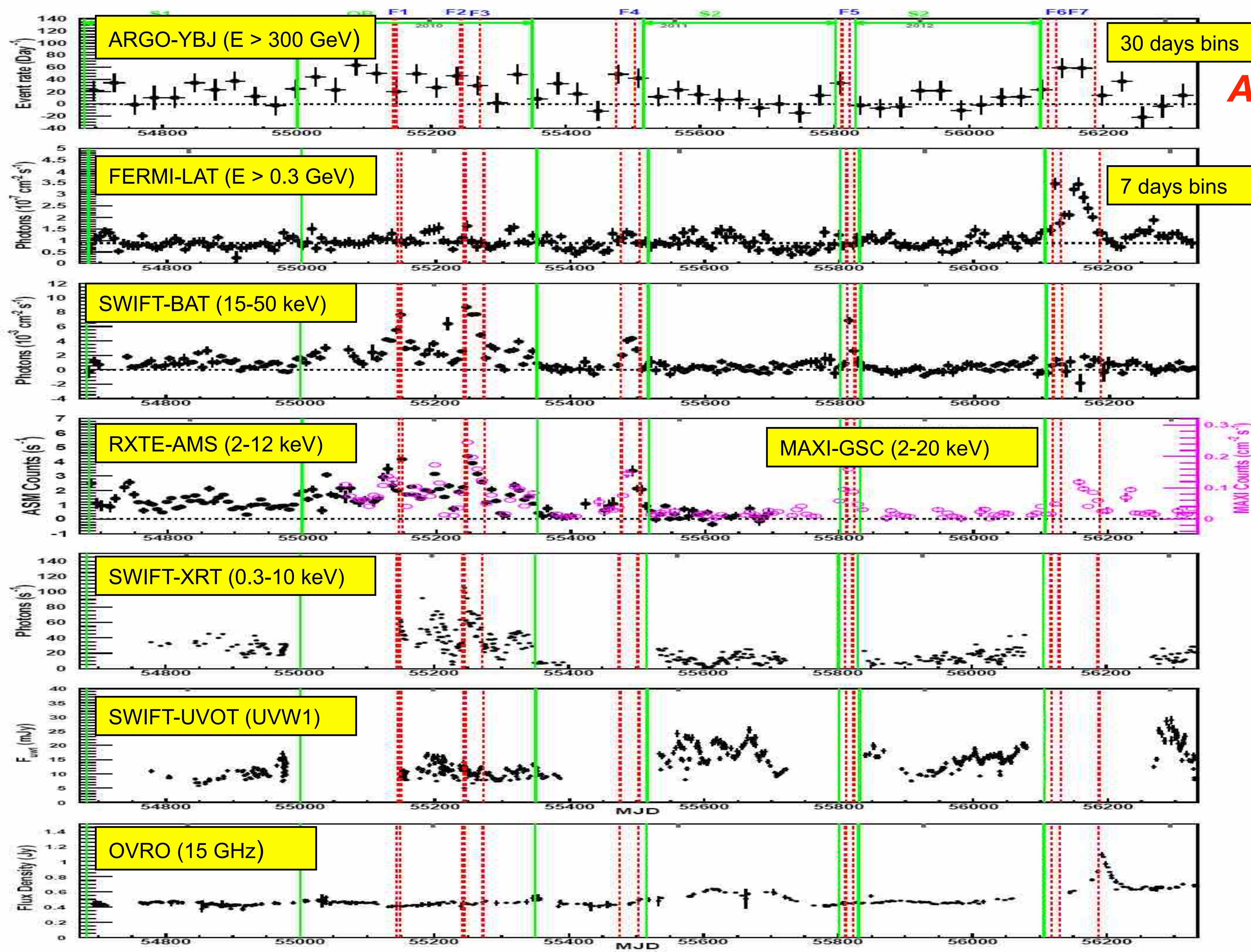

ARGO-YBJ
5 years

One-zone Synchrotron Self-Compton model

Consider a population of relativistic electrons in a magnetized region. They will produce *synchrotron radiation*, and therefore they will fill the region with photons. These synchrotron photons will have some probability to interact again with the electrons, by the *Inverse Compton* process.

Since the *electron "work twice"* (first making synchrotron radiation, then scattering it at higher energies) this particular kind of process is called *synchrotron self–Compton*, or *SSC* for short.

ApJ Supplement, 222 (2016) 6

The *one-zone model* assumes that non-thermal radiations are produced in a single, homogeneous and spherical region in the jet.

The emission region moves relativistically toward us, and consequently the intrinsic radiation is strongly amplified due to the Doppler boosting.

Three parameters are needed to characterise the emission region: the comoving magnetic field, the Doppler factor and the comoving radius of the emission region.

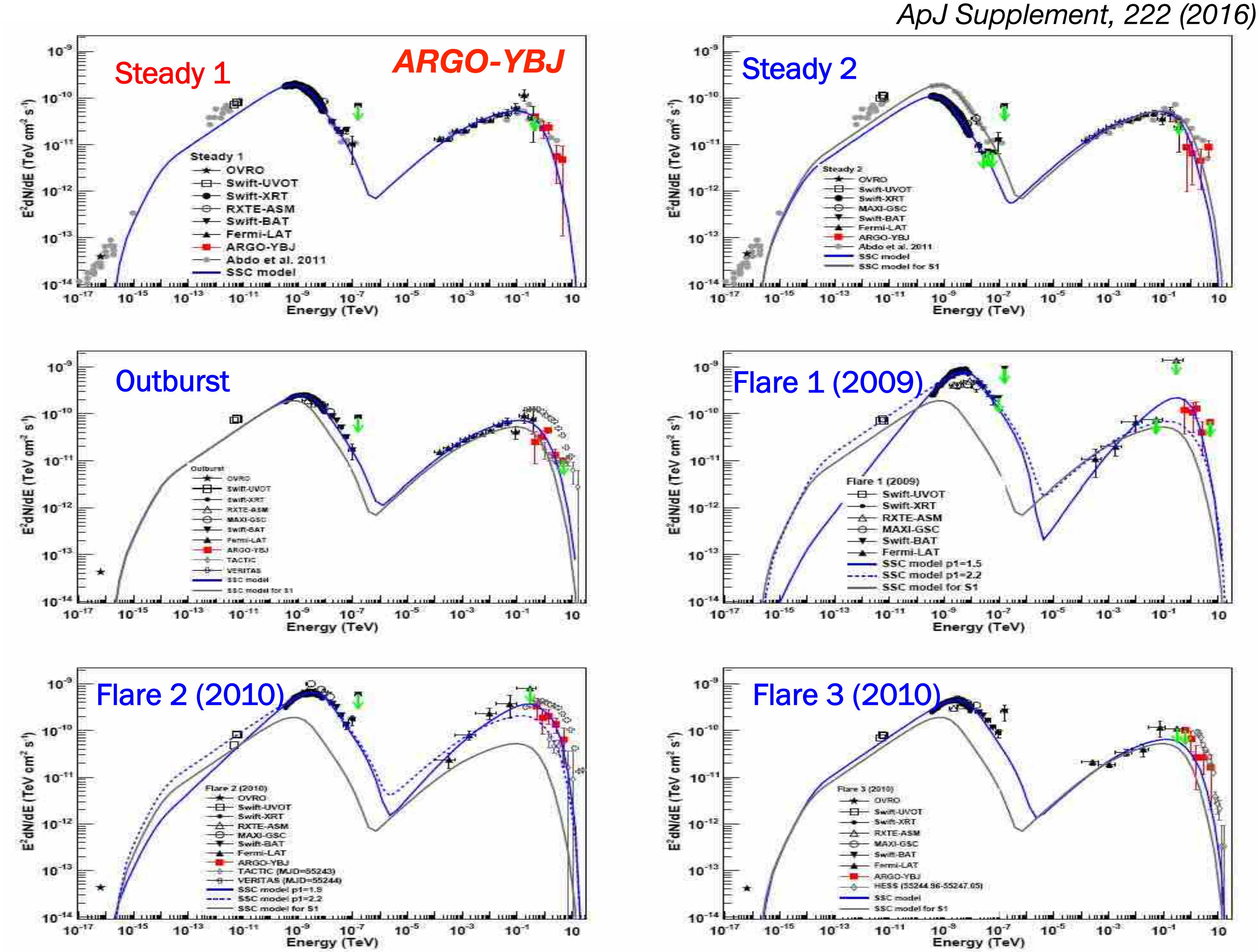

CR energy spectrum: the overall picture

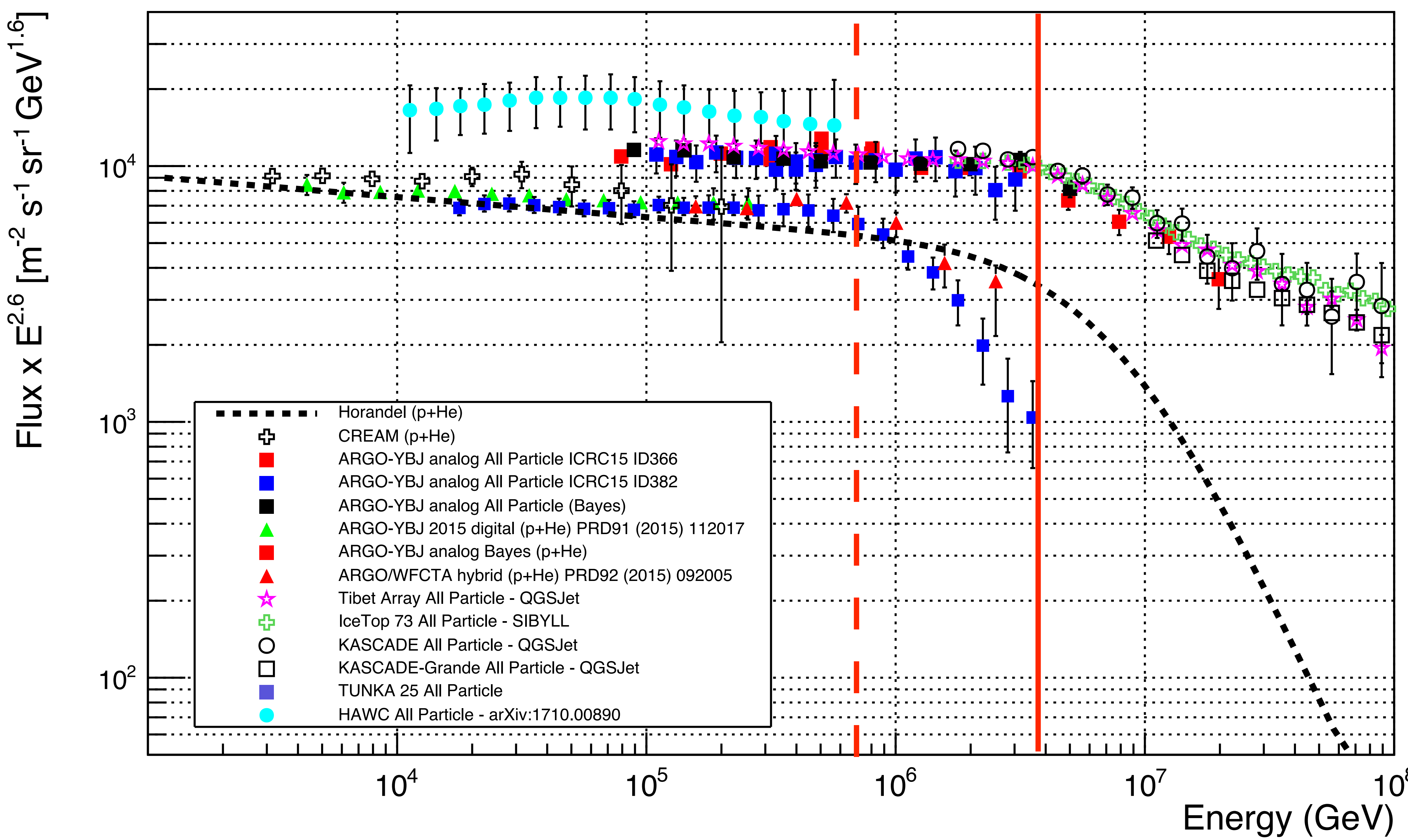

Experimental results in the knee region still conflicting:

ARGO-YBJ reports evidence for a *proton knee starting at about 700 TeV*

The proton knee is connected to the maximum energy of accelerated particles in CR sources !

Full-Sky Cosmic Ray Anisotropy

HAWC

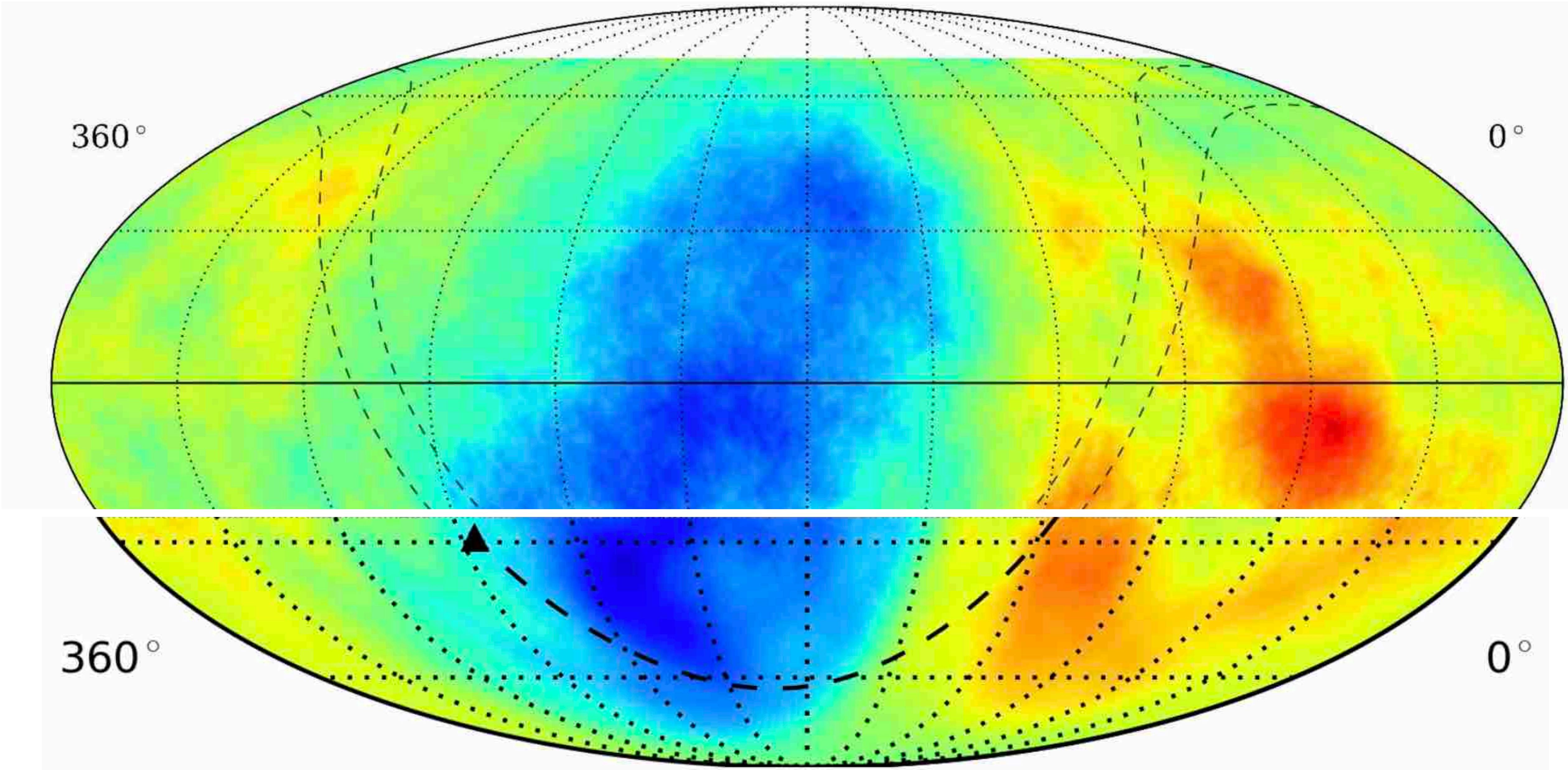

Credit: P. Desiati & J.C. Diaz Velez

IceCube

Cosmic Ray mass dependency ?

Energy dependency (< knee)

Anisotropy depends on primary energy

CR composition changes as well with energy

After IceCube/IceTop observations we know very well the anisotropy in the Southern Hemisphere at different angular scales but…

…we need anisotropy observations vs CR particle rigidity !

A *combined measurement* of CR energy spectrum, mass composition and anisotropy inevitably probes the properties and spatial distribution of their sources as well as of the long propagation journey through the magnetized medium.

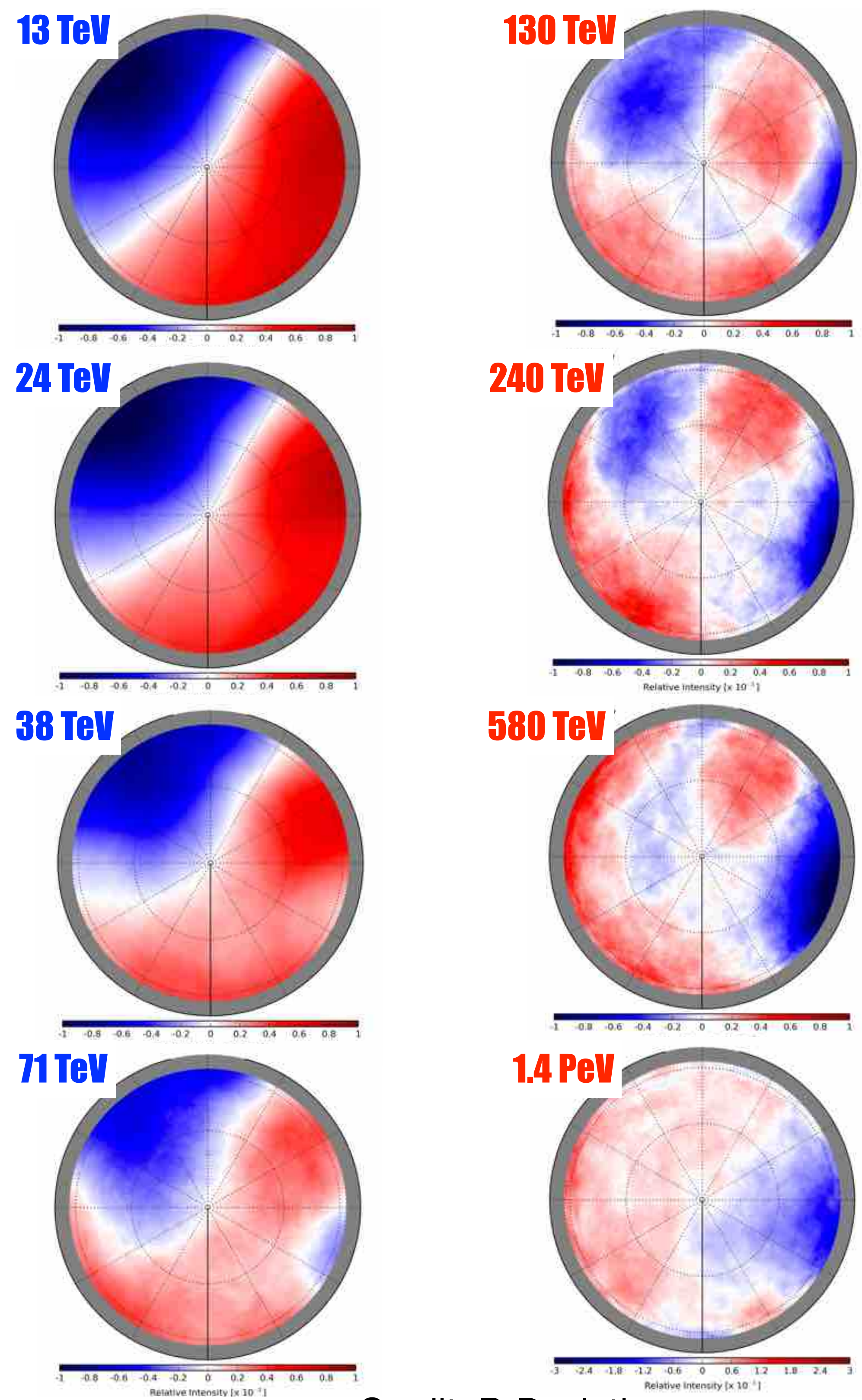

Credit: P. Desiati

CTA and a new Wide FoV observatory

A future Wide FoV Observatory to be useful to CTA needs:

- <10% Crab sensitivity below TeV
- *Low energy threshold* (≈ 100 GeV)
- Ability to detect extragalactic transient (AGN, GRBs)
- *Southern hemisphere site*

★ Is this possible ?

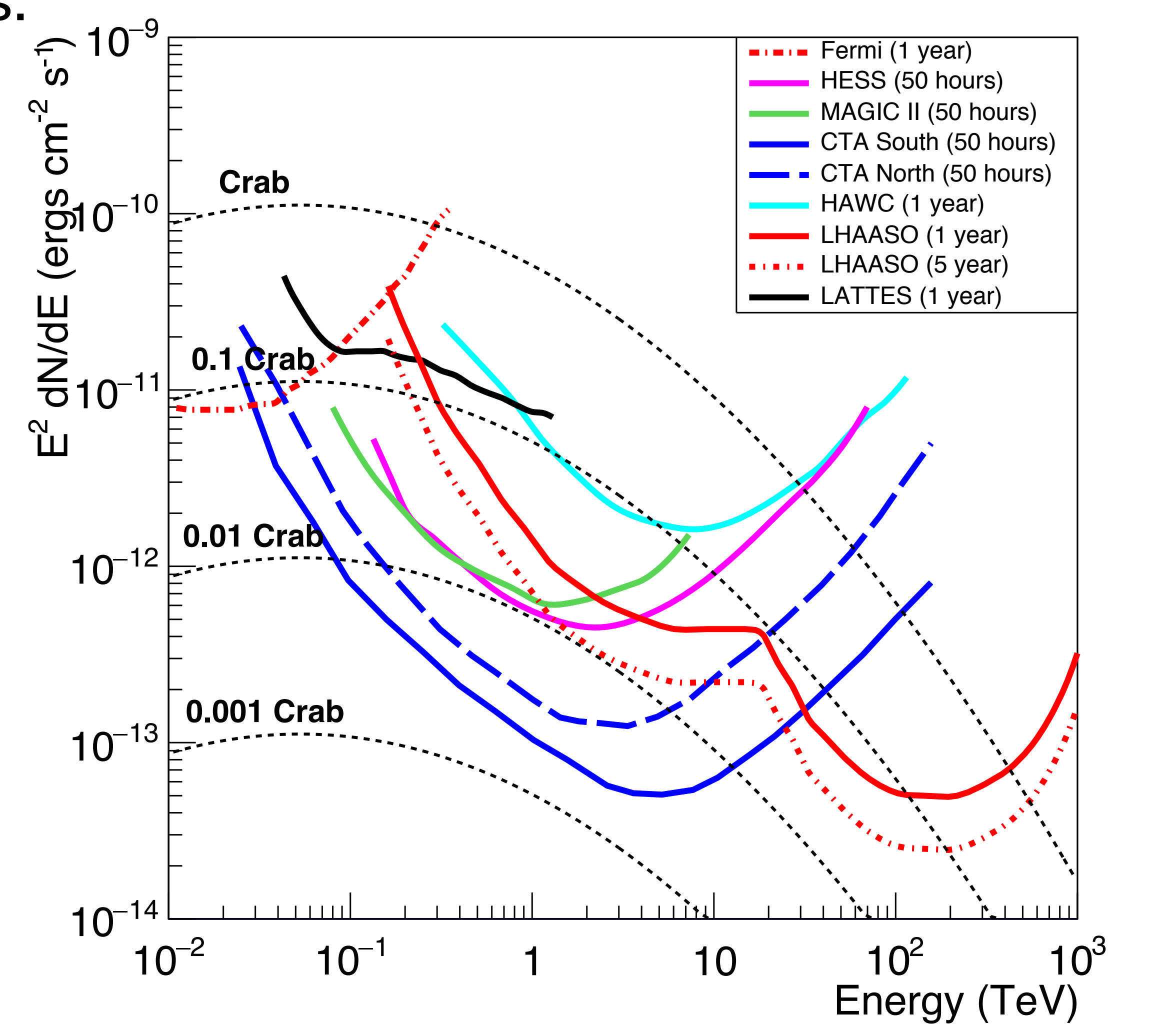

Minimum Detectable Gamma-Ray Flux (1 year):

$$\boxed{\Phi_\gamma^{MDF} \propto \sqrt{\Phi_B} \cdot \frac{1}{R \cdot \sqrt{A_{eff}^\gamma}} \cdot \psi_{70} \cdot \frac{1}{Q_f}}$$

Φ_B = background flux

ψ_{70} = opening angle

$A_{eff}^{\gamma,p}(E)$ = effective area

$$\boxed{R = \sqrt{\frac{A_{eff}^\gamma(E)}{A_{eff}^B(E)}}}$$

$$\boxed{Q_f = \frac{\text{fraction of surviving photons}}{\sqrt{\text{fraction of surviving hadrons}}}}$$

The key parameters

$$S \propto \frac{\Phi_\gamma}{\sqrt{\Phi_{bkg}}} \cdot R \cdot \sqrt{A^{\gamma}_{eff}} \cdot \frac{1}{\sigma_\theta} \cdot Q$$

For the integral fluxes we can write $\Phi_\gamma \sim E_{thr}^{-\gamma}$, $\Phi_{bkg} \sim E_{thr}^{-\gamma_{bkg}}$ and we obtain $\frac{\Phi_\gamma}{\sqrt{\Phi_{bkg}}} \sim E_{thr}^{-(\gamma-\gamma_{bkg}/2)} \sim E_{thr}^{-2/3}$

being $\gamma \sim 1.5$ and $\gamma_{bkg} \sim 1.7$.

The *key parameters* to improve the sensitivity are

- The energy threshold
- R, the signal/background relative trigger efficiency
- The angular resolution
- Q-factor, the background rejection capability

Milagro vs ARGO-YBJ

2 different approaches in the last decade for ground-based survey instruments

Milagro
Water Cherenkov Technology

- operated from 2000 to 2008
- *2600 m* above sea level
- angular resolution ≈0.5°
- 1700 Hz trigger rate
- *Median Energy at the threshold: ≈ 2 TeV*
- *Energy range: 2 - 40 TeV*
- poor background rejection via muons
- conversion of secondary photons in water

Widely used technology in cosmic ray physics

ARGO-YBJ
Resistive Plate Chamber Technology

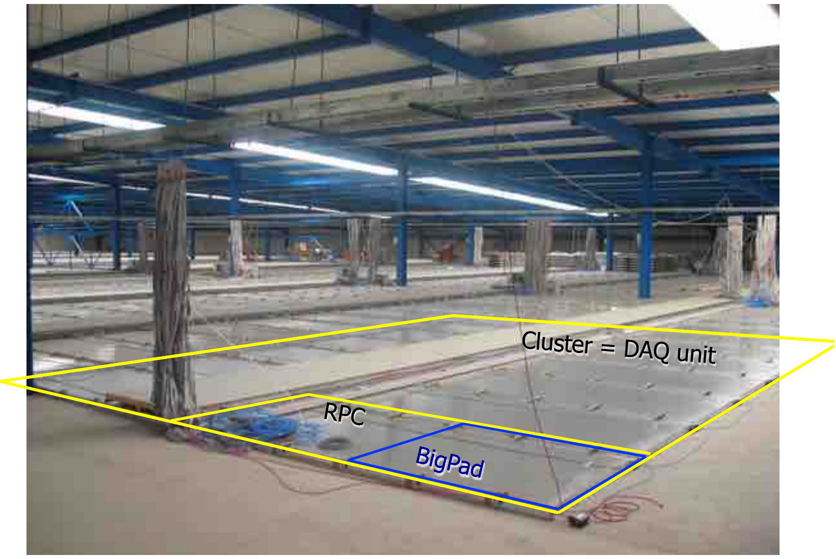

- operated from 2007 to 2012 (final configuration)
- *4300 m* above sea level
- angular resolution ≈0.5°
- 3500 Hz trigger rate
- high granularity of the readout
- *Median Energy at the threshold: ≈360 GeV*
- *Energy Range: 360 GeV - 10 PeV*
- NO background rejection (no muons identification)
- NO conversion of secondary photons (no lead)

Widely used technology in accelerator physics

Milagro vs ARGO-YBJ

Milagro
Water Cherenkov Technology

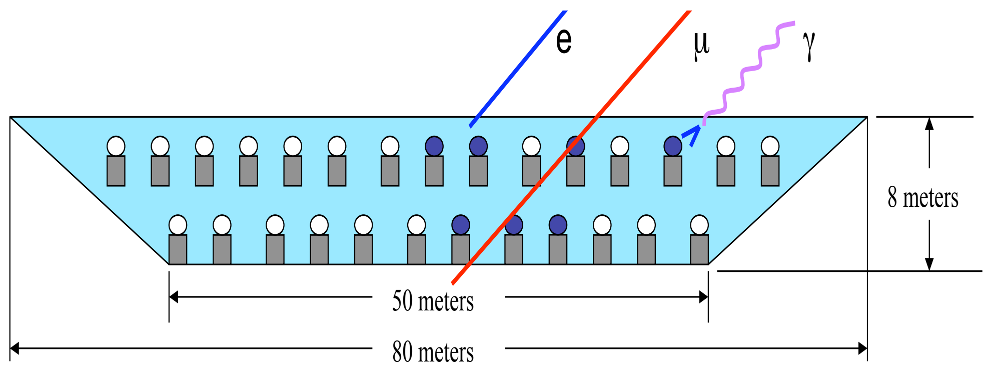

Central 80 m x 60 m x 8 m water reservoir, containing two layers of PMTs

- 450 PMTs at 1.4 m below the surface (top layer)
- 273 PMTs at 6 m below the surface (bottom layer)

Outrigger Array, consisting of 175 tanks filled with water and containing one PMT, distributed on an area of 200 m x 200 m around the central water reservoir.

→ ***HAWC*** and ***LHAASO***

ARGO-YBJ
Resistive Plate Chamber Technology

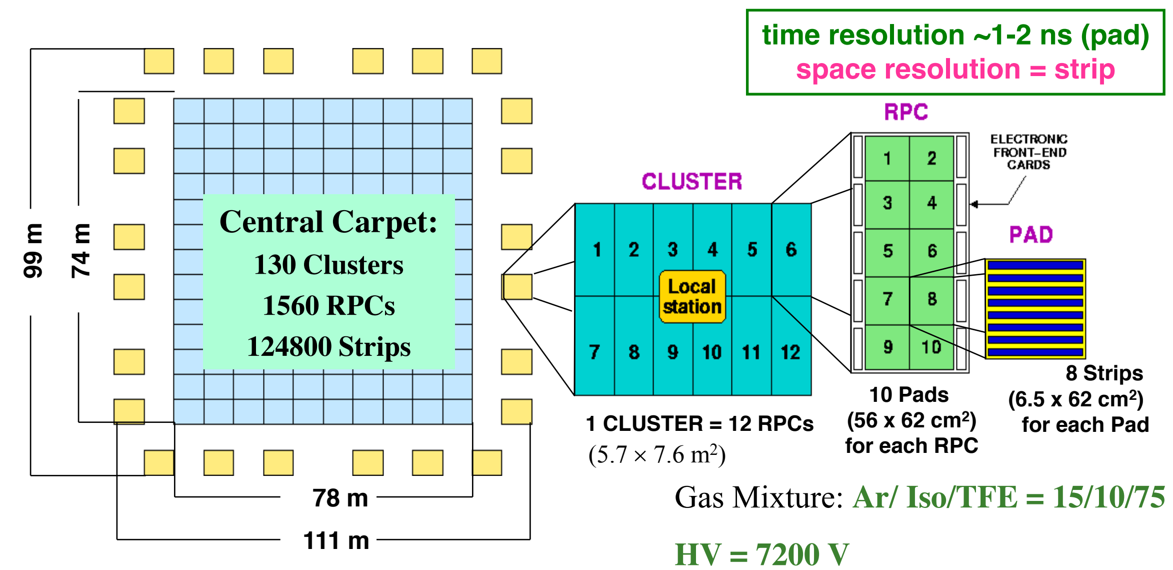

Single layer of Resistive Plate Chambers (RPCs) with a full coverage (92% active surface) of a large area (5600 m^2) + sampling guard ring (6700 m^2 in total)

Space pixels: *146,880 strips* (7×62 cm^2)
Time pixels: *18,360 pads* (56×62 cm^2)

2 read-outs:

$$\rho_{max-strip} \approx 20\ particles/m^2$$

$$\rho_{max-analog} \approx 10^4\ particles/m^2$$

→ ***MATHUSLA*** proposal, CR and hadronic physics at CERN (RPC carpet above ATLAS)

Shower detection by ARGO-YBJ

Small and compact events

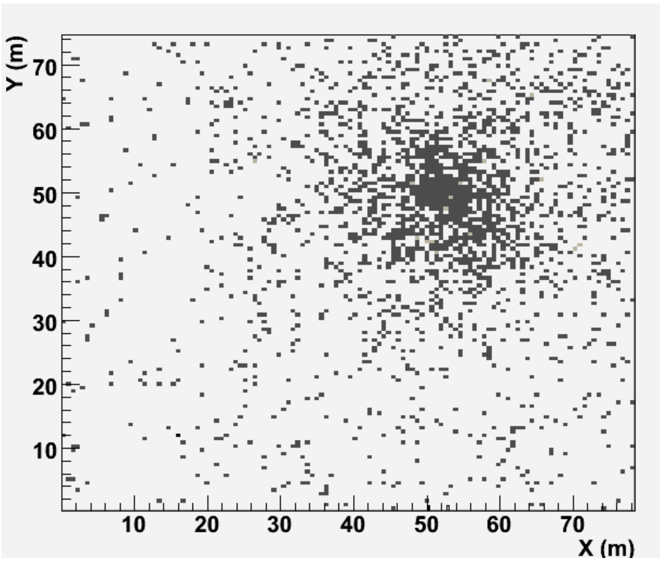

Fired pads on the carpet

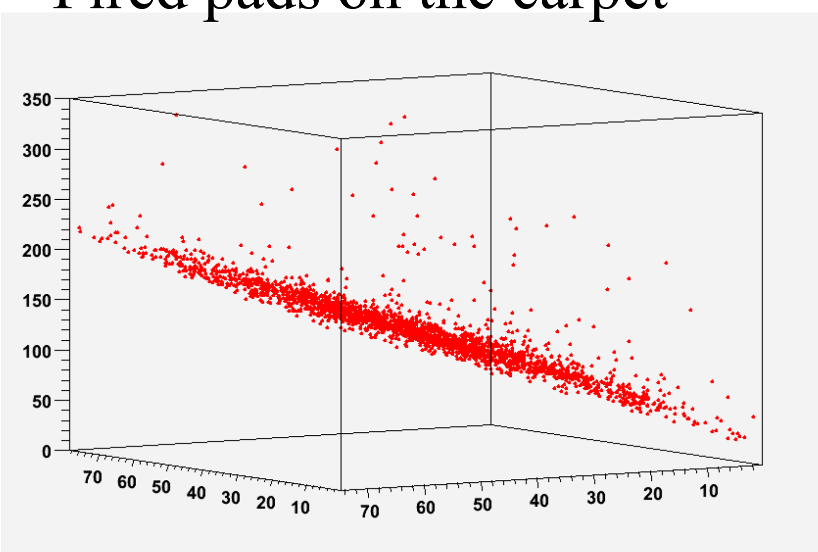

Arrival time vs position

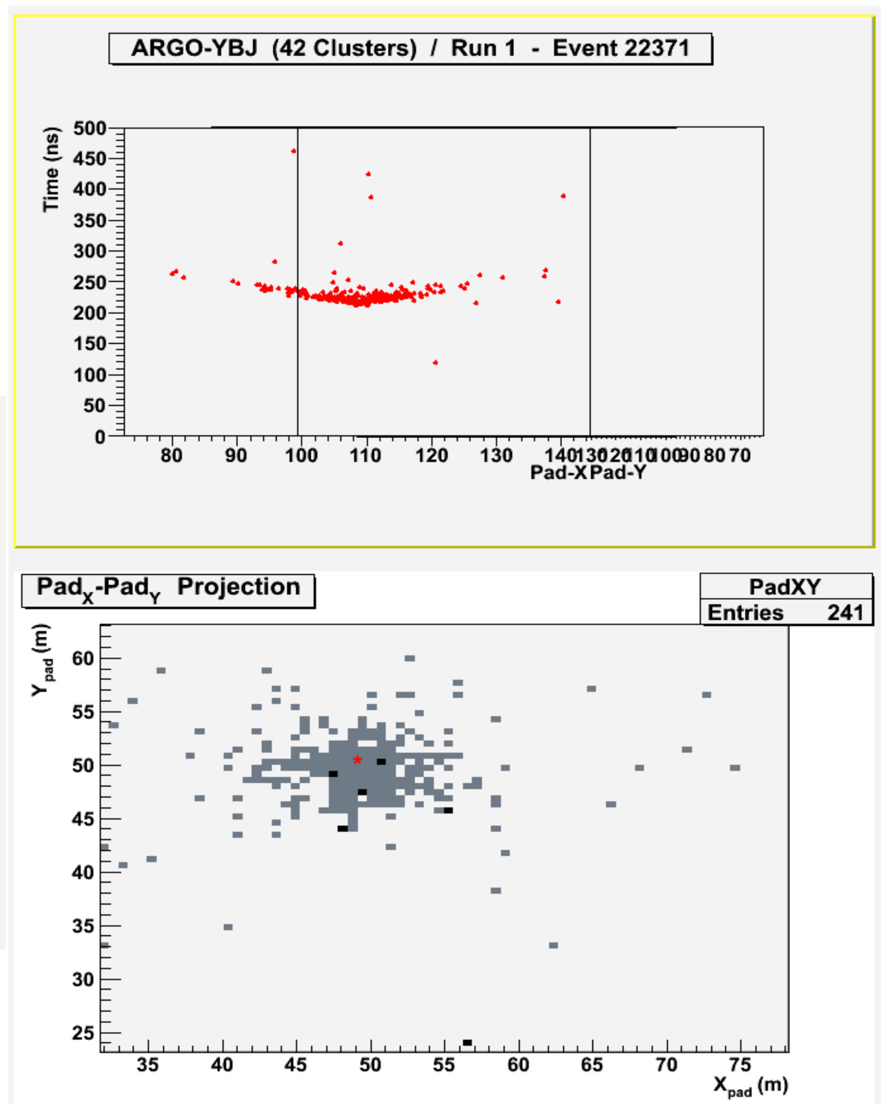

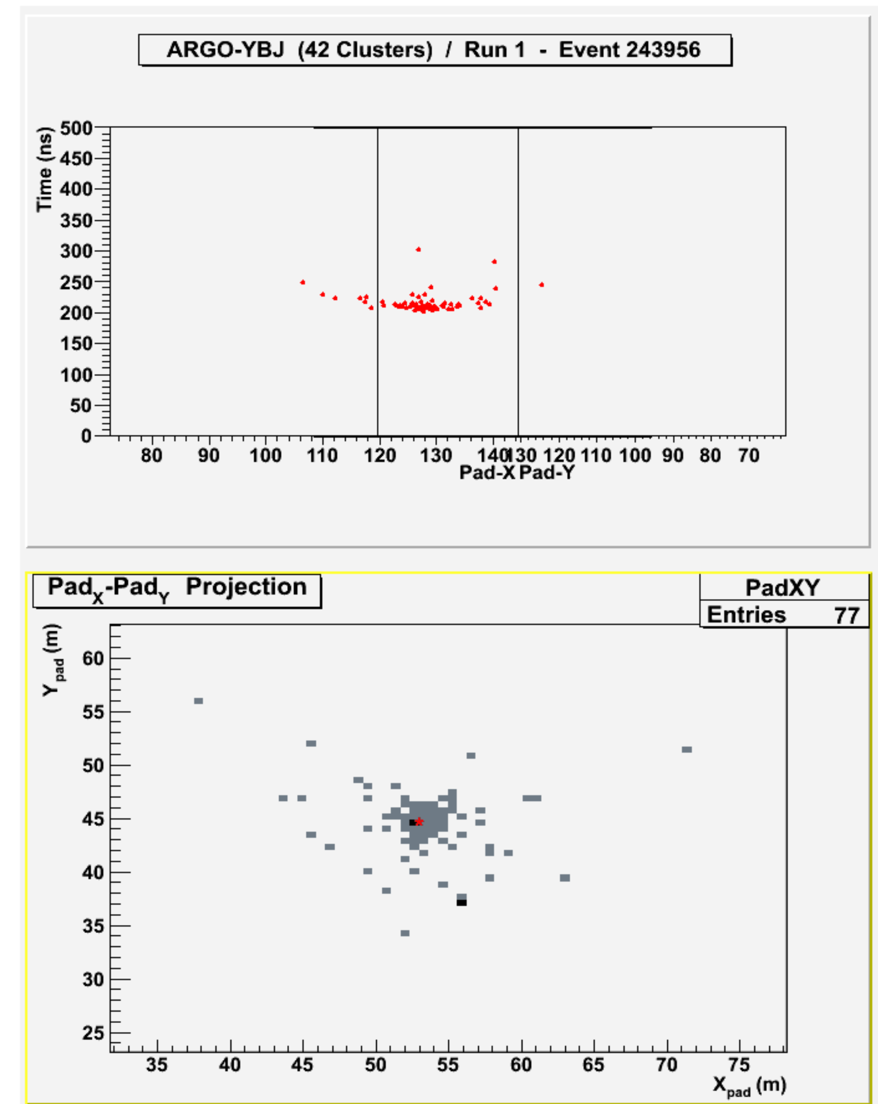

Scientific results

Milagro

Water Cherenkov Technology

- Gamma-ray Astronomy
- CR anisotropy
- *No results on selection of different primary masses and spectra of different elements*

ARGO-YBJ

Resistive Plate Chamber Technology

- Gamma-ray Astronomy
- CR anisotropy
- All-particle energy spectrum up to the knee
- Study of the shower core region
- Selection of light component (p+He) and *observation of the proton knee*

HAWC

Water Cherenkov Technology

- Gamma-ray Astronomy
- CR anisotropy
- All-particle energy spectrum
- *Still no results on the selection of different primary masses*

→ *The capability of Water Cherenkov facilities in extending the energy range to PeV and in selecting primary masses at the knee must be investigated*

Lowering the energy threshold: extreme altitude

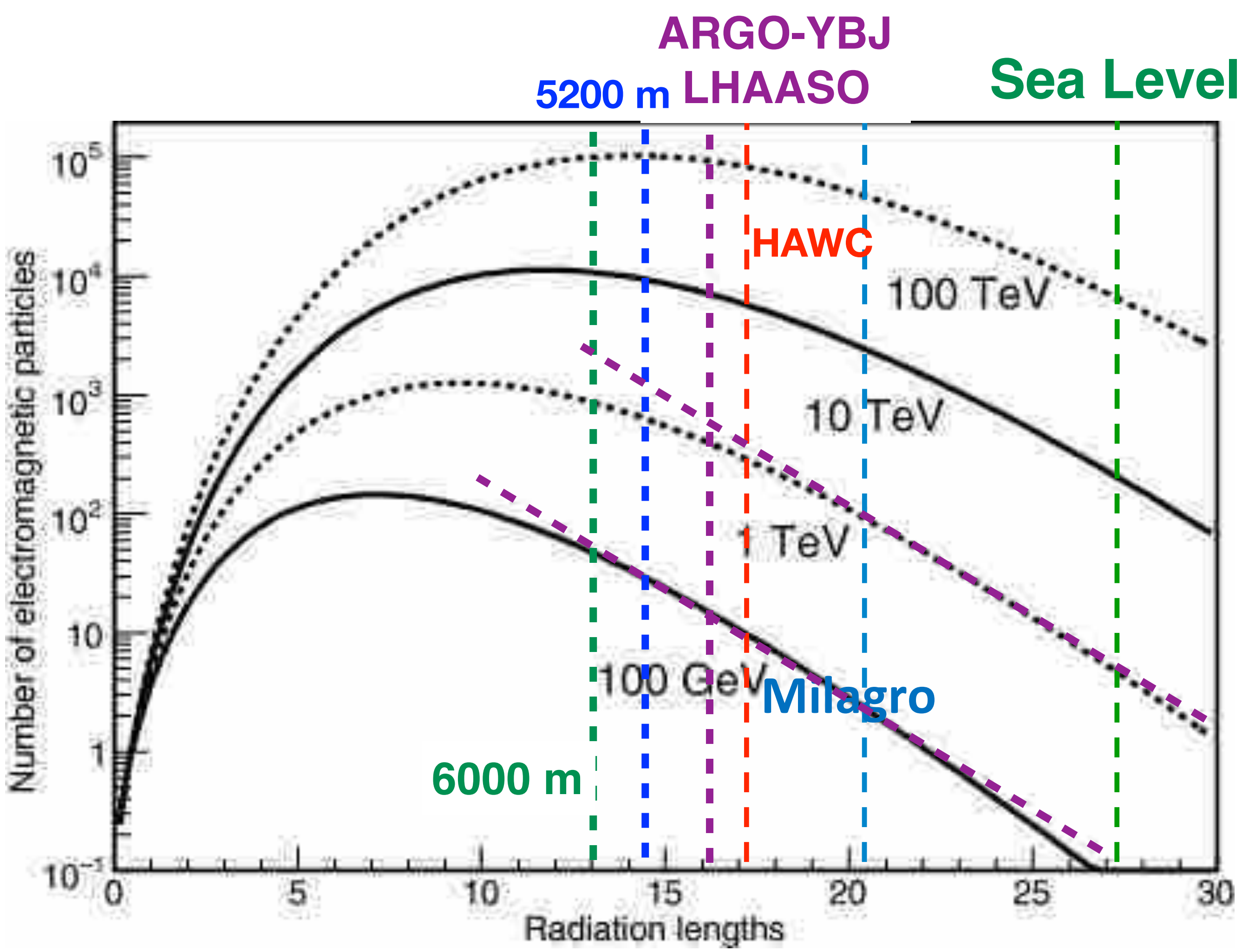

Showers of all energies have the same slope after shower maximum: ≈1.65x decrease per r.l. .
So, for all energies, if a detector is located one radiation length higher in atmosphere, the result will be a ≈1.65x decrease in the energy observable.

Lowering the energy threshold:

- *Extreme altitude (≈5000 m asl)*
- *Detector and layout*
- *Coverage and granularity of the read-out*
- *Trigger logic*
- *Detection of secondary photons*

This imply that the effective areas of EAS detectors increases at low energies.

The full coverage approach

ARGO-YBJ is a high altitude full coverage EAS-array
optimized for the detection of small size air showers.

ARGO-YBJ central carpet

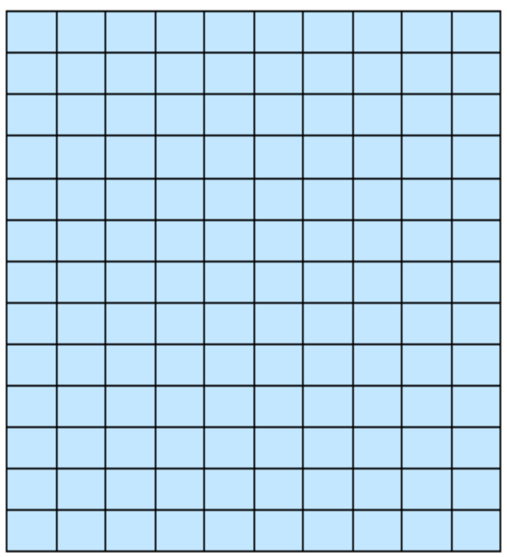

a continuous carpet of detectors
coverage factor ≈ 0.92

sparse array

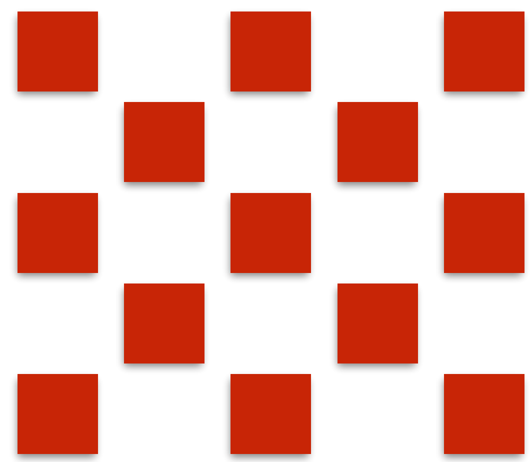

coverage factor ≈ 10^{-3} - 10^{-2}

The full coverage approach

ARGO-YBJ is a high altitude full coverage EAS-array
optimized for the detection of small size air showers.

ARGO-YBJ central carpet

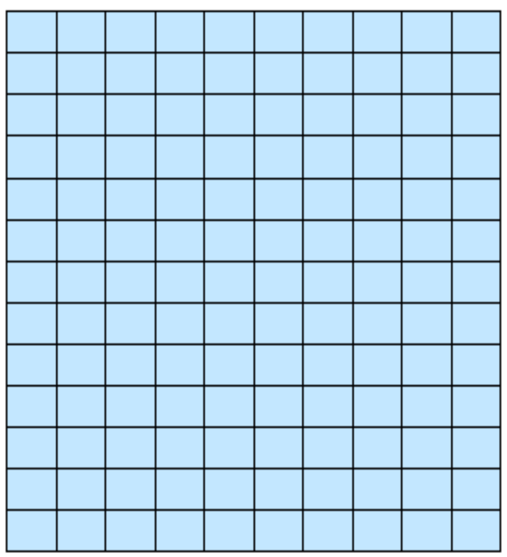

a continuous carpet of detectors
coverage factor ≈ 0.92

sparse array

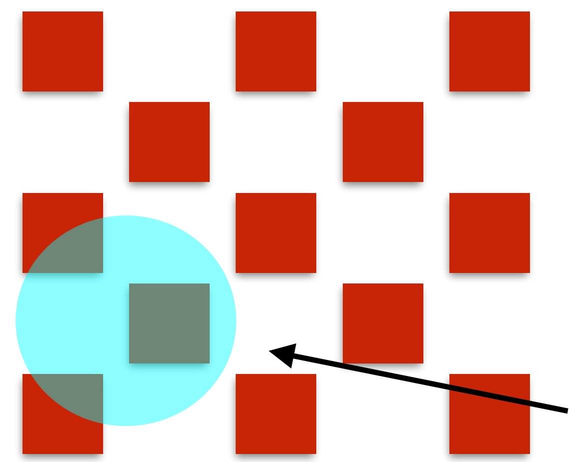

high energy shower = big shower
➔ trigger

coverage factor ≈ 10^{-3} - 10^{-2}

The full coverage approach

ARGO-YBJ is a high altitude full coverage EAS-array
optimized for the detection of small size air showers.

ARGO-YBJ central carpet

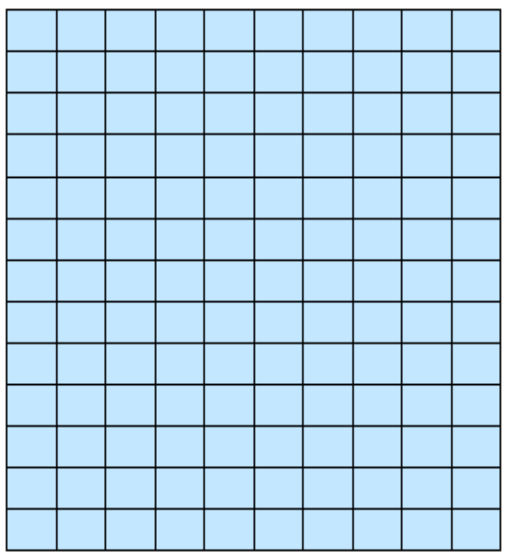

a continuous carpet of detectors
coverage factor ≈ 0.92

sparse array

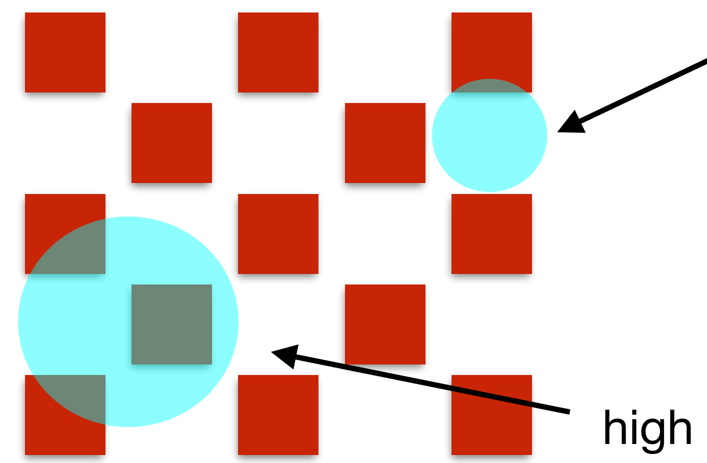

low energy shower = small shower
➔ NO trigger

high energy shower = big shower
➔ trigger

coverage factor ≈ 10^{-3} - 10^{-2}

The full coverage approach

ARGO-YBJ is a high altitude full coverage EAS-array
optimized for the detection of small size air showers.

ARGO-YBJ central carpet

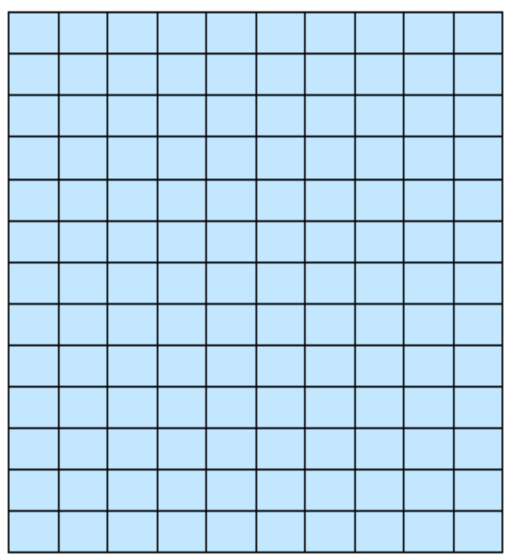

a continuous carpet of detectors
coverage factor ≈ 0.92

sparse array

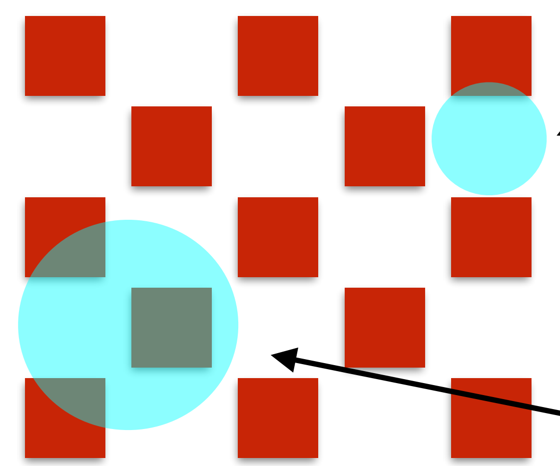

low energy shower = small shower
➔ NO trigger

high energy shower = big shower
➔ trigger

coverage factor ≈ 10^{-3} - 10^{-2}

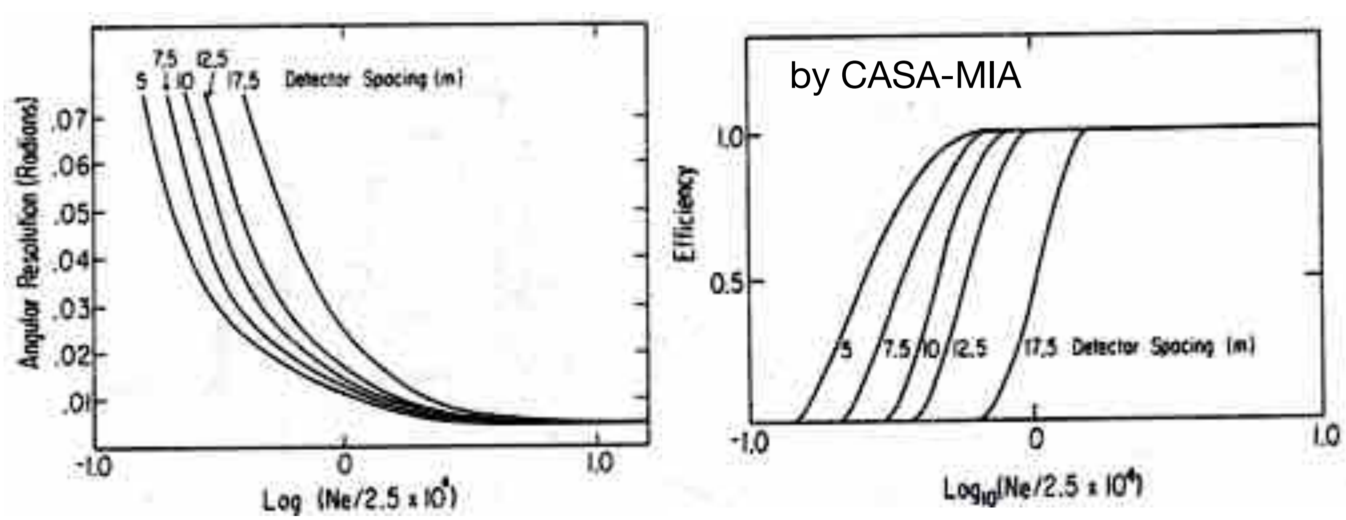

Increasing the sampling (~1% ➔100%)

- Improves angular resolution
- Lowers energy threshold

Energy threshold

ARGO-YBJ

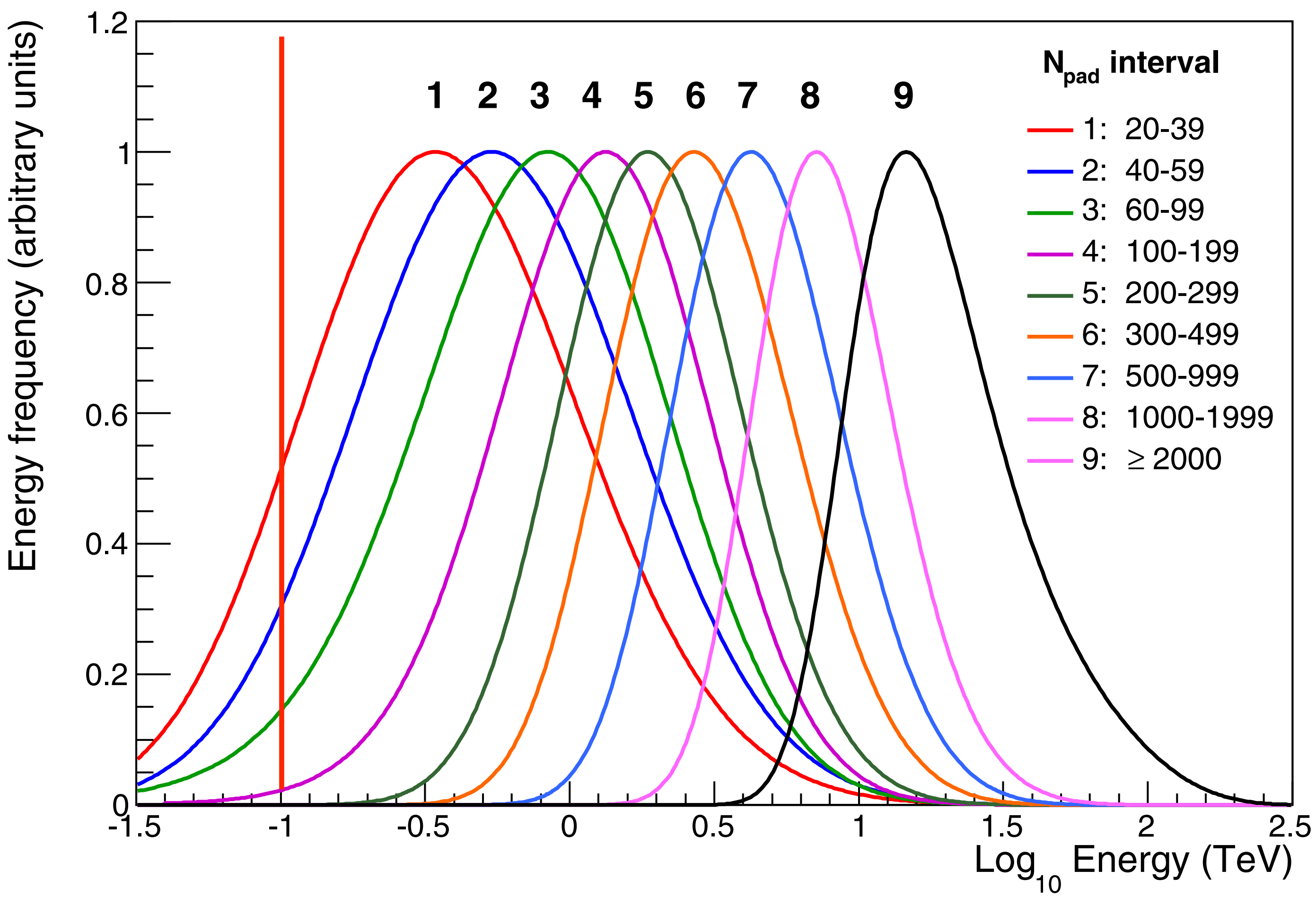

full coverage RPC carpet operated at 4300 m asl

coverage ≈ 92%

high granularity (cm level)

Topological-based Trigger logic;

>20 pads out of 15,000 bkg free !

Median energy first bin = 360 GeV

HAWC (2017)

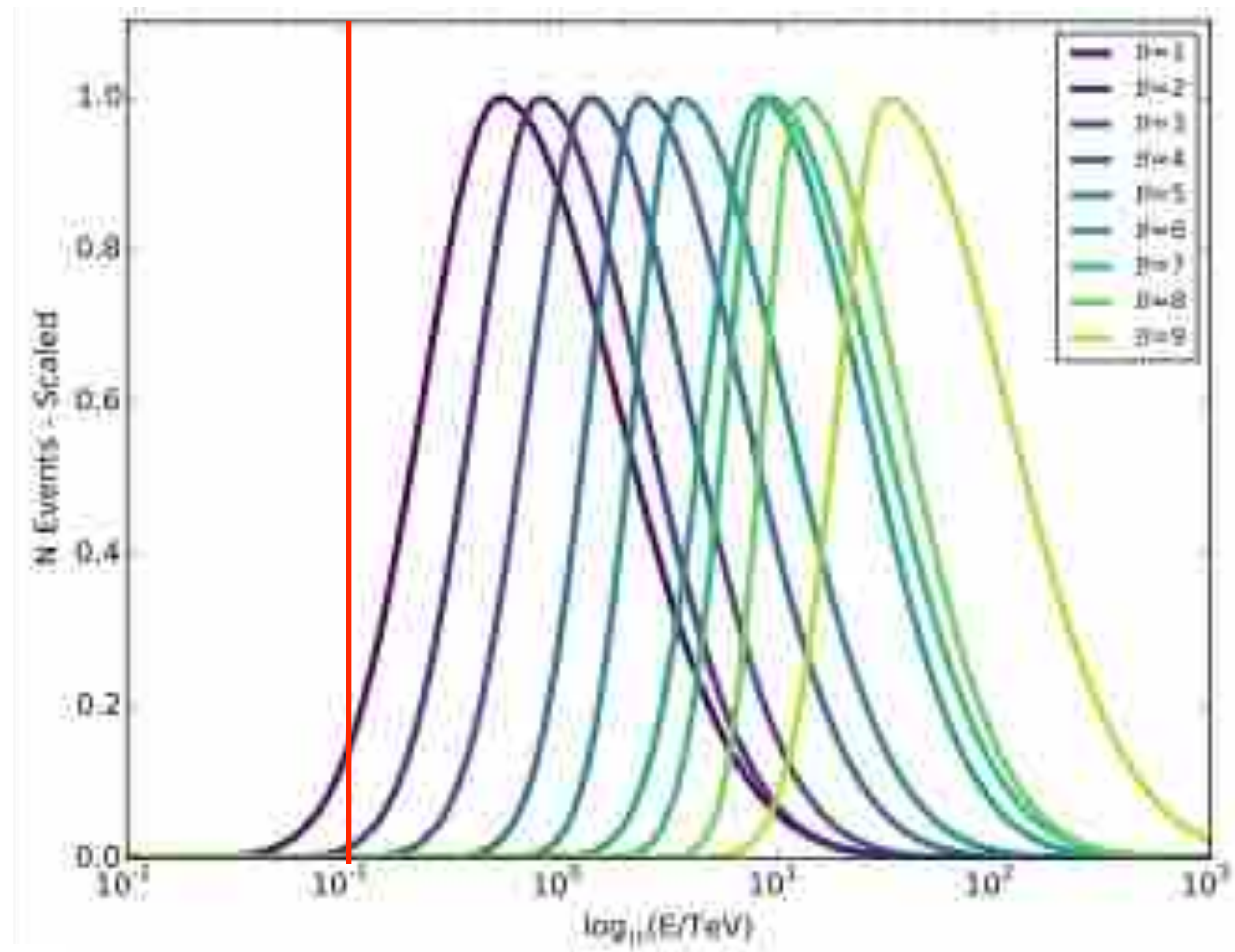

array of water tanks operated at 4100 m asl

coverage ≈ 60%

poor granularity (m level)

free running

Median energy first bin = 700 GeV

Extreme Altitude

1. *All nuclei produce showers with similar size* $N^{A}_{e,\max} \approx N^{p}_{e,\max}$
2. *Unbiased trigger threshold* for all nuclei
3. Primary *energy reconstruction mass-independent* $Ne(E_0, A) = \alpha(A) \cdot E^{\beta(A)}$
4. *Small fluctuations:* shower maximum
5. *Low energy threshold:* absolute energy scale calibration with the Moon

   Shadow technique and overposition with direct measurements
6. Trigger probability larger for γ-showers than for p-showers

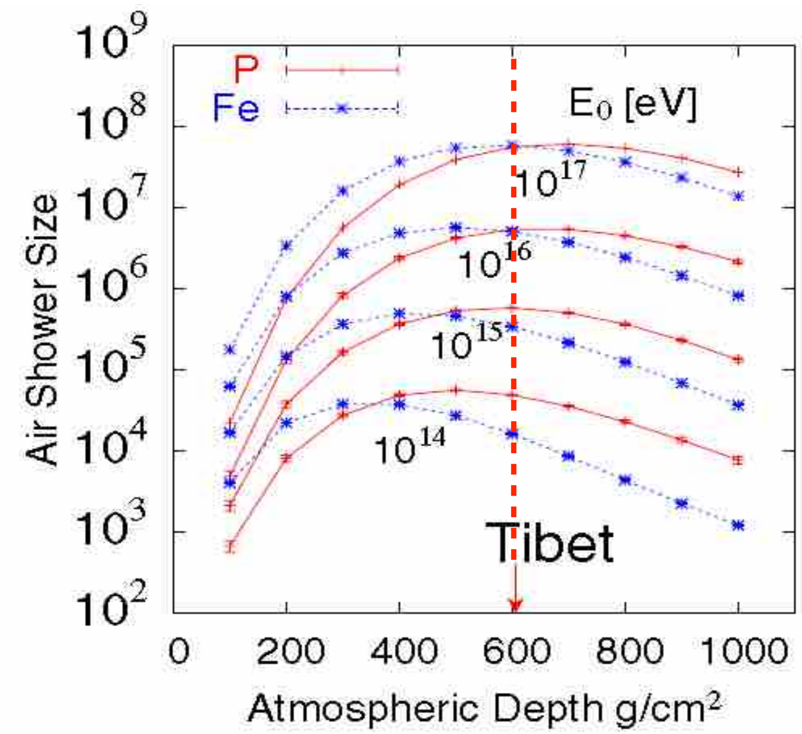

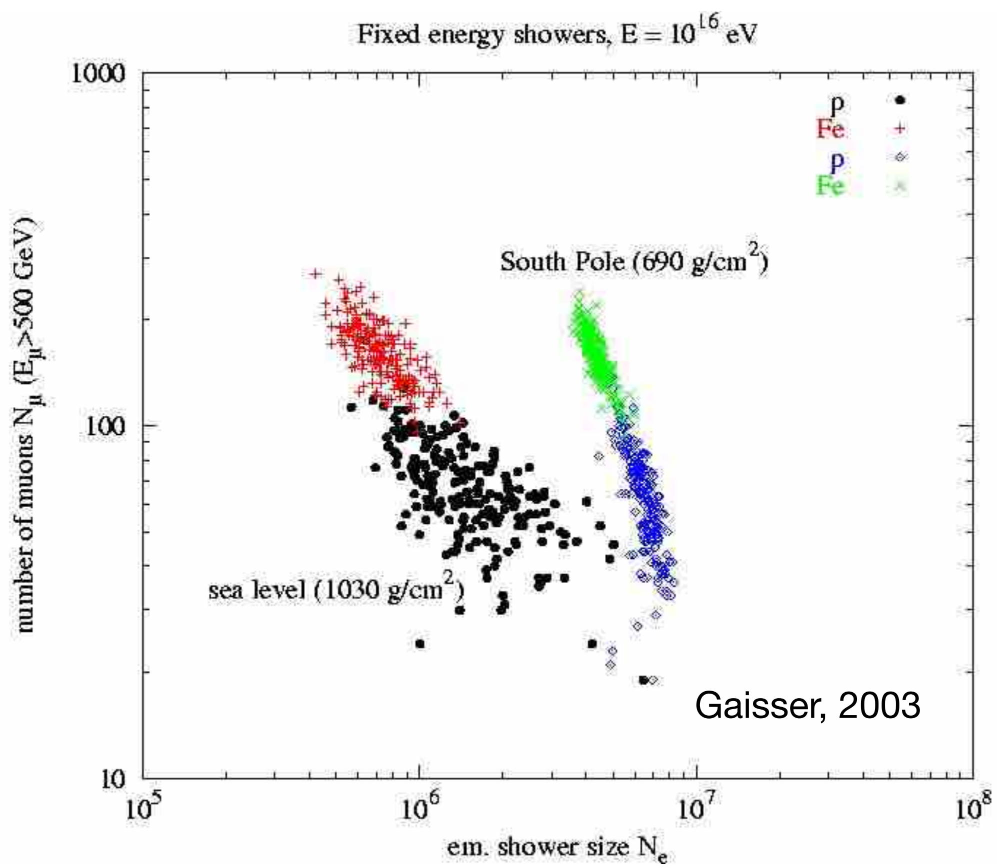

Fluctuations smaller but *reduced sensitivity of the N_e/N_μ technique in selecting primary masses*

➜ Different technique to select primary masses: ARGO-YBJ, Tibet ASγ, BASJE-MAS exploited *characteristics of the shower core region.*

No muons ? ➜ results nearly independent on hadronic interaction models !

Secondary photons

gamma rays dominate the particles on ground (≈7:1 for 100 GeV γ-showers at 4300 m asl)

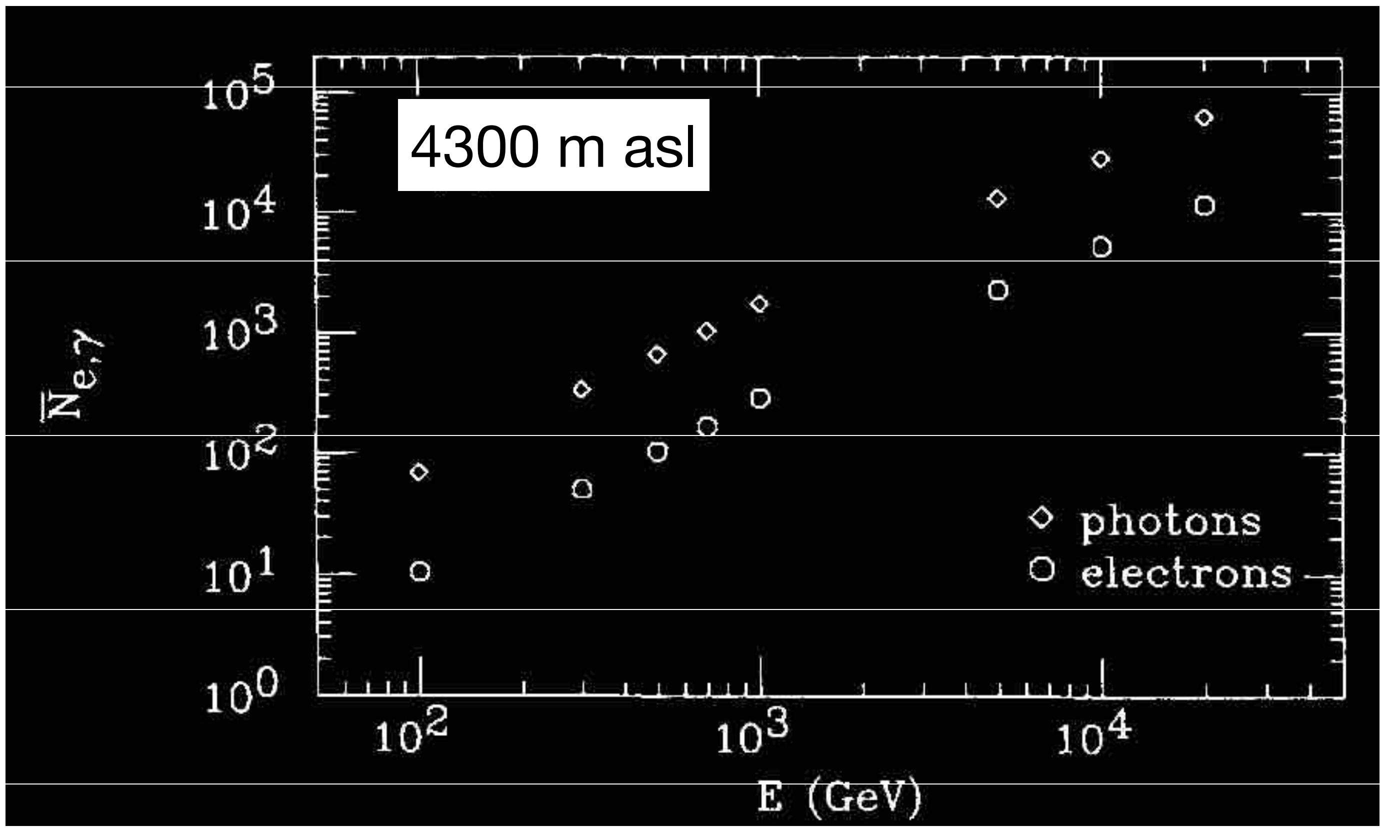

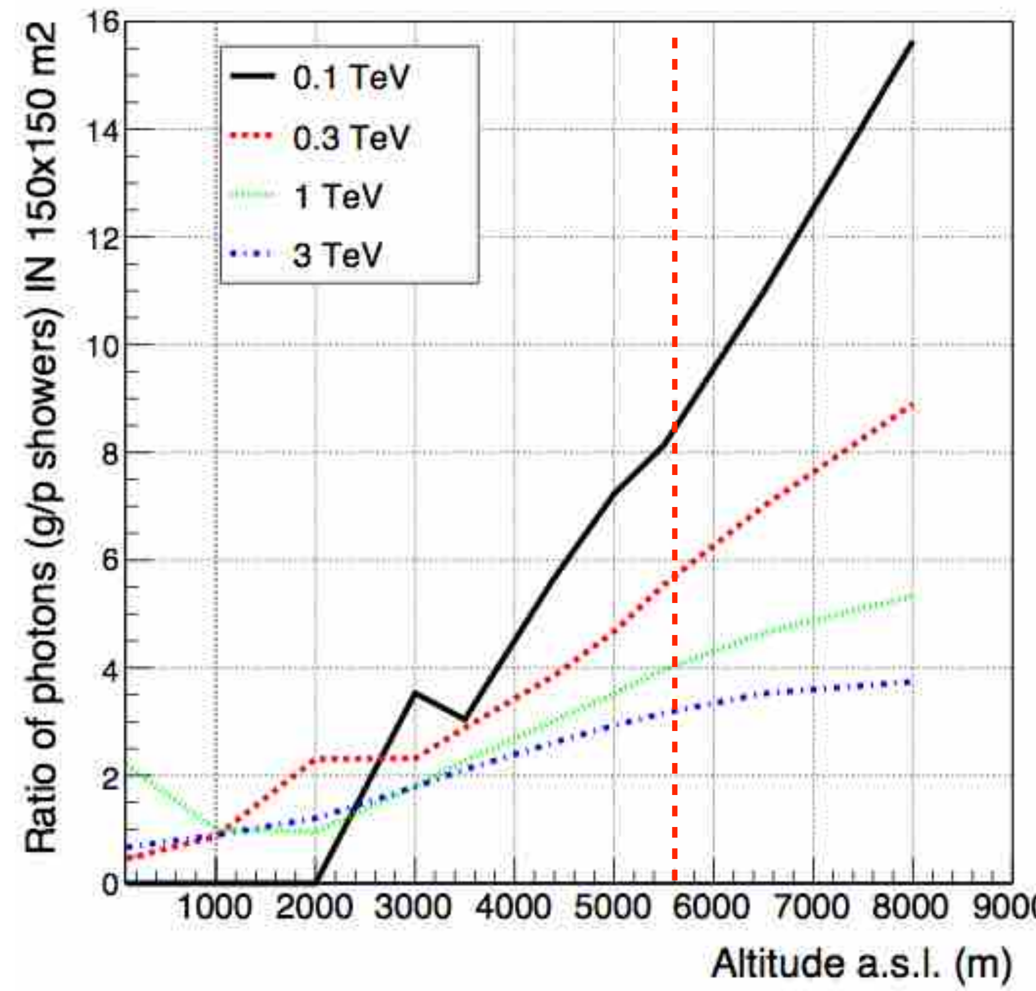

In γ-showers the ratio Nγ/Nch decreases if the comparison is restricted to a small area around the shower core. For instance, we get Nγ/Nch ≈3.5 at a distance *r* < 50 m from the core for 100 GeV showers.

The number of secondary photons in γ-showers exceeds the number of gammas in p-showers with increasing altitude.

Detection of secondary photons very important to lower the energy threshold and to improve the angular resolution

γ/p detection efficiency

High altitude → rejection of the background ‘for free’ !

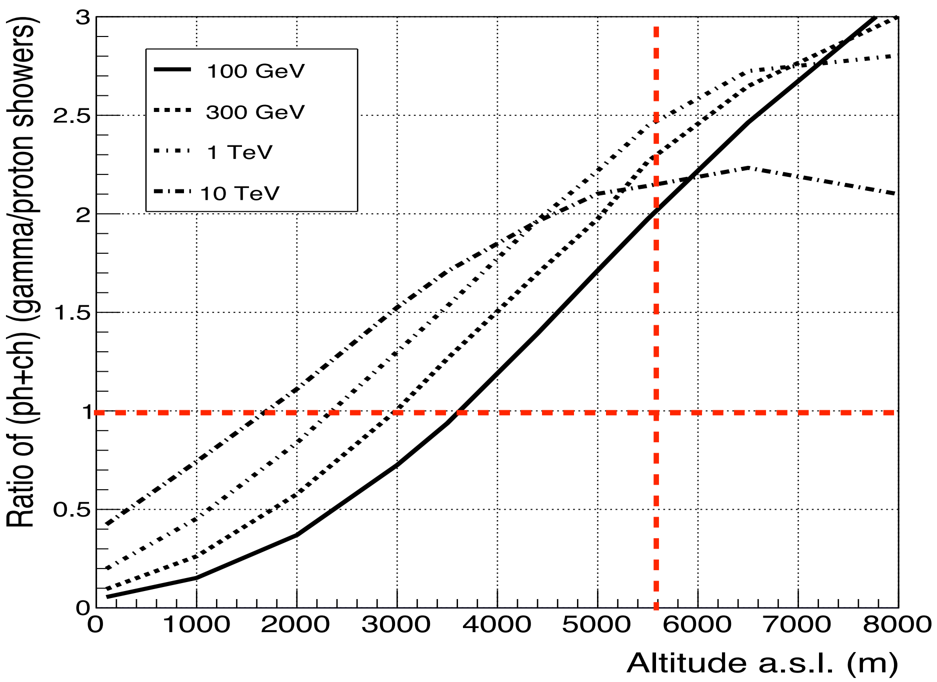

$$R = \sqrt{\frac{A^{\gamma}_{eff}(E)}{A^{B}_{eff}(E)}}$$

γ/hadron relative trigger efficiency

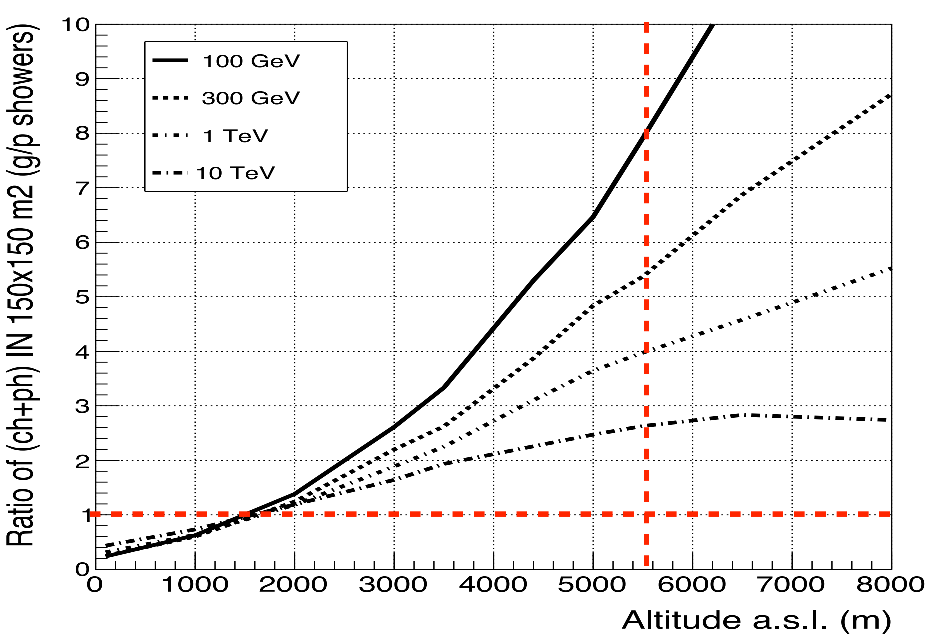

The number of particles in γ-showers exceeds the number of particles in p-showers at extreme altitude.

Trigger probability of a detector larger for γ-showers than for p-showers at extreme altitude.

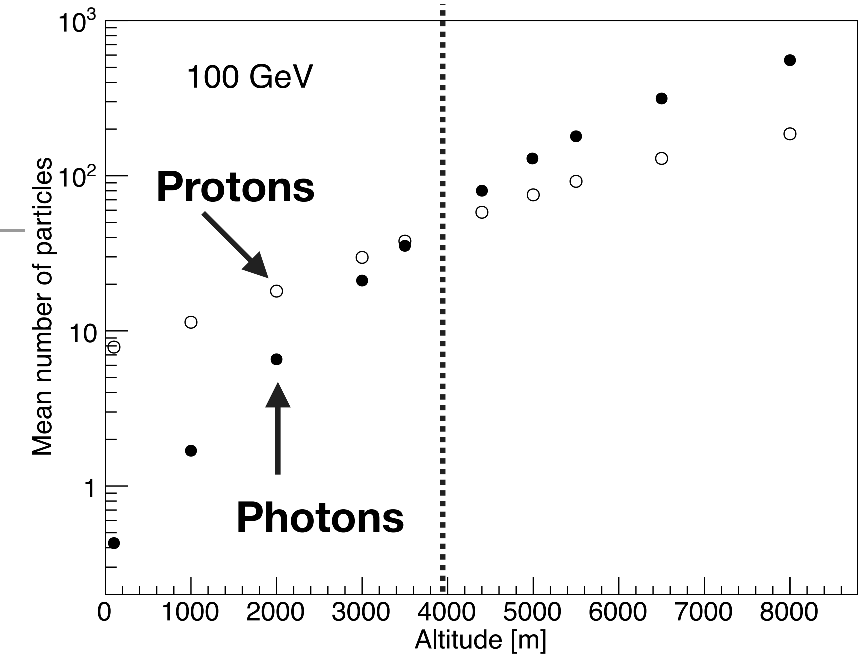

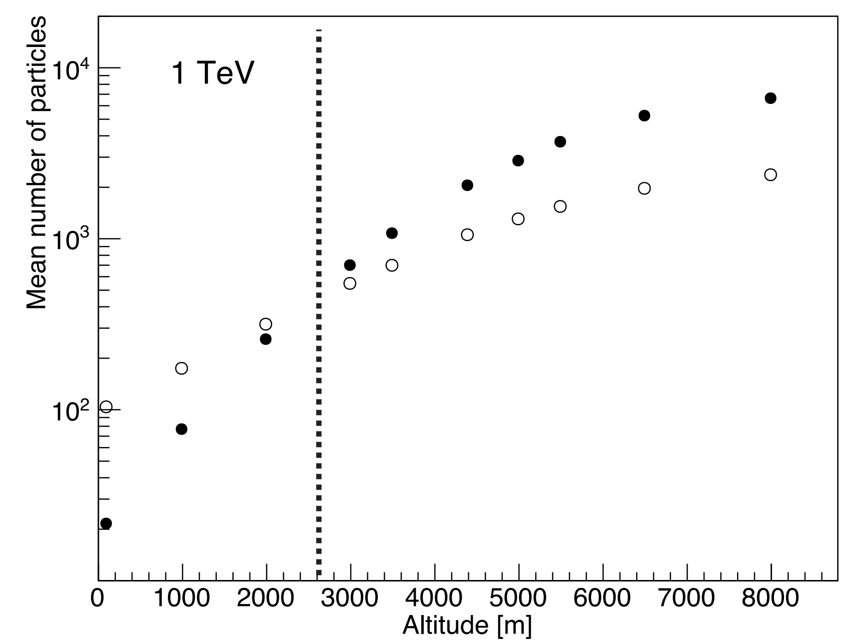

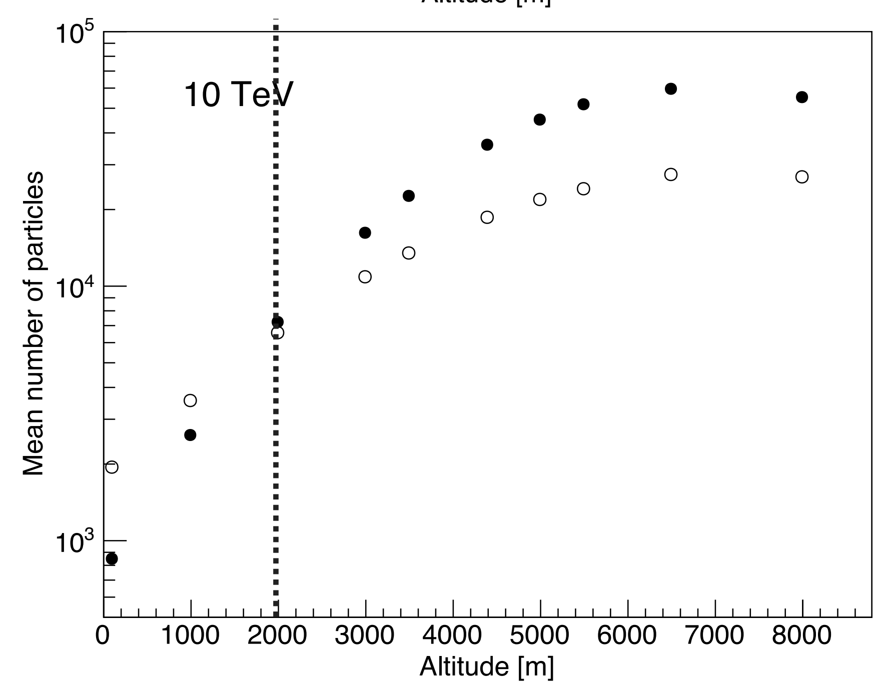

Southern Gamma-Ray Survey Observatory

SOUTHERN
GAMMA-RAY
SURVEY
OBSERVATORY

Who are we?…

H. Schoorlemmer
Recontres du Vietnam 2018

The alliance

- Advancement of this effort in the Southern-Hemisphere
- **Organizing the writing of a white-paper on the science case**
- Documentation on site-candidates
- No decision on technical design (for now)
- Currently **75 members** from **11 countries**
- Next meeting **8-9 October Heidelberg**, Germany

www.sgso-alliance.org

Science Case White Paper by SGSO

SCIENCE CASE FOR A WIDE FIELD-OF-VIEW VERY-HIGH-ENERGY GAMMA-RAY OBSERVATORY IN THE SOUTHERN HEMISPHERE

ANDREA ALBERT, R. ARCEO, SEGEV BENZVI, THOMAS BRETZ, ALBERTO CARRAMIÑANA, SABRINA CASANOVA, PAOLO DESIATI, DANIELA DORNER, JUAN CARLOS DÍAZ-VÉLEZ, GIUSEPPE DI SCIASCIO, NISSIM FRAIJA, JAVIER GONZALEZ, H. MARTÍNEZ-HUERTA, MIGUEL MOSTAFA, MAGDALENA GONZALEZ, JIM HINTON, JEAN-PHILIPPE LENAIN, R. LÓPEZ-COTO, FILIPE DE O. SALLES, ANA PICHEL, ELISA PRANDINI, ANDREAS REISENEGGER, JÉRÔME RODRIGUEZ, ADRIAN C. ROVERO, MARCOS SANTANDER, HARM SCHOORLEMMER, FABIAN SCHÜSSLER, ANDRES SANDOVAL, MONICA SEGLAR-ARROYO, AION VIANA, THOMAS WEISGARBER, FELIX WERNER, AND YOUR NAME CAN BE HERE...

Contents

1

- Community wide contributions
- Focus on how the science will drive detector requirements
- *First version ready this Fall*
- Public tools for writing and calculations
- Regular calls for coordination

H. Schoorlemmer
Recontres du Vietnam 2018

A straw mans design: point source sensitivity

Size & Fill factor

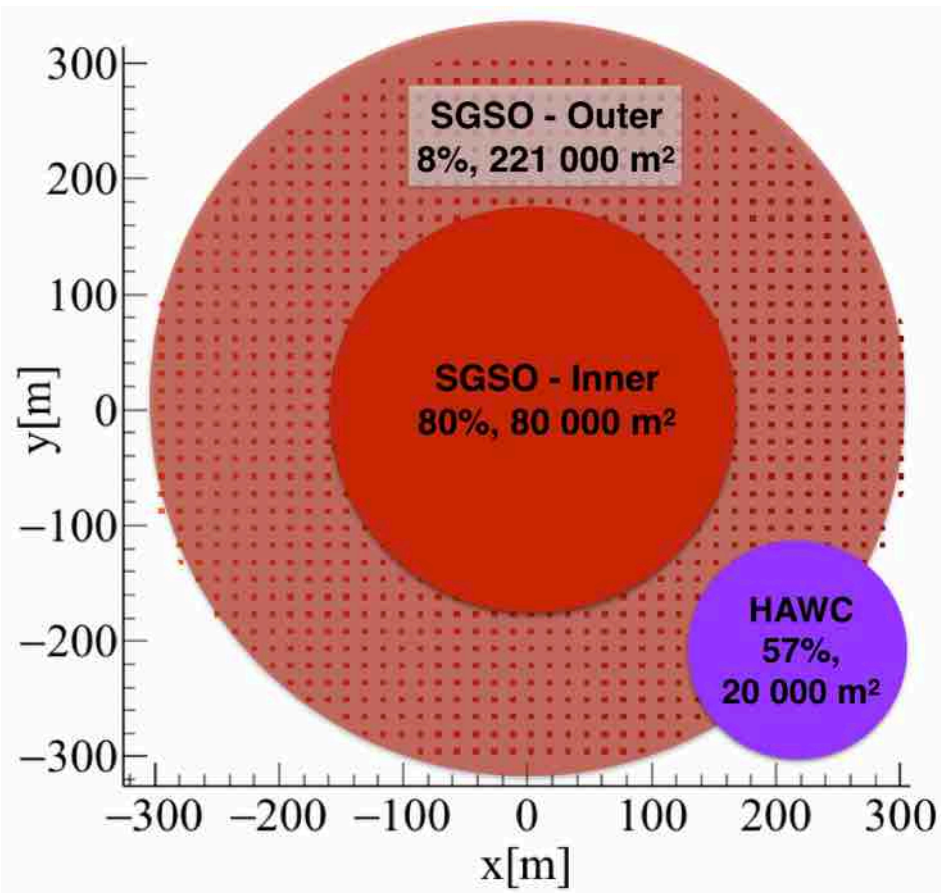

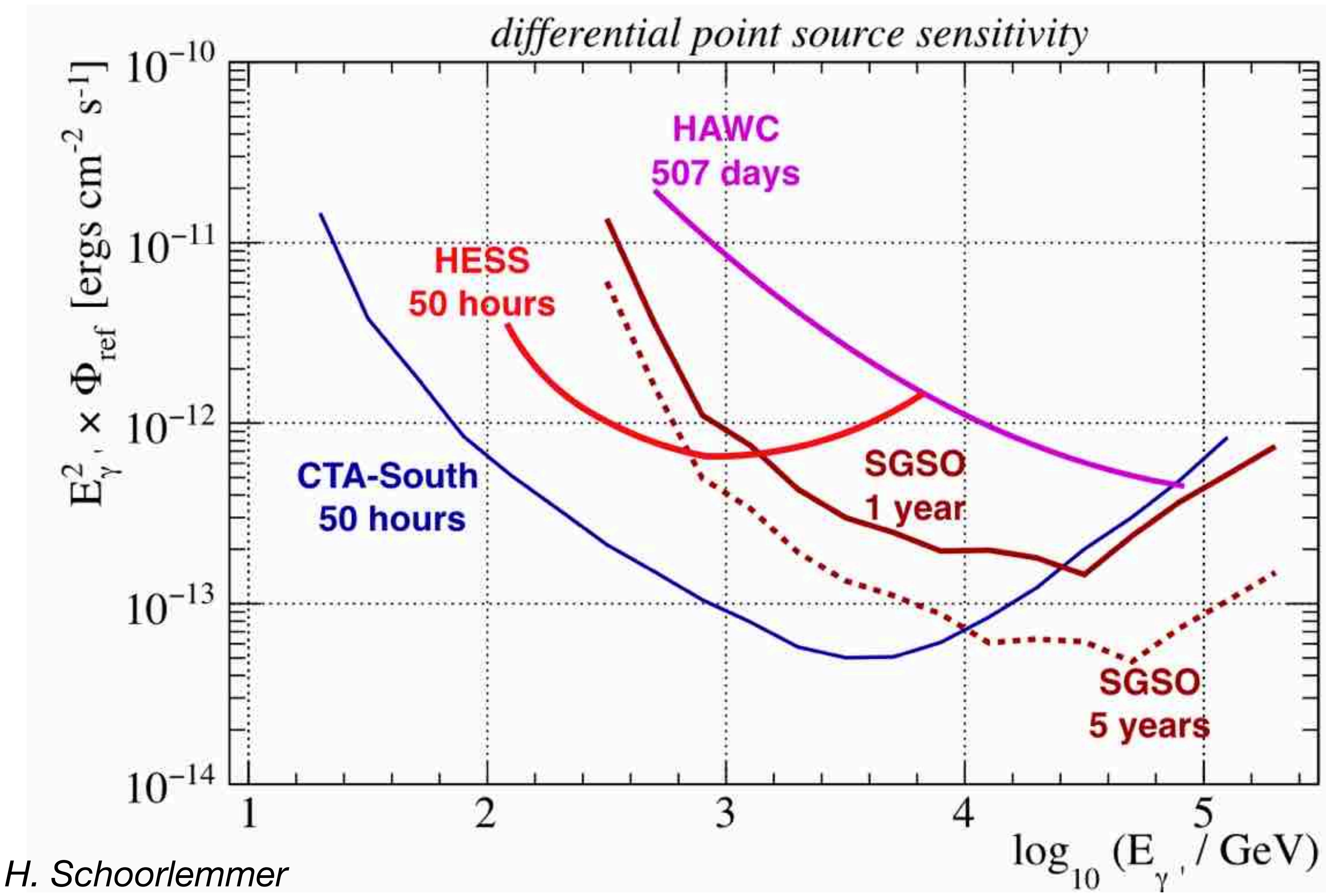

H. Schoorlemmer
Recontres du Vietnam 2018

5 km above sea level

HAWC-based layout

If you are interested join SGSO at

www.sgso-alliance.org

Conclusions

Open problems in cosmic ray physics push the construction of new generation Wide FoV experiments.

In the next decade CTA-North and LHAASO are expected to be the most sensitive instruments to study γ-ray astronomy in the Northern hemisphere from ≈20 GeV up to PeV.

- *An all-sky detector in the Southern Hemisphere should be a high priority* to face a broad range of topics.
- Extragalactic transient detection requires *low threshold, ≈100 GeV*.
- *Extreme altitude* (≈5000 m asl), *high coverage* and *high granularity of the read-out* are key.
- *Background rejection below TeV challenging ➜ RPCs + Water Cherenkov ?*
- *Selection of primary masses* crucial ➜ *RPCs + Water Cherenkov ?*
- Capability of Water Cherenkov Facilities in selecting primary masses at the knee must be investigated.
- Different groups are studying different experimental solutions (ALPACA, ALTO, LATTES, STACEX)
- High energy gamma-ray astronomy (>10 TeV) and CR physics covered by ALPACA ?

Hybrid detector: LATTES

Astroparticle Physics 99 (2018) 34–42

Design and expected performance of a novel hybrid detector for very-high-energy gamma-ray astrophysics

P. Assis[a,b], U. Barres de Almeida[c], A. Blanco[d], R. Conceição[a,b,*], B. D'Ettorre Piazzoli[e], A. De Angelis[f,g,b,a], M. Doro[h,f], P. Fonte[d], L. Lopes[d], G. Matthiae[i], M. Pimenta[b,a], R. Shellard[c], B. Tomé[a,b]

An array of hybrid detectors constituted by

1. one Water Cherenkov Detector (WCD) with a rectangular horizontal surface of 3 m × 1.5 m and a depth of 0.5 m, with signals read by PMTs at both ends of the smallest vertical face of the block.

2. On top of the WCD there are two MARTA RPCs, each with a surface of (1.5 × 1.5) m^2 and with 16 charge collecting pads. Each RPC is covered with a thin (5.6 mm) layer of lead.

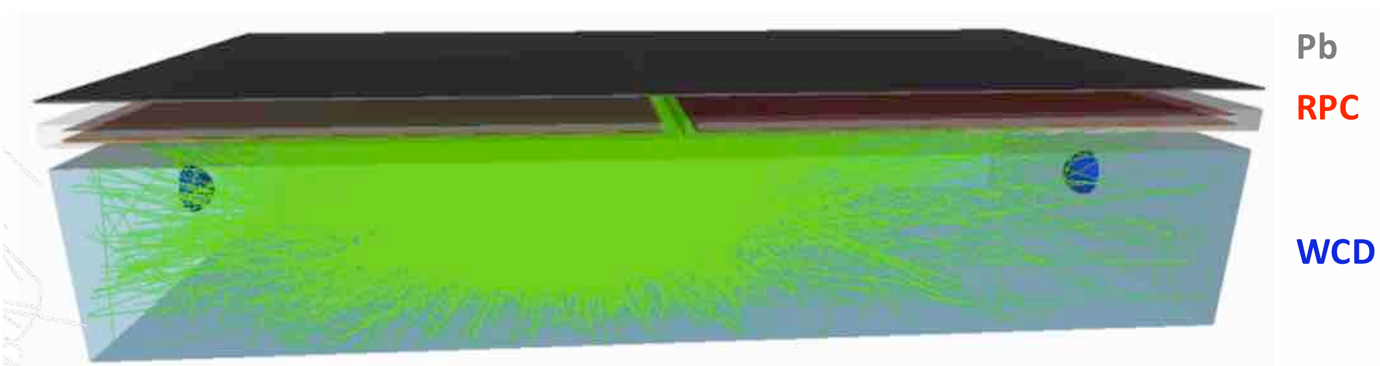

– Thin lead plate (Pb)
  - 5.6 mm (one radiation lenght)
– Resistive Plate Chambers (**RPC**)
  - 2 RPCs per station
  - Each RPC with 4x4 readout pads
– Water Cherenkov Detector (**WCD**)
  - 2 PMTs (diameter: 15 cm)
  - Dimensions: 1.5 m x 3 m x 0.5 m

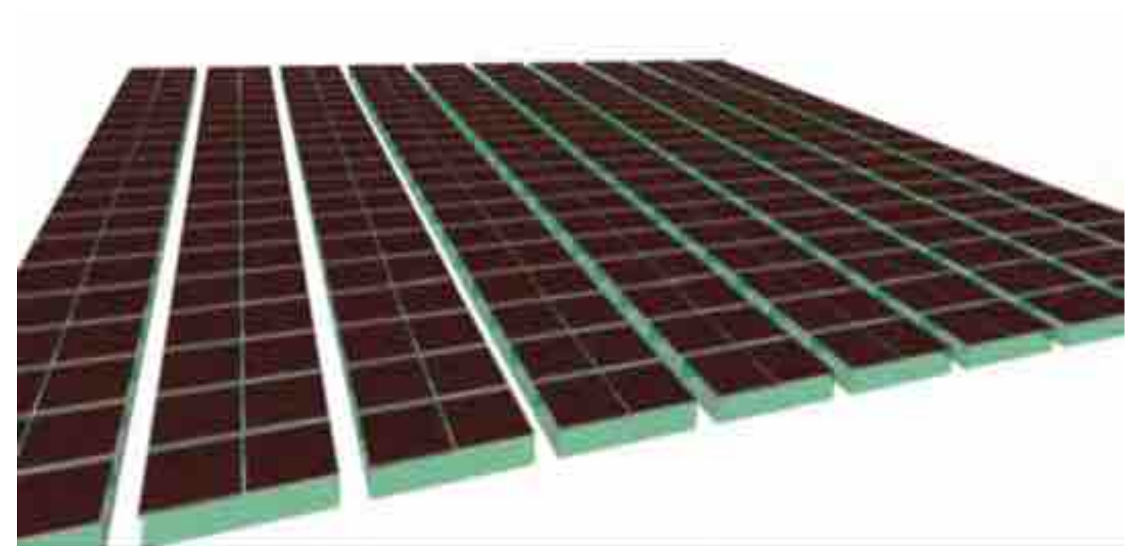

Glass-based RPCs

LATTES performance

Instrumented area ≈20,000 m^2

Simulated site at 5200 m asl

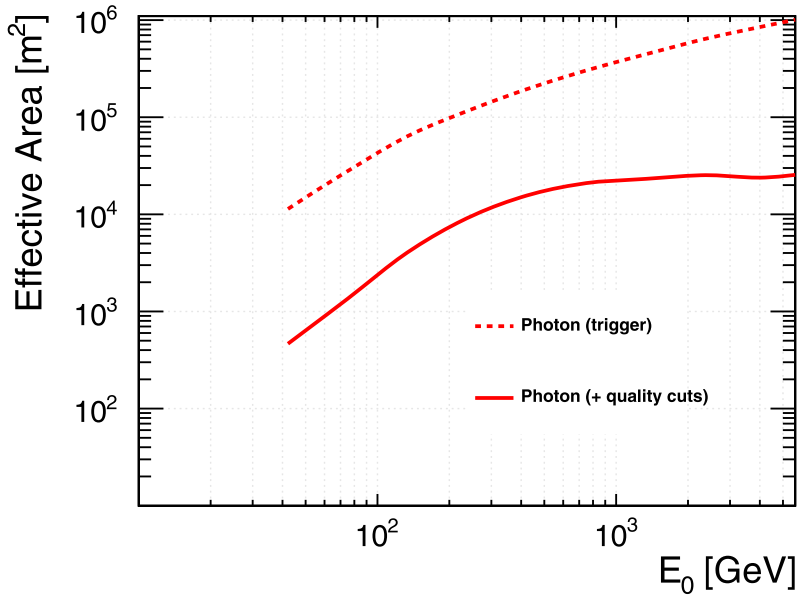

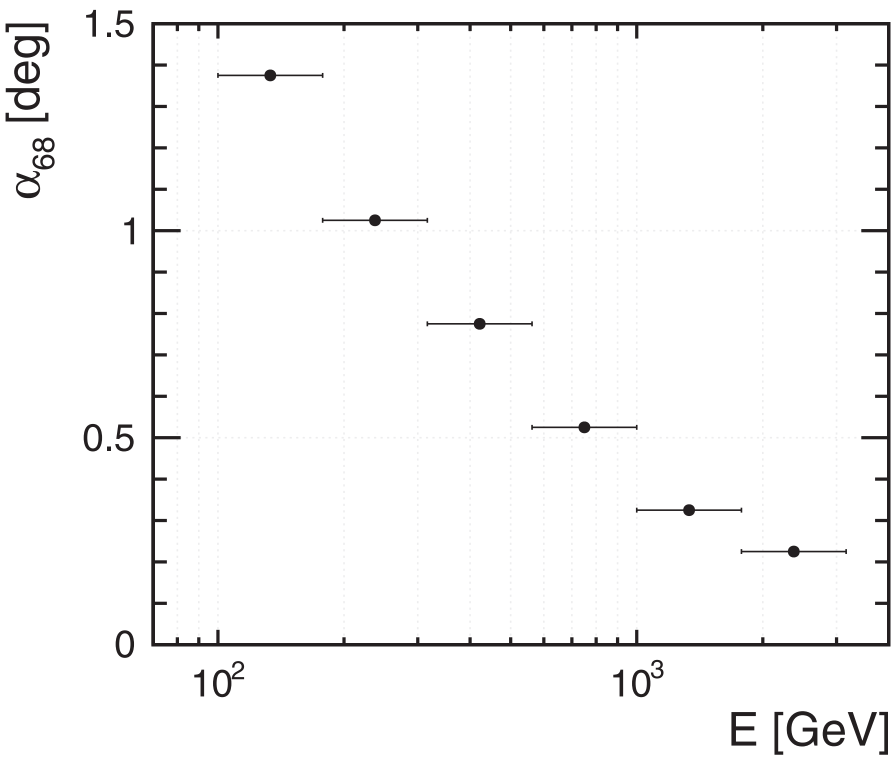

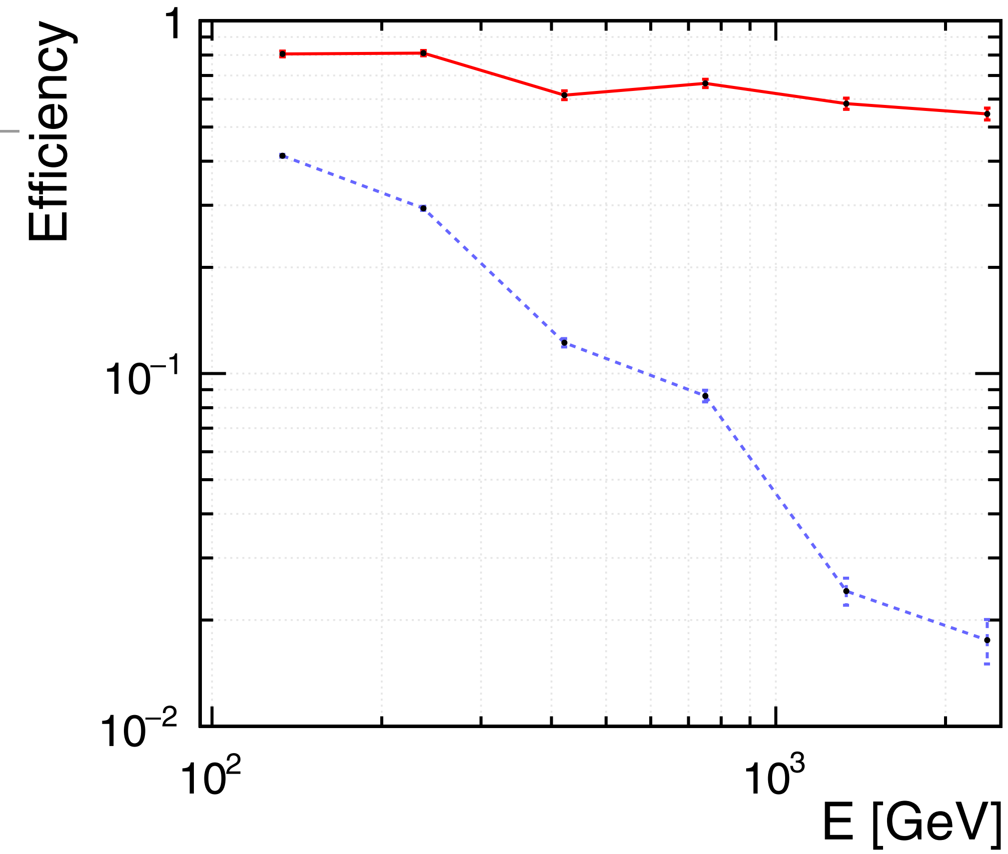

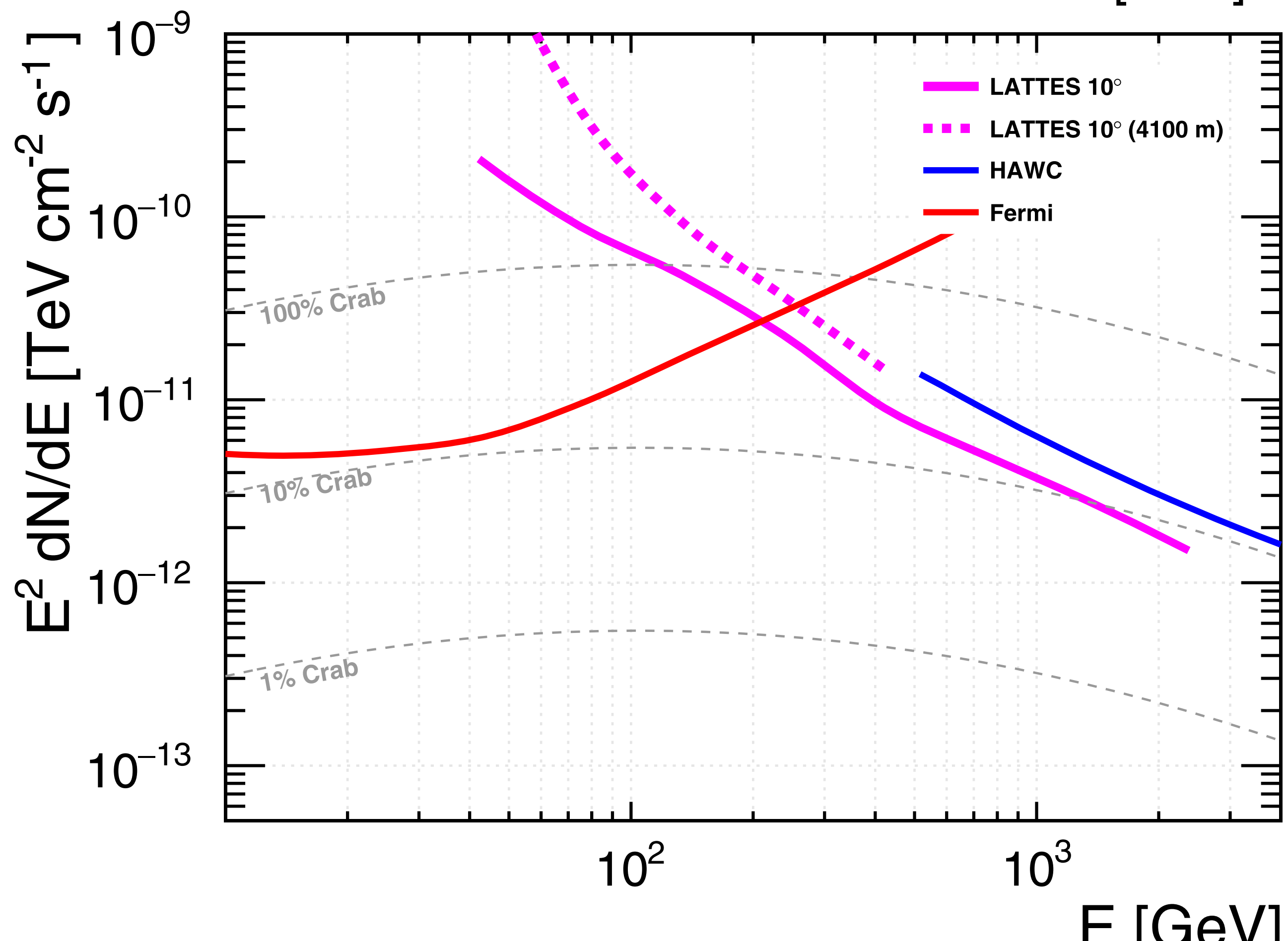

Southern Hemisphere: ALPACA

Andes
Large area
PArticle detector for Cosmic ray physics
and Astronomy

Location: 4,740 m above sea level (16˚23’S, 68˚08’W)

# of scintillation detectors	1 m^2 x 401 detectors
Effective area of	~83,000 m^2
modal energy	~5TeV
angular resolution	~0.2 @100 TeV
energy resolution	~30% @100TeV
field of view	~2 sr
CR rejection power	>99.9%@100 TeV
(γ ray efficiency ~ 90 %)	

MD Array 56m^2 x 96 detectors
- Effective area for muons ~5400m^2
- CR rejection power >99.9% @100TeV (gamma ray efficiency ~90%)

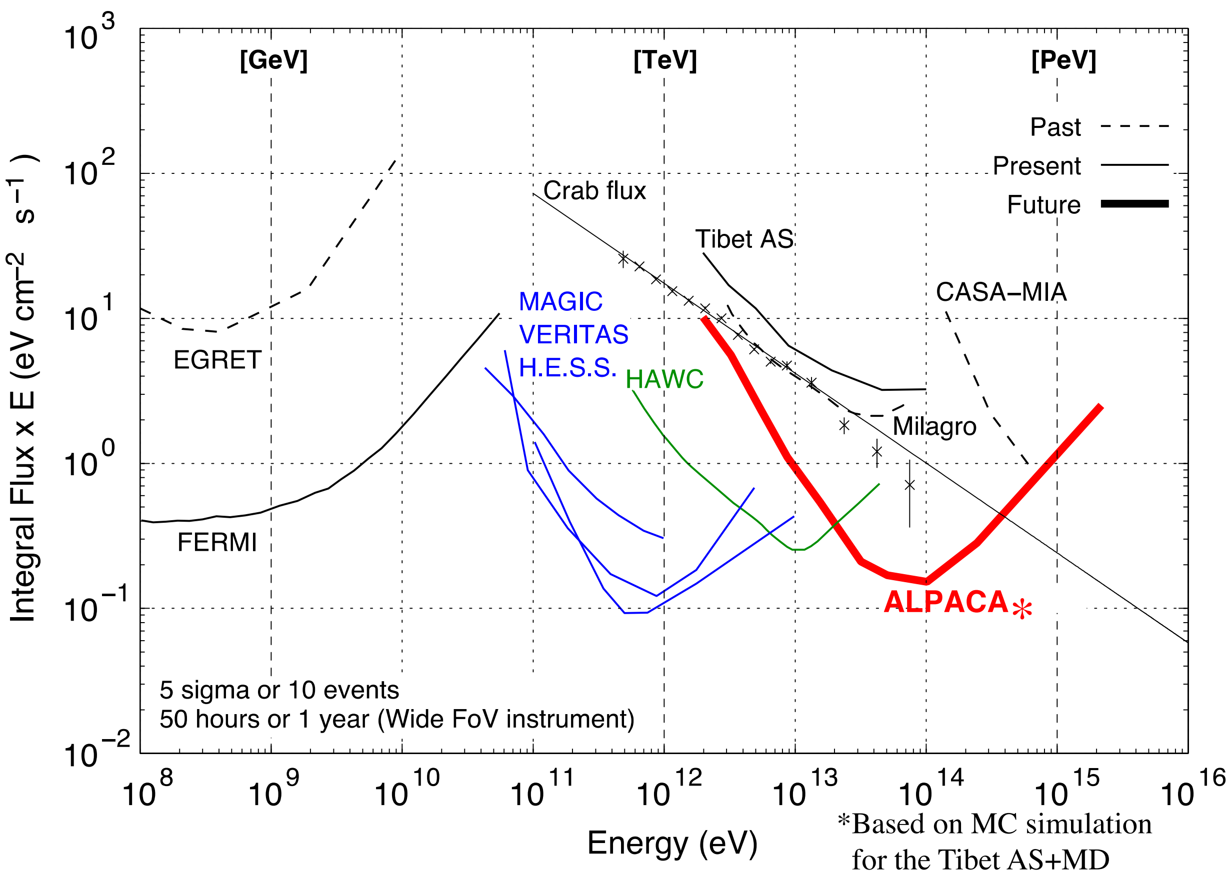

*Based on MC simulation for the Tibet AS+MD

Similar to the Tibet ASγ experiment operated in Tibet

ALPACA layout

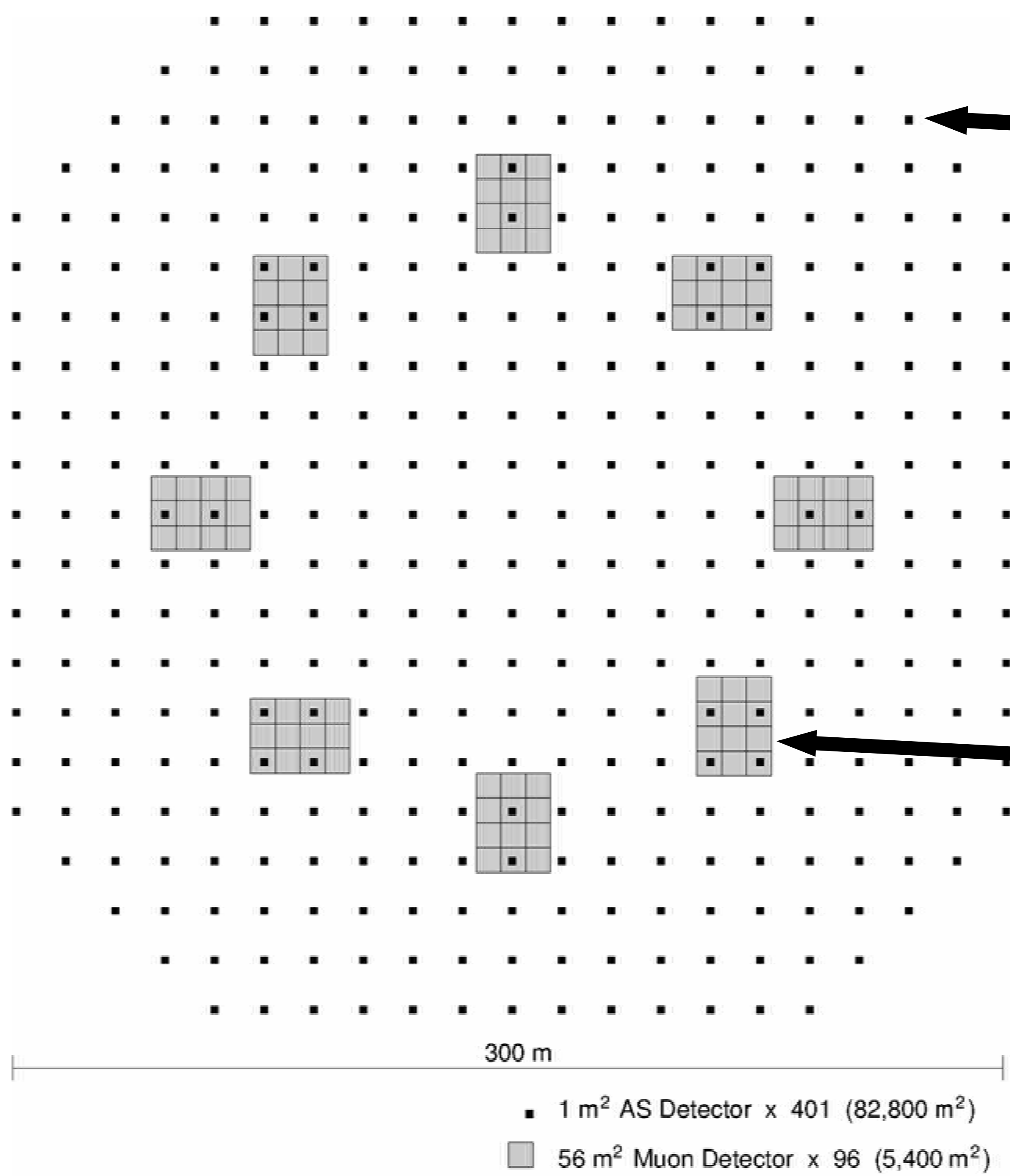

AS

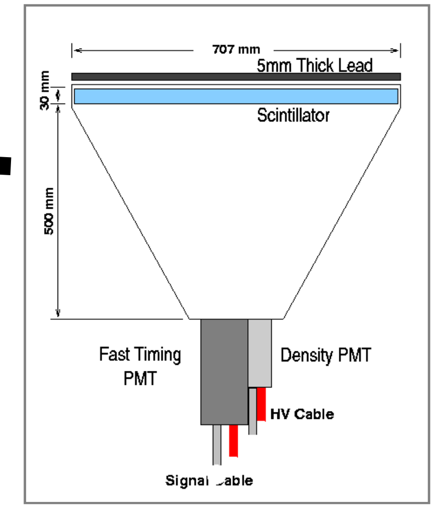

Image of 1m² plastic scintillation detector

MD

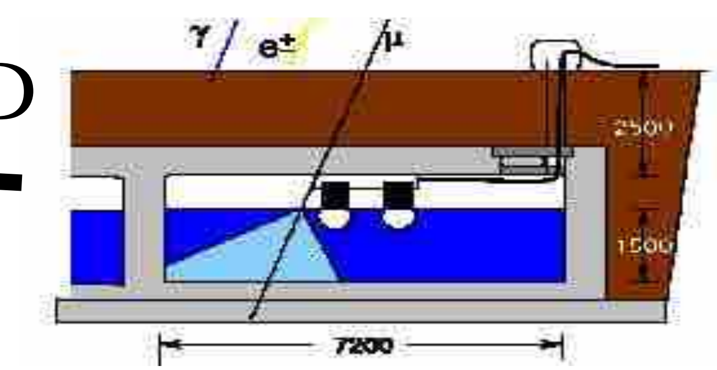

Image of unit (56m²) underground water Cherenkov muon detector

ALPAQUITA (1/10 scale ALPACA AS , in 2017)

The RPC charge readout

…extending the dynamical range up to 10 PeV

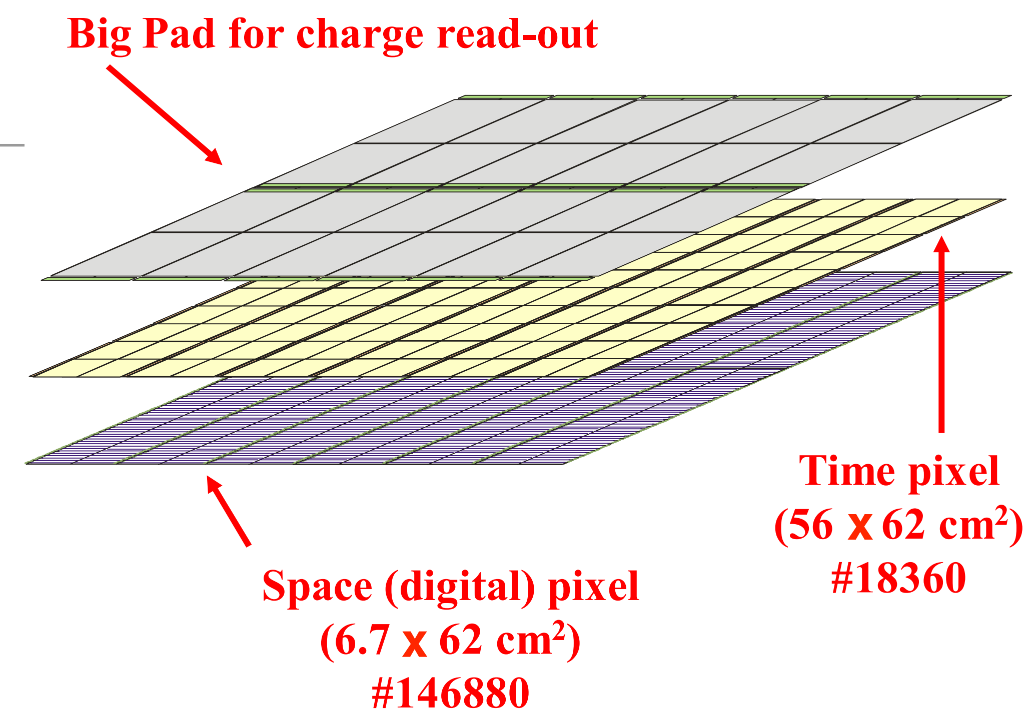

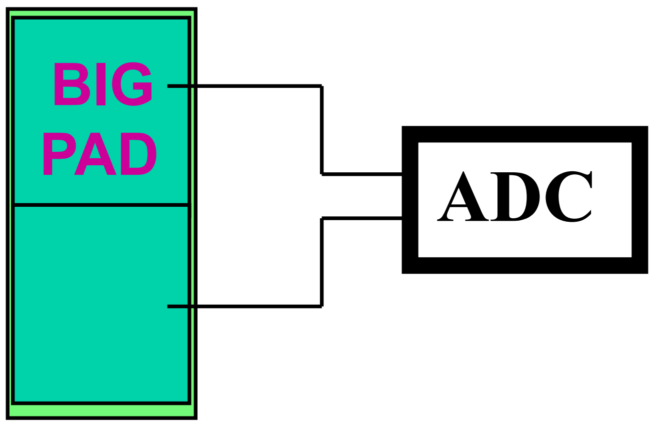

4 different gain scales used to cover a wide range in particle density:

$$\rho_{max-strip} \approx 20\ \text{particles/m}^2$$

$$\rho_{max-analog} \approx 10^4\ \text{particles/m}^2$$

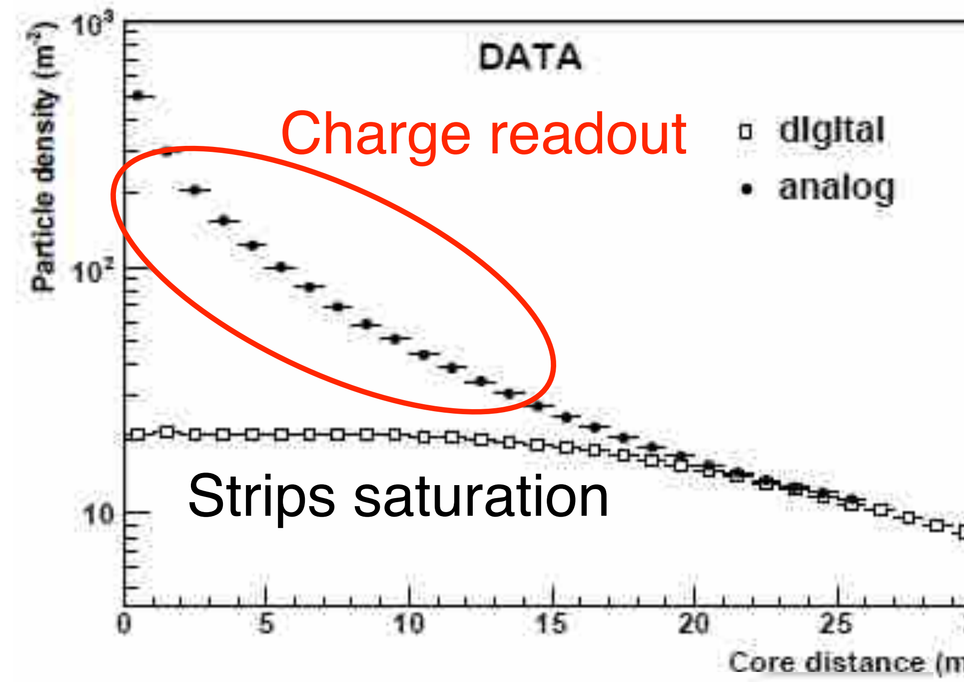

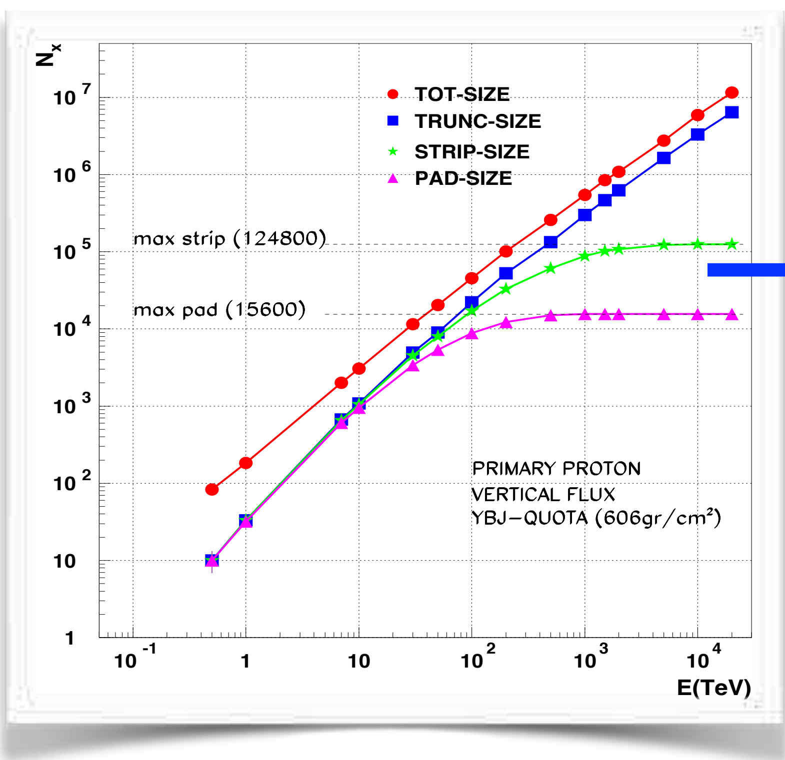

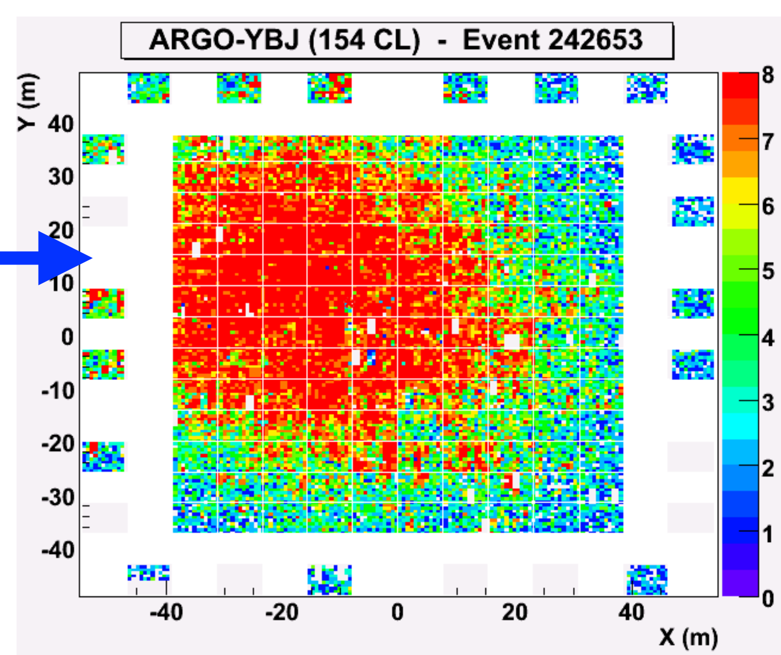

Intrinsic linearity: test at the BTF facility

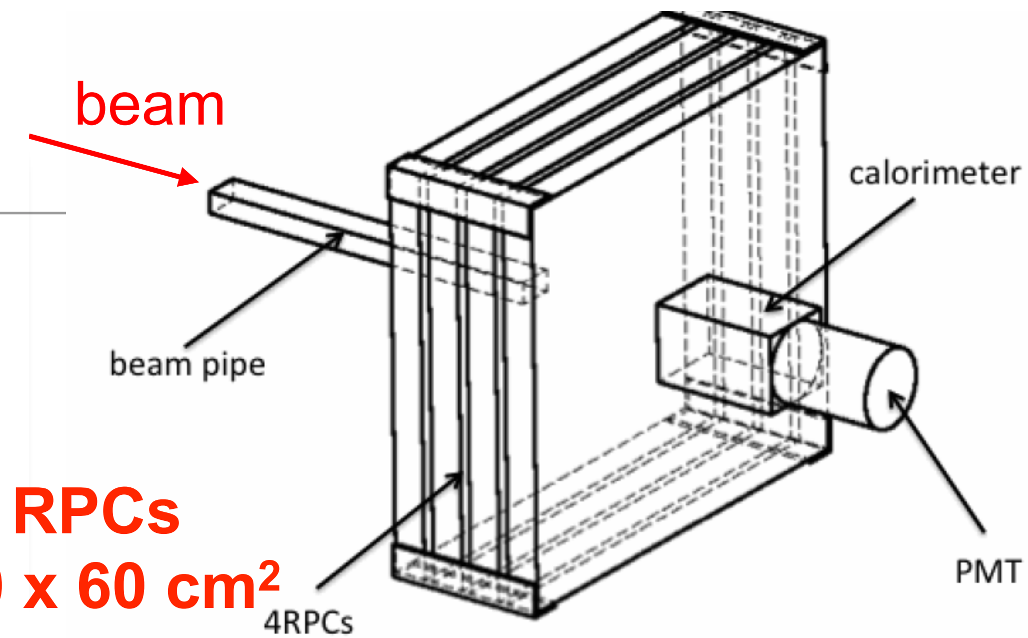

Calorimeter: lead glass block from OPAL, PMT a Hamamatsu R2238.

Linearity of the RPC @ BTF in INFN Frascati Lab:

- *electrons (or positrons)*
- *E = 25-750 MeV (0.5% resolution)*
- *<N>=1÷10^8particles/pulse*
- *10 ns pulses, 1-49 Hz*
- *beam spot uniform on 3×5 cm*

Good overlap between 4 scales with the maximum density of the showers spanning over three decades

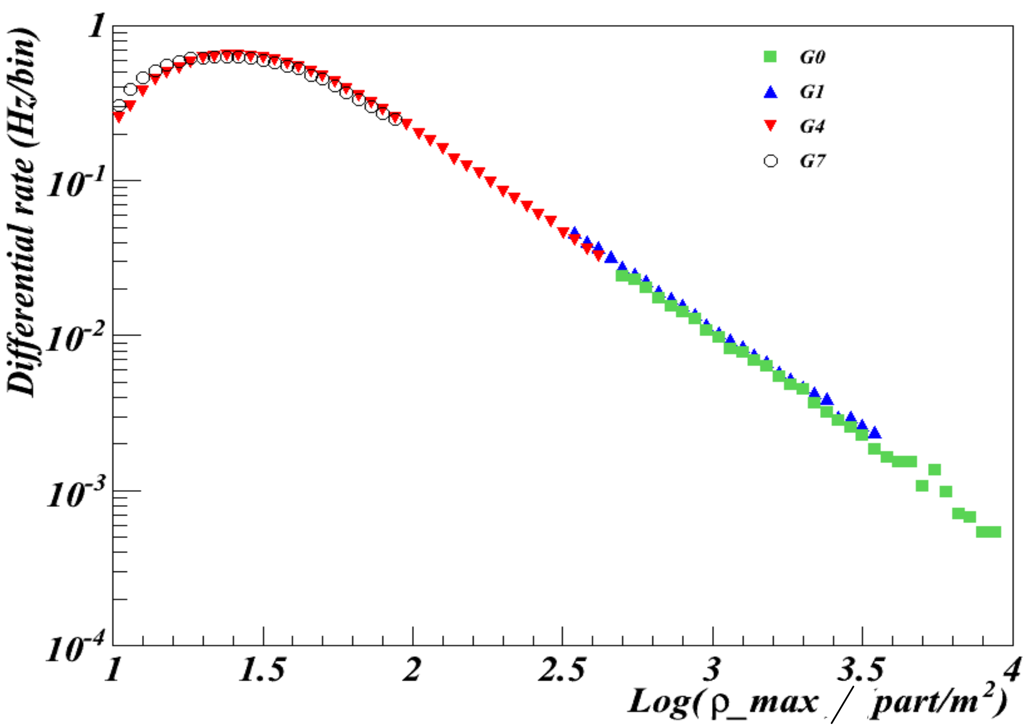

Astrop. Phys. 67 (2015) 47

The RPC signal vs the calorimeter signal

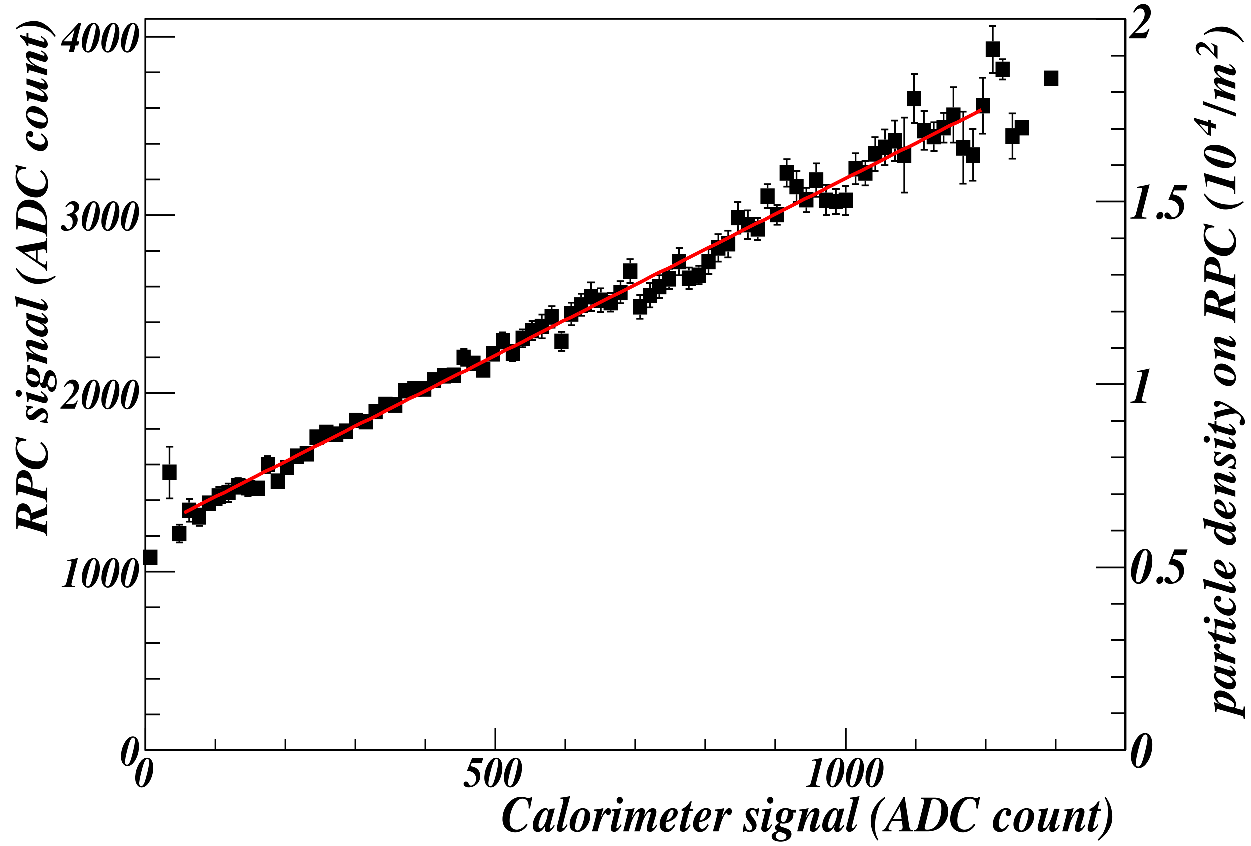

➔ Linearity up to ≈ 2 · 10^4 particle/m^2

The RPC charge readout: the core region

MC: 100 TeV

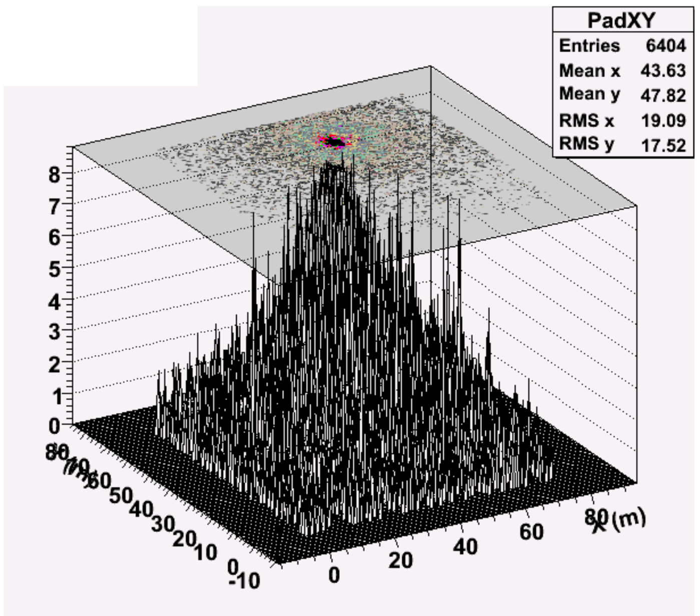

Strip read-out

MC: 1000 TeV

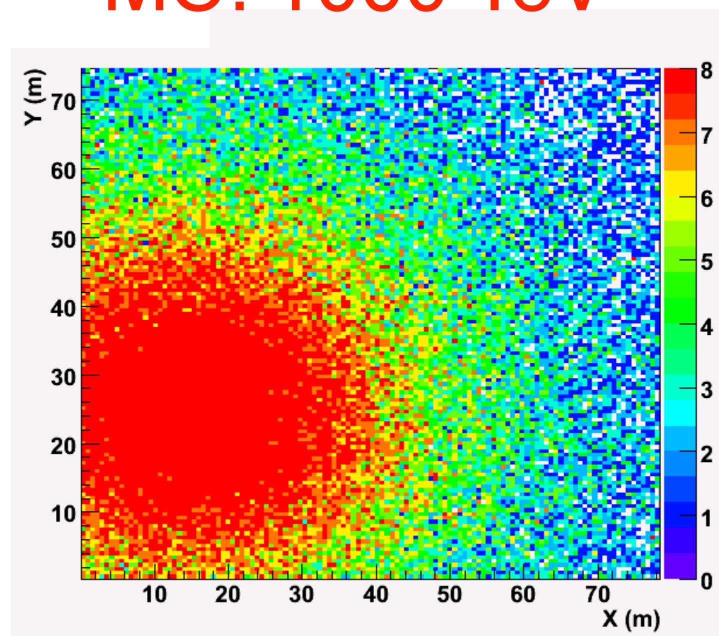

Strip read-out

Data

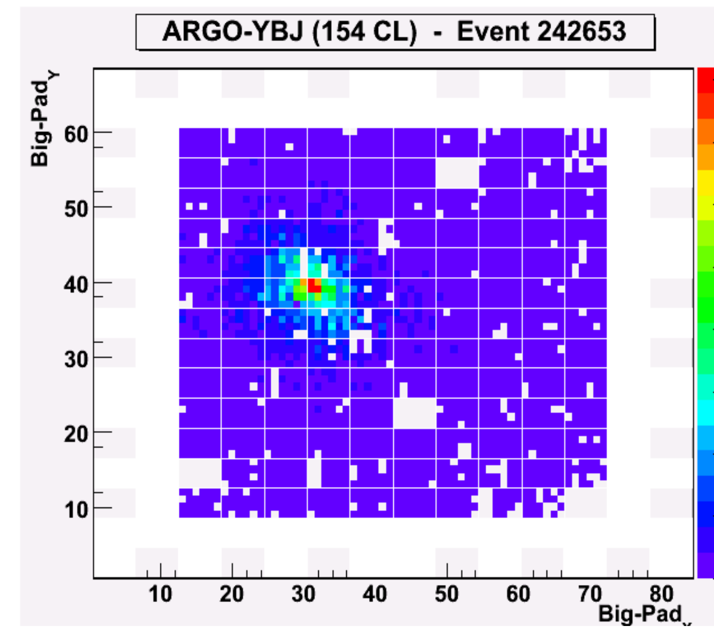

Strip read-out

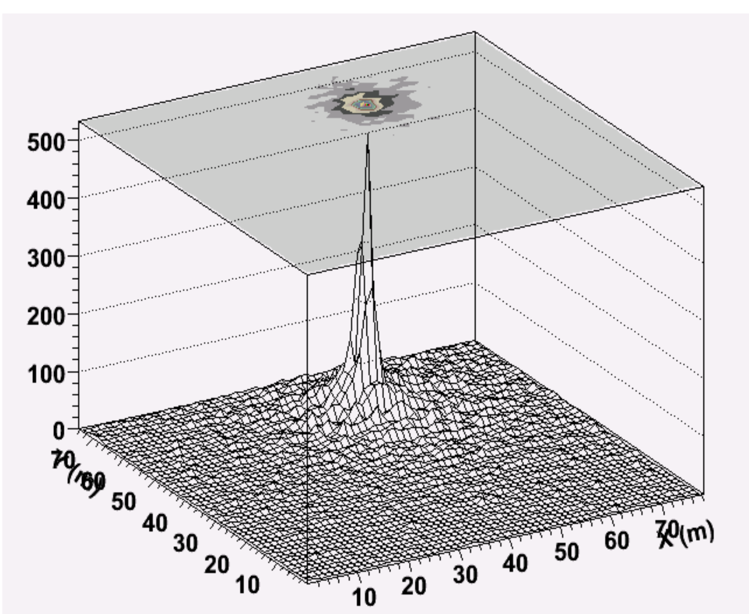

Charge read-out

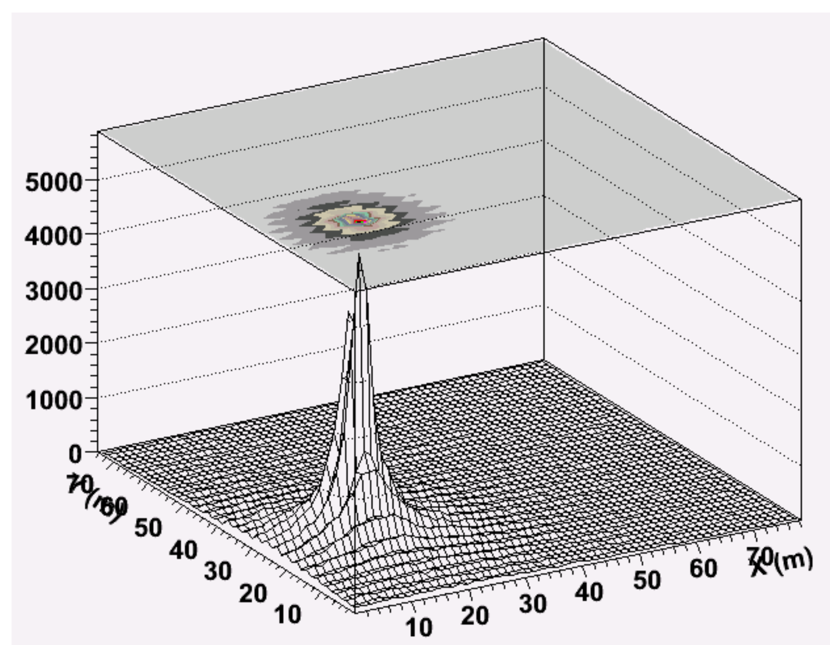

Charge read-out

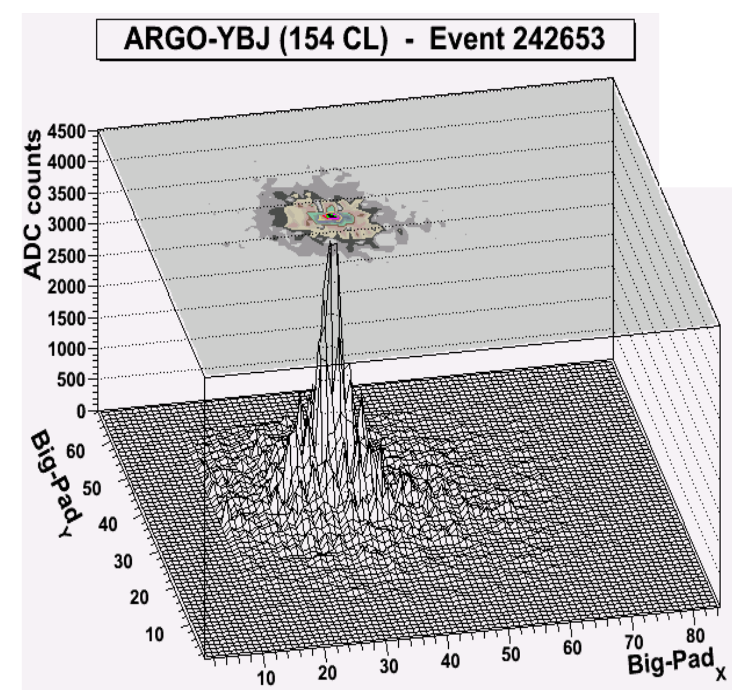

Charge read-out

The RPC charge readout: the core region

MC: 100 TeV

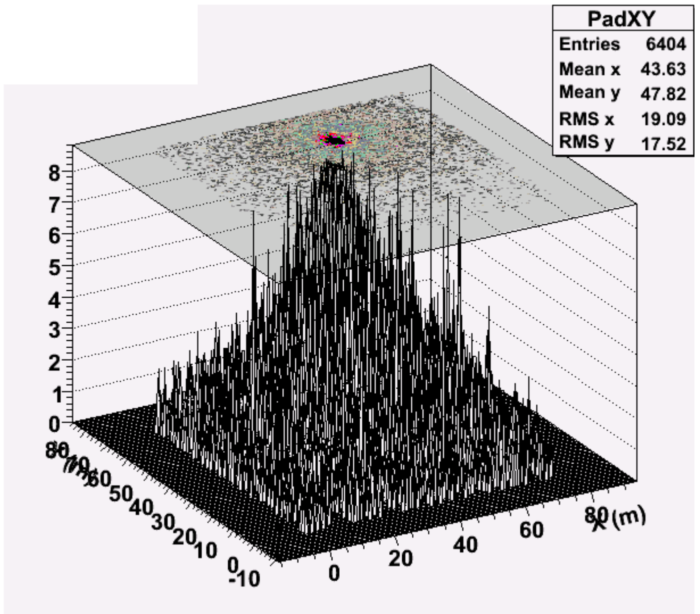

Strip rea

MC: 1000 TeV

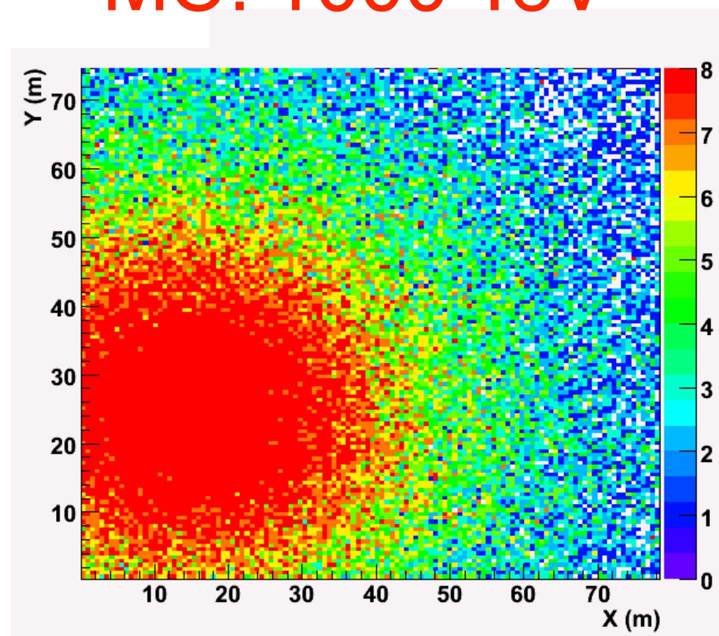

Strip read-out

Data

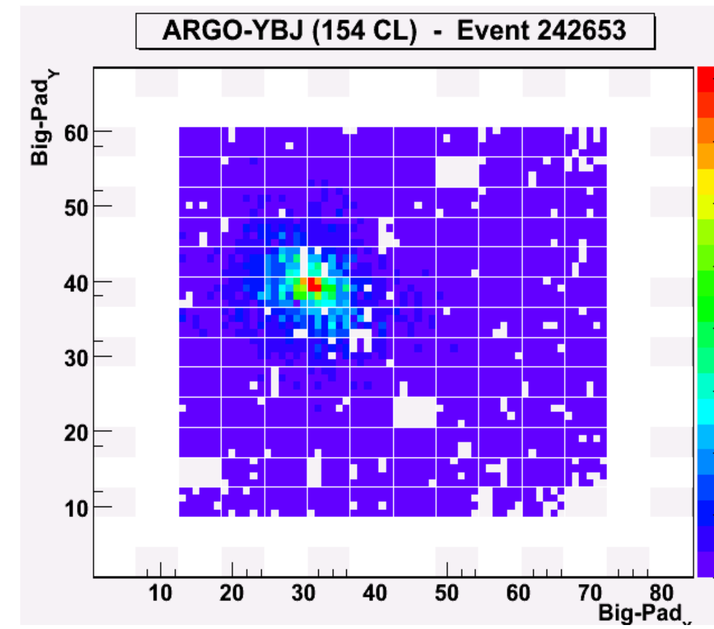

Strip read-out

Shower Core = study of hadronic interactions in a region with pseudorapidity > 8 !!!

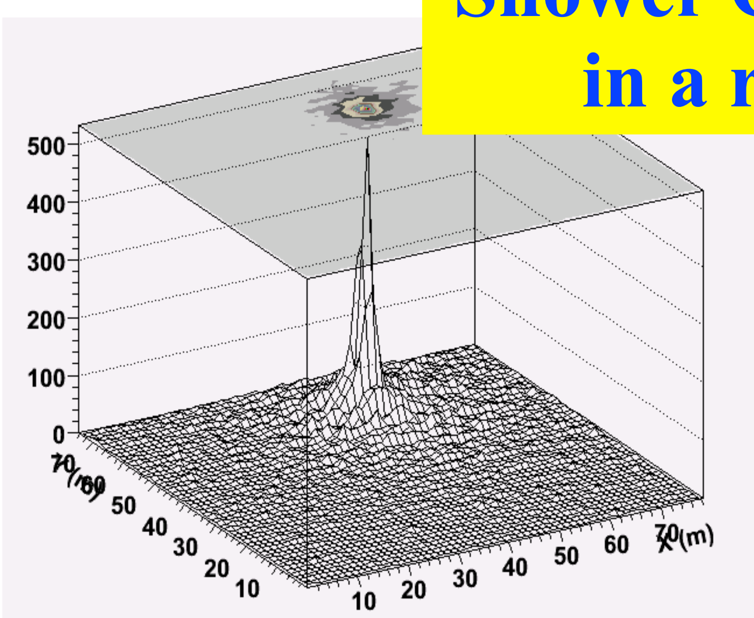

Charge read-out

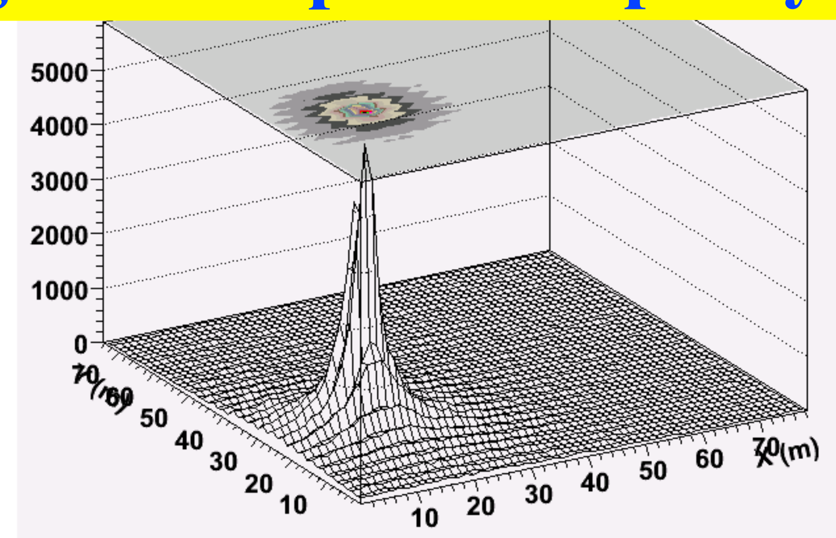

Charge read-out

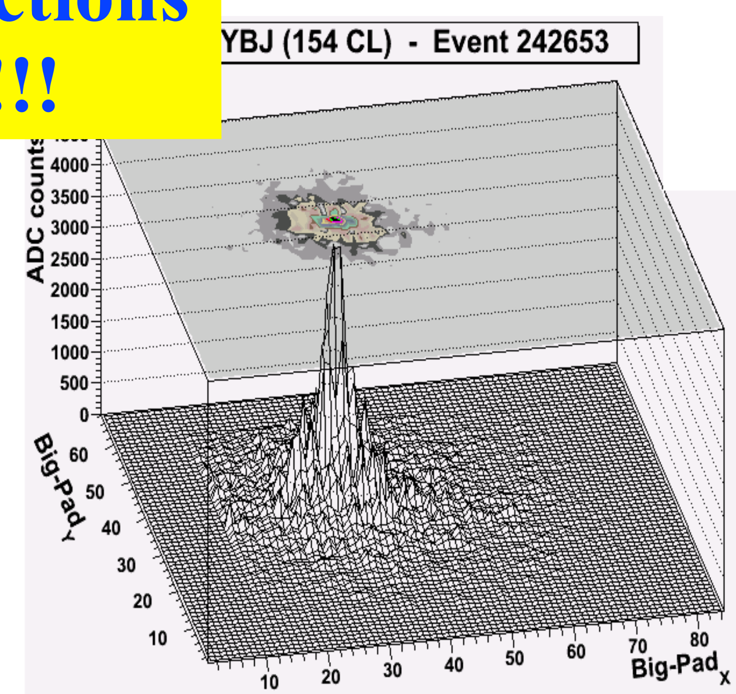

Charge read-out

Sensitivity

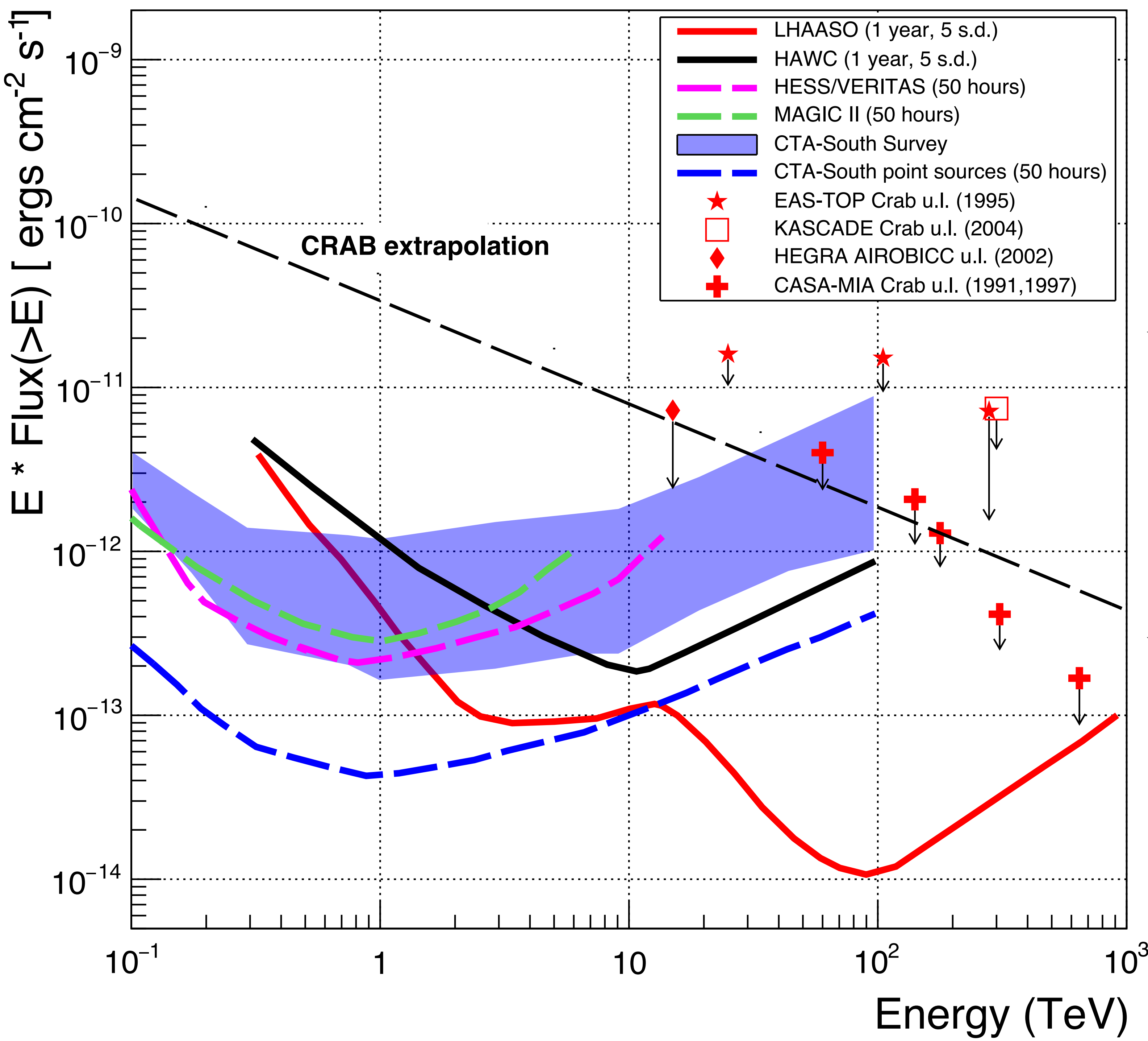

EAS-array: 5 s.d. in 1 year

Cherenkov: 5 s.d. in 50 h *on source*

★ 1 year for EAS arrays means:

(5 h × 365 d) ~1500 - 2200 of observation hours for each source (about 4-6 hours per day).

★ For Cherenkov:

(5 h × 365 d) × d.c. (≈ 15%) ≈ 270 h/y for each source.

Effect of a lead converter above a detector

The consequences of placing a thin sheet of dense, high-Z material, above detectors are, qualitatively:

(1) low-energy electrons are absorbed and no longer contribute to the signal (low-energy photons are also absorbed),

(2) high-energy electrons produce an enhanced signal size through multiplication,

(3) high-energy photons materialise, producing additional signal contributions similar in size to those produced by (2).

The number of particles gained from processes (2) and (3) exceeds that lost through (1) and hence the *Rossi transition effect* is observed.

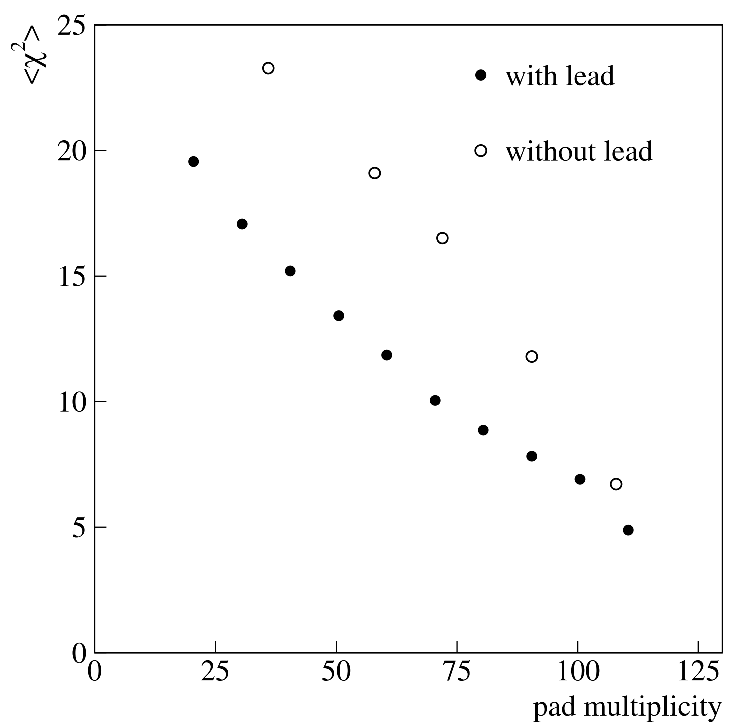

$(\chi^2)^{1/2}$ represents (approximately) the average time spread

The enhanced signal alone, arising from this, will reduce the timing fluctuations.

In addition, the contributions gained are concentrated near the ideal time because the higher energy electrons and photons travel near the front of the particle swarm (they suffer from smaller time delays) while those lost tend to lag far behind.

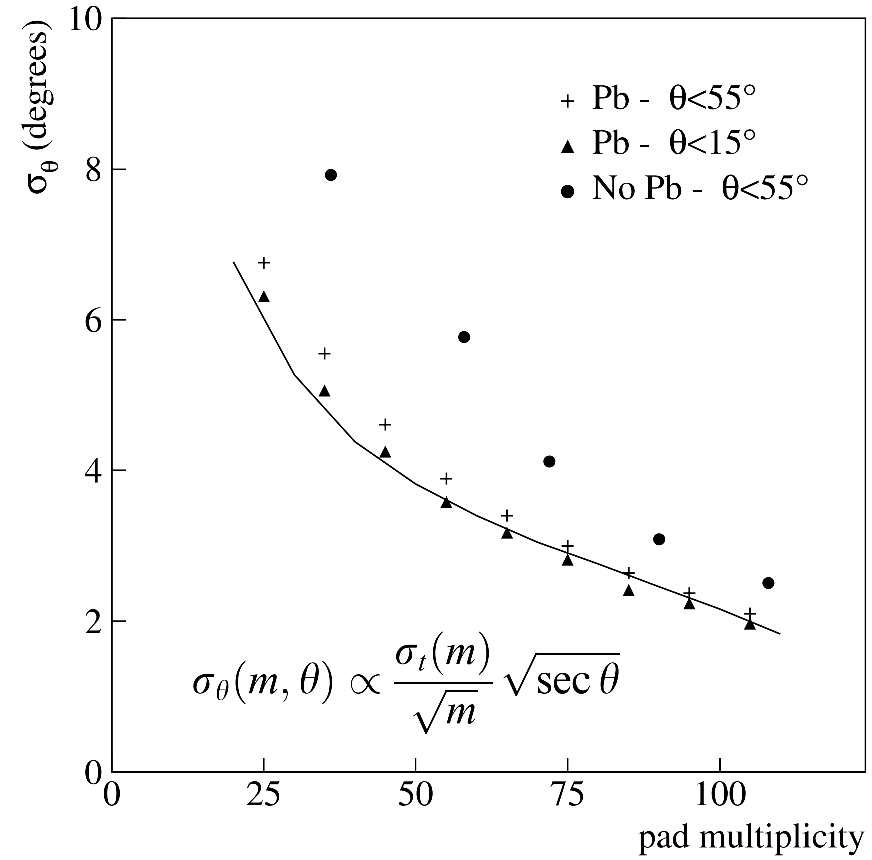

Measurement with ARGO at YBJ

Calibration of the energy scale

ARGO-YBJ: *Moon shadow* tool

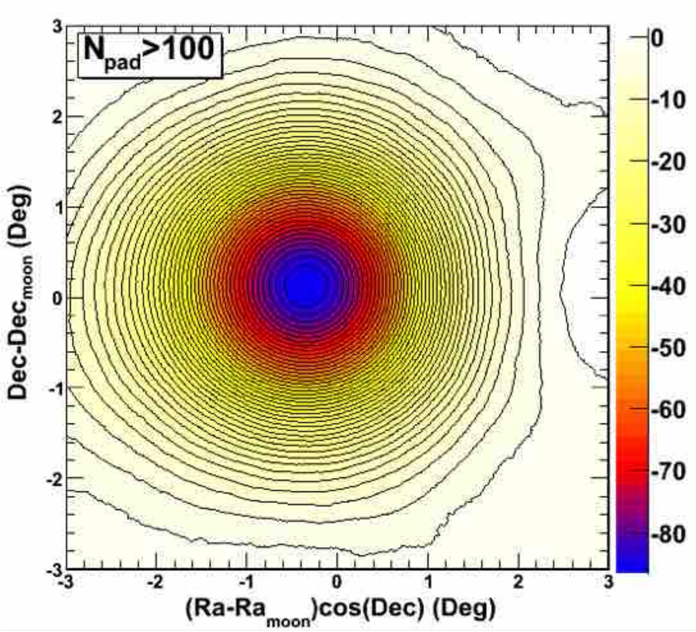

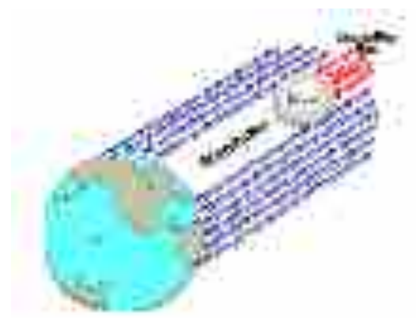

PRD 84 (2011) 022003

The energy scale uncertainty is estimated at 10% level in the energy range 1 – 30 (TeV/Z).

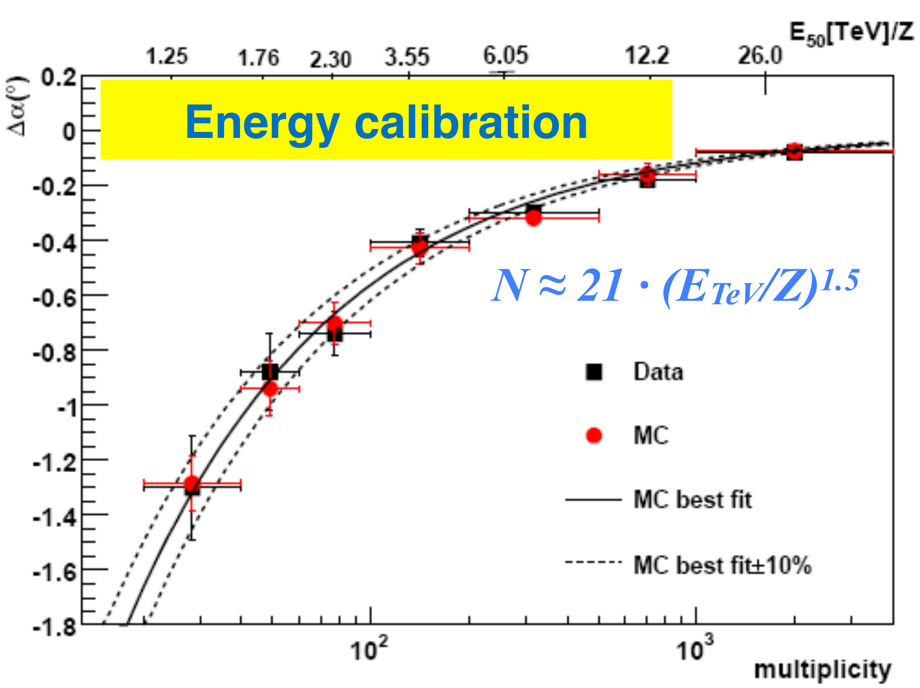

(p+He) spectrum (2 - 700) TeV

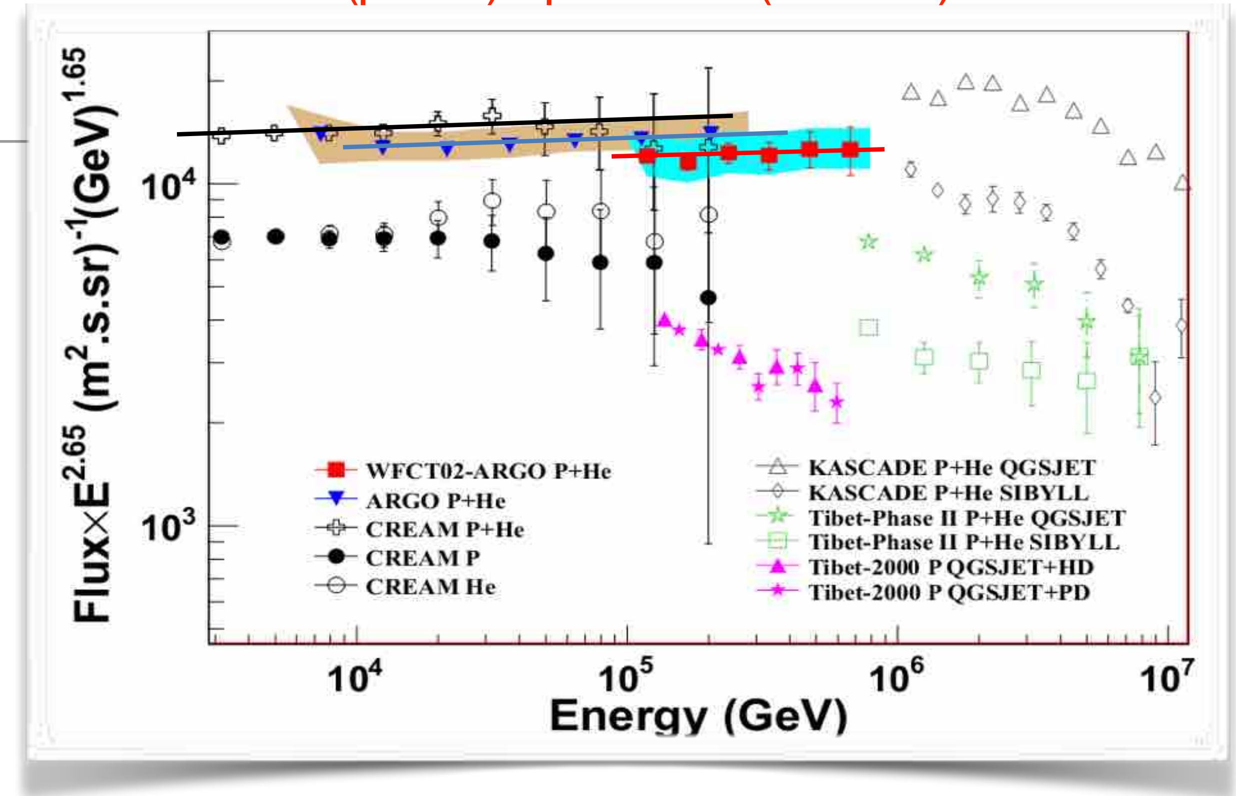

Chin. Phys. C 38, 045001 (2014)

- CREAM: 1.09 × 1.95 × 10^{-11} (E/400 TeV)$^{-2.62}$
- ARGO-YBJ: 1.95 × 10^{-11} (E/400 TeV)$^{-2.61}$
- Hybrid: 0.92 × 1.95 × 10^{-11} (E/400 TeV)$^{-2.63}$

Single power-law: 2.62 ± 0.01

Flux at 400 TeV:

1.95 × 10^{-11}± 9% (GeV^{-1} m^{-2} sr^{-1} s^{-1})

The 9% difference in flux corresponds to a difference of ± 4% in energy scale between different experiments.

Gamma/Hadron discrimination

Very difficult at low energy (< 1 TeV)

Muon size very small

HAWC/LHAASO approach requires large area: discrimination based on topological cut in the pattern of energy deposition far from the core (>40 m).

Requires sufficient number of triggered channels (>70 - 100)
→ minimum energy required E > 0.5 TeV

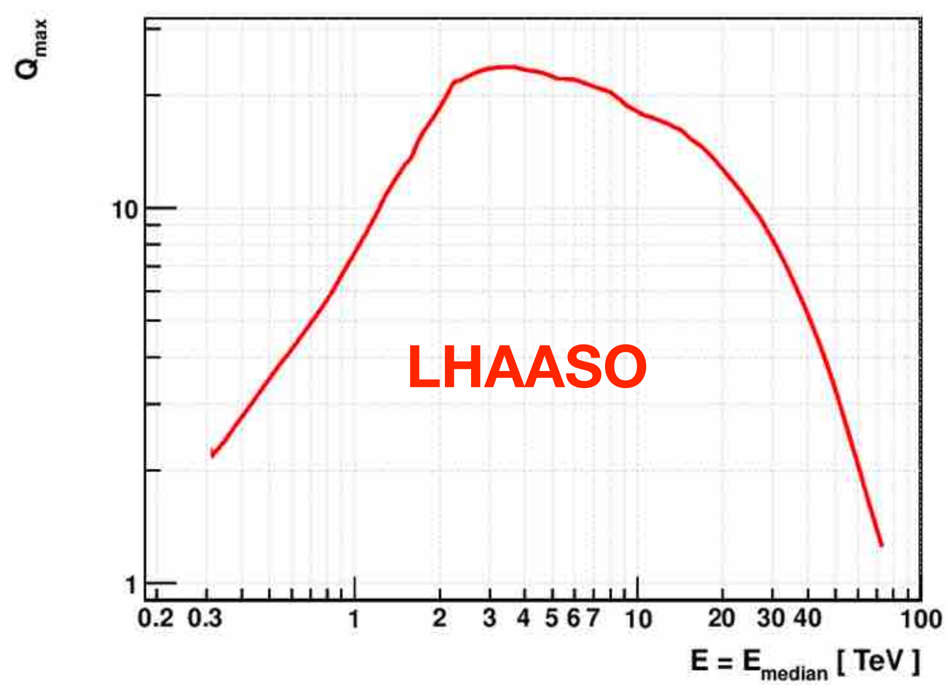

LHAASO Q-factor: 3 at 500 GeV, 7 at 1 TeV, 22 at 5 TeV.

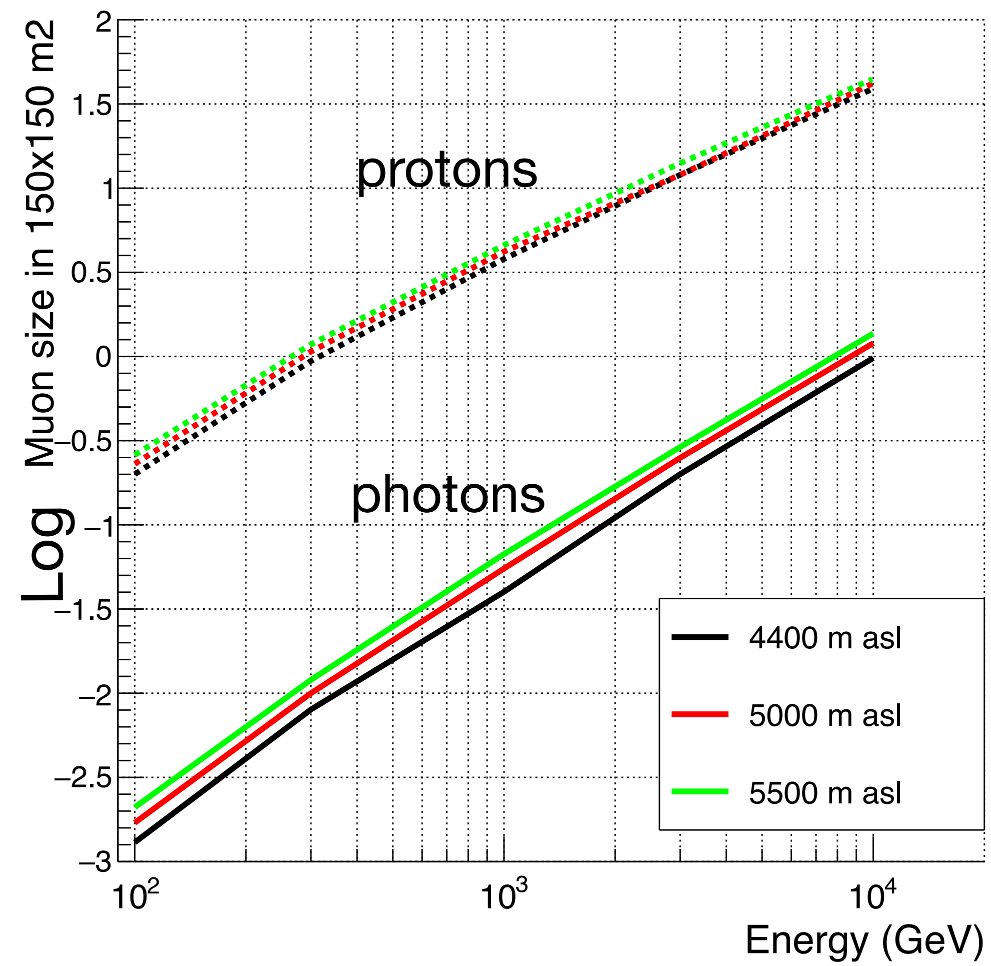

Discrimination capability depends on detector area

→ according to HAWC/LHAASO calculations sensitivity $\approx A_{eff}^{0.8}$ and not $A_{eff}^{0.5}$ up to ≈ 300 x 300 m² at TeV energies

New ideas ?

Extended sources

$$S_{ext} \sim \boxed{\frac{\Phi_\gamma(>E)}{\sqrt{\Phi_{bkg}(>E)}} \cdot R \cdot \sqrt{A^\gamma_{eff}} \cdot \sqrt{T} \cdot Q \times \frac{1}{\theta_{ext}} \cdot \frac{\theta_{ext}}{\theta_{PSF}}} \cdot \frac{\theta_{PSF}}{\theta_{ext}}$$

S point-source

$$\boxed{S_{ext} = S_{point} \cdot \frac{\theta_{PSF}}{\theta_{ext}}}$$

dimension of the extended source

Detectors with a 'poor' angular resolution are favoured in the extended source studies.

The minimum integral flux (in Crab units) detectable by LHAASO and CTA-South as a function of the source angular diameter, for two different photon energies.